ORNL/TM-2006/132

OAK RIDGE
NATIONAL LABORATORY
MANAGED BY UT-BATTELLE
FOR THE DEPARTMENT OF ENERGY

DURABILITY OF DEPLETED URANIUM AGGREGATES IN DUCRETE SHIELDING APPLICATIONS

C. H. Mattus
L. R. Dole

November 2006

UT-BATTELLE
ORNL-27 (4-00)

DOCUMENT AVAILABILITY

Reports produced after January 1, 1996, are generally available free via the U.S. Department of Energy (DOE) Information Bridge.

Web site http://www.osti.gov/bridge

Reports produced before January 1, 1996, may be purchased by members of the public from the following source.

National Technical Information Service
5285 Port Royal Road
Springfield, VA 22161
Telephone 703-605-6000 (1-800-553-6847)
TDD 703-487-4639
Fax 703-605-6900
E-mail info@ntis.fedworld.gov
Web site http://www.ntis.gov/support/ordernowabout.htm

Reports are available to DOE employees, DOE contractors, Energy Technology Data Exchange (ETDE) representatives, and International Nuclear Information System (INIS) representatives from the following source.

Office of Scientific and Technical Information
P.O. Box 62
Oak Ridge, TN 37831
Telephone 865-576-8401
Fax 865-576-5728
E-mail reports@adonis.osti.gov
Web site http://www.osti.gov/contact.html

This report was prepared as an account of work sponsored by an agency of the United States Government. Neither the United States Government nor any agency thereof, nor any of their employees, makes any warranty, express or implied, or assumes any legal liability or responsibility for the accuracy, completeness, or usefulness of any information, apparatus, product, or process disclosed, or represents that its use would not infringe privately owned rights. Reference herein to any specific commercial product, process, or service by trade name, trademark, manufacturer, or otherwise, does not necessarily constitute or imply its endorsement, recommendation, or favoring by the United States Government or any agency thereof. The views and opinions of authors expressed herein do not necessarily state or reflect those of the United States Government or any agency thereof.

ORNL/TM-2006/132

Nuclear Science and Technology Division

DURABILITY OF DEPLETED URANIUM AGGREGATES IN DUCRETE SHIELDING APPLICATIONS

C. H. Mattus
L. R. Dole

Date Published: November 2006

Prepared by
OAK RIDGE NATIONAL LABORATORY
Oak Ridge, Tennessee 37831-6254
managed by
UT-BATTELLE, LLC
for the
U.S. DEPARTMENT OF ENERGY
under contract DE-AC05-00OR22725

CONTENTS

LIST OF FIGURES v
LIST OF TABLES vii
ACRONYMS, ABBREVIATIONS, AND INITIALISMS ix
EXECUTIVE SUMMARY xi
ACKNOWLEDGMENTS xv
ABSTRACT xvii

1. INTRODUCTION 1

2. EXPERIMENTAL 3
   2.1 DESCRIPTION OF THE DURABILITY/LEACHING TEST 3
   2.2 DUO_2 MATERIALS TESTED 4
   2.3 PREPARATION OF THE LEACHING SOLUTIONS 6
      2.3.1 Leaching solutions for the testing of DUAGG 6
      2.3.2 Leaching solutions for the testing of high-fired DUO_2 7
   2.4 EXPERIMENTAL SETUP 7

3. RESULTS AND DISCUSSION 10
   3.1 CHEMICAL ANALYSES OF THE LEACHATES 10
   3.2 RELEASE OF URANIUM FROM THE DUO_2 AGGREGATES 15
      3.2.1 The release of uranium is lower from DUAGG than from the DUO_2 pellet 15
      3.2.2 The release of uranium increases when the temperature increases in almost all cases 18
      3.2.3 DI water is the worst solution when considering the inhibition of the release of uranium 18
      3.2.4 Cement pore solutions have a beneficial effect for both DUAGG and DUO_2 on the reduction of uranium release 18
   3.3 RELEASE OF THE BASALT COMPONENTS FROM DUAGG 23
   3.4 SEM EXAMINATION OF THE PELLETS 28
      3.4.1 High fired DUO_2 pellets 28
      3.4.2 DUAGG 44

4. CONCLUSIONS 59

5. REFERENCES 61

LIST OF FIGURES

1. DUAGG pellet 5
2. High-fired DUO_2 pellet 5
3. View of the Teflon liner used in the high-temperature experiment and the vessel receiving it 8
4. Fraction of uranium released from DUAGG kept in DI water and NaOH solution 16
5. Fraction of uranium released from DUAGG kept in OPC and BFS cement pore solutions 16
6. Fraction of uranium released from DUO_2 kept in DI water and NaOH solution 17
7. Fraction of uranium released from DUO_2 kept in OPC and BFS pore solutions 17
8. Release rate of uranium at 20°C 22
9. Release rate of uranium at 67°C 22
10. Release rate of uranium at 150°C 23
11. Fraction of silicon released from DUAGG kept in DI water and NaOH solution 25
12. Fraction of silicon released from DUAGG kept in OPC and BFS pore solutions 25
13. Fraction of aluminum released from DUAGG kept in DI water and NaOH solution 26
14. Fraction of aluminum released from DUAGG kept in OPC and BFS pore solutions 26
15. Fraction of iron released from DUAGG 27
16. Fraction of titanium released from DUAGG 27
17. Fraction of zirconium released from DUAGG 28
18. SEM pictures of DUO_2 cylinder kept in NaOH solution at 20°C for 9 months 30
19. SEM pictures of DUO_2 cylinder kept in NaOH solution at 67°C for 9 months 31
20. SEM pictures of DUO_2 cylinder kept in NaOH solution at 150°C for 9 months 32
21. SEM pictures of DUO_2 cylinder kept in DI water at 20°C for 9 months 33
22. SEM pictures of DUO_2 cylinder kept in DI water at 67°C for 9 months 34
23. SEM pictures of DUO_2 cylinder kept in DI water at 150°C for 9 months 35
24. SEM pictures of DUO_2 cylinder kept in BFS pore solution at 20°C for 9 months 38
25. SEM pictures of DUO_2 cylinder kept in BFS pore solution at 67°C for 9 months 39

26. SEM pictures of DUO_2 cylinder kept in BFS pore solution at 150°C for 9 months 40
27. SEM pictures of DUO_2 cylinder kept in OPC pore solution at 20°C for 9 months 41
28. SEM pictures of DUO_2 cylinder kept in OPC pore solution at 67°C for 9 months 42
29. SEM pictures of DUO_2 cylinder kept in OPC pore solution at 150°C for 9 months 43
30. SEM pictures of DUAGG pellet kept in DI water at 20°C for 27 months 45
31. SEM pictures of DUAGG pellet kept in DI water at 67°C for 27 months 46
32. SEM pictures of DUAGG pellet kept in DI water at 150°C for 27 months 47
33. SEM pictures of DUAGG pellet kept in NaOH solution at 20°C for 27 months 49
34. SEM pictures of DUAGG pellet kept in NaOH solution at 67°C for 27 months 50
35. SEM pictures of DUAGG pellet kept in NaOH solution at 150°C for 27 months 51
36. SEM pictures of DUAGG pellet kept in OPC pore solution at 20°C for 27 months 53
37. SEM pictures of DUAGG pellet kept in OPC pore solution at 67°C for 27 months 54
38. SEM pictures of DUAGG pellet kept in OPC pore solution at 150°C for 27 months 55
39. SEM pictures of DUAGG pellet kept in BFS pore solution at 20°C for 27 months 56
40. SEM pictures of DUAGG pellet kept in BFS pore solution at 67°C for 27 months 57
41. SEM pictures of DUAGG pellet kept in BFS pore solution at 150°C for 27 months 58

LIST OF TABLES

1. Physical characteristics of the two types of DUO_2 pellets used 5
2. Elemental composition of the DUO_2 materials 6
3. Analyses (mg/L) of the solutions used for curing the DUAGG and DUO_2 pellets 7
4. Quantity of some elements leached in DI water (percentage of the original amount present in the pellet) 11
5. Quantity of some elements leached in NaOH 1*N* solution (percentage of the original amount present in the pellet) 12
6. Quantity of some elements leached in OPC cement solution (percentage of the original amount present in the pellet) 13
7. Quantity of some elements leached in BFS cement solution (percentage of the original amount present in the pellet) 14
8. Comparison of the maximum release for uranium in each conservation medium 15
9. Uranium release rates ($mg \bullet m^{-2} \bullet d^{-1}$) obtained for DUAGG and high-fired DUO_2 19
10. Comparison of uranium release rate with data from the literature 21

ACRONYMS, ABBREVIATIONS, AND INITIALISMS

AAR	alkali-aggregate reaction
ALARA	as low as reasonably achievable
ANS	American Nuclear Society
ASTM	American Society for Testing and Materials
BFS	blast furnace slag
CSH	hydrated calcium cilicates
cm^3	cubic centimeters
DI	deionized water
DOE	U.S. Department of Energy
DU	depleted uranium
DUAGG	depleted uranium aggregate
DUCRETE	depleted uranium concrete
DUO_2	depleted uranium oxide
EDX	energy-dispersive X-ray fluorescence
EPA	U.S. Environmental Protection Agency
EPRI	Electric Power Research Institute
g	gram
HDPE	high-density polyethylene
HLW	high-level waste
ICP	inductively coupled plasma
ICP-AES	inductively coupled plasma–atomic emission spectroscopy
INL	Idaho National Laboratory
h	hour
kg	kilogram
L	liter
LDPE	low-density polyethylene
m	meter
mg	milligram
min	minute
mL	milliliter
NaOH	sodium hydroxide
OPC	ordinary Portland cement
OPC-DUAGG	ordinary Portland cement-pore solution
ORNL	Oak Ridge National Laboratory
PFA	perfluoroalkoxy
ppm	parts per million
PWR	pressurized water reactor
sec	second
SEM	scanning electron microscope
ShaRE	Shared Research Equipment

SIMFUEL	simulated fuel
SNF	spent nuclear fuel
TFE	tetrafluoroethylene
UO_2	uranium oxide
vol %	volume percent
wt %	weight percent

EXECUTIVE SUMMARY

In 1993, the U.S. Department of Energy (DOE) Office of Environmental Management began investigating the potential use of depleted uranium (DU) in heavy concretes, or DU concrete (DUCRETE) [1]. The depleted uranium aggregate (DUAGG) material was developed at Idaho National Laboratory (INL) and consists of DU dioxide (DUO_2) sintered with a synthetic basalt–based binder that coats the sintered DUO_2 particles and retards their surface reactions [2,3]. The DUCRETE material would be of beneficial use in the fabrication of casks for the transport and storage of spent nuclear fuels because of the additional shielding it provides [4].

The uranium release from UO_2 and spent fuel has been studied by many researchers. Most of the studies agree on the stages that occur when spent fuel is dissolved under repository conditions. In the first stage, the oxidized layer at the surface of the matrix is released into the leaching solution. Then, the oxidants attack the UO_2 surface, and more uranium is released and oxidized. The oxidized uranium precipitates as U(VI), and the reaction continues. Oxidizing conditions in a repository enhance the corrosion of UO_2 [5]; however, secondary uranyl alteration minerals can form and grow onto the surface, thus protecting the fuel material from further dissolution [6]. Uranyl oxide hydrates are the first to precipitate, but when the surrounding medium provides other species, uranyl silicates can be found [7,8]. The durability of basaltic glass, both synthetic in the laboratory and as natural analog found in nature, has also been studied extensively, especially to determine the long-term durability of the high-level waste immobilized in glass.

The principal area of concern regarding the stability of DUAGG pellets in concrete is the possible reaction between the sintered DUO_2 particles and the cement pore solution, which is a very basic medium (pH ~12.6) and contains alkalies (sodium and potassium). The potential reaction products of the UO_2 and/or the constituents of the basaltlike binder could create deleterious expansive mineral growths, similar to alkali-aggregate (alkali-silica) reactions (AAR), which can disrupt normal concrete structures [9,10,11]. To assess the potential impacts of DUO_2-DUAGG aggregates on the longevity and durability of DUCRETE casks, Oak Ridge National Laboratory (ORNL) used modified standardized American Society for Testing and Materials (ASTM) exposure tests that accelerate such surface interactions. Subsequent SEM examination of the surface of the uranium aggregate shows the alteration products that were formed.

The corrosion of DUAGG pellets was studied for as long as 27 months at three temperatures, 20, 67, and 150˚C in deionized (DI) water, 1 *N* NaOH solution, saturated cement pore solution made of (a) ordinary Portland cement (OPC) and (b) saturated cement pour solutions made of a mix of OPC, blast furnace slag (BFS), and fly ash. The pellets were completely immersed in the solution with a 10 to $1cm^{-1}$ ratio of the volume

of leachant to the surface area of the pellets with no change of the solution during the test (static cumulative test). No special handling of the pellet or the solutions was made to control the oxidation state nor was there any control of the air atmosphere in these experiments. The analyses of the leachates were made, and the pellets were observed by scanning electron miscrope (SEM) to identify the nature of the products formed during the exposure. For comparison, the same conditions and testing were performed on pellets of high-fired DUO_2 for 9 months. The following conclusions can be drawn from the results gathered:

- The total release of uranium was minimal in the conditions of the tests. After 27 months at 150°C, maxima ranging from 0.40 to 0.0003% uranium (amount leached divided by the total amount of uranium present in the pellet before testing) was released from DUAGG; and 0.90 to 0.0005% was released from high-fired DUO_2 after 9 months at 150°C.

- The release of uranium from DUAGG was lower than that released from a DUO_2 pellet. Under most conditions, at least one order of magnitude difference existed between DUAGG and DUO_2.

- The release of uranium was greater in DI water than in the 1*N* NaOH solution.

- The cement pore solutions had a beneficial effect for both DUAGG and DUO_2 on the uranium release. For DUO_2, the maximum release was as much as 260 times lower in BFS and 750 times lower for OPC than in DI water. For DUAGG, the maximum release was as much as 600 times lower in BFS and 70 times lower in OPC than in DI water.

- The release rate of uranium has been compared with data found in the literature for release rates of uranium from UO_2 or simulated nuclear fuel; the release rate was lower for DUAGG. The release rate was comparable for DUO_2 in the presence of DI water, but the contact of pure uranium pellet with cement pore solutions decreased the release rate.

The combination of uranium and basalt in DUAGG resulted in a competition between the different species (uranium, aluminum, silicon, iron, titanium, and zirconium) for interaction with the solution species. The examination of the samples after more than 2 years of cure provided strong evidence that the basalt phase effectively protected the UO_2. A protective coating of recrystallized basalt dissolution products covered the DU particles and formed a very dense layer that slowed or stopped the exchange of species between the pellets and the solution. The examination showed no deleterious crystals that may have resulted from AAR when the samples were kept in the cement pore solution. The nature of the compounds formed after curing for the high-fired DUO_2 was similar to that

reported in the literature for spent nuclear fuel or surrogate simulated fuel (SIMFUEL) in which crystals such as schoepite were observed. For the DUAGG pellets, such products were not visible, and protective crystals, such as those found in altered nuclear glasses, were observed. The results obtained tended to prove that DUAGG behaves as a nuclear glass, partly because of the basalt component—a metal that behaves similar to high-level waste (HLW) glass. Such glasses are currently used for the long-term storage of high-level nuclear wastes; they have been studied extensively in the past and are approved as safe for storage of long-lived radionuclides.

ACKNOWLEDGMENTS

The funding for this research was provided by the Depleted Uranium Uses Research and Development Program (DOE EM-30). The authors want to acknowledge Dr. J. M. Haire for his support of this work.

ABSTRACT

The depleted uranium (DU) inventory in the United States exceeds 500,000 metric tonnes. To evaluate the possibilities for reuse of this stockpile of DU, the U.S. Department of Energy (DOE) has created a research and development program to address the disposition of its DU. One potential use for this stockpile material is in the fabrication of nuclear shielding casks, for the storage, transport, and disposal of spent nuclear fuels. The use of the DU-based shielding would reduce the size and weight of the casks while allowing a level of protection from neutrons and gamma rays comparable to that afforded by steel and concrete. Depleted uranium aggregate (DUAGG) is formed of depleted uranium dioxide (DUO_2) sintered with a synthetic basalt–based binder. This study was designed to investigate possible deleterious reactions that could occur between the cement paste and the DUAGG. The same tests were also performed on some pellets of high-fired DUO_2 specifically to compare the action of the basalt addition in DUAGG.

The curing of the pellets lasted 27 months for DUAGG and 9 months for DUO_2. Four curing solutions were used: deionized distilled (DI) water, 1 *N* NaOH solution, a cement pore solution from ordinary Portland cement (OPC) and a cement pore solution from a mixture of OPC with blast furnace slag (BFS) and fly ash. The samples were subjected to three different temperatures: 20, 67 and 150°C in room atmospheric conditions. At the end of specified time intervals the leaching solutions were analyzed and the surfaces of the pellets were examined by scanning electron microscope (SEM) for identification of the products formed.

After 27 months of exposure to cement pore solutions, no deleterious expansive mineral phases were observed to form either with the DUO_2 or with the simulated basalt sintering phases from DUAGG. The release of uranium was found to be lower in DUAGG than in DUO_2 pellets. The uranium release was found to be lower in cement pore solutions than in DI water for both DUAGG and DUO_2. The SEM examination of DUO_2 showed the formation of schoepite or dehydrated schoepite in the samples kept in NaOH solution. In the cement pore solutions, these recrystallization phases were not visible. Some DUAGG samples exhibited the presence of crystals of hydrotalcite, a mineral found in the alteration of basaltic and nuclear waste glass. A layer of products from the basalt dissolution was seen around the DUAGG pellets, providing a protective layer that slowed or stopped the exchange of species between the pellet and the surrounding solution. This finding may indicate that DUAGG in depleted uranium concrete (DUCRETE) casks could have service lives sufficient to meet the projected needs of DOE and the commercial nuclear power industry.

1. INTRODUCTION

In 1993, the U.S. Department of Energy (DOE) Office of Environmental Management began investigating the potential use of depleted uranium (DU) in heavy concretes, or depleted uranium concrete (DUCRETE) [1]. This concrete consists of depleted uranium ceramic or depleted uranium aggregate (DUAGG), which replaces the coarser aggregate that is mixed with Portland cement, sand, and water for use in normal concrete. The DUAGG material was developed at Idaho National Laboratory (INL) and consists of depleted uranium dioxide (DUO_2) sintered with a synthetic basalt–based binder that coats the sintered DUO_2 particles and retards their surface reactions [2,3]. The preliminary work on DUAGG and DUCRETE properties has been performed at INL [4,5]. The DUCRETE material would be of beneficial use in the fabrication of casks for the transport and storage of spent nuclear fuel (SNF) because of the additional shielding it provides [6]. However, more information is required to fully evaluate the long-term stability and durability of these materials.

Because DUO_2 grains are embedded into a basalt sintering phase (mostly SiO_2• Al2O_3•TiO_2-ZrO_2) close to the composition of a basaltic glass, the possible alteration of the DUAGG material in a corrosive environment is unknown. The uranium release from uranium oxide (UO_2)and spent fuel has been studied by many researchers [7–28], several of them using UO_2 as a surrogate for irradiated spent fuels, which are highly radioactive and therefore difficult to use for experiments [20]. Using UO_2 provides a good correlation with spent fuels as to the nature of the alteration products that can be formed; however, the influence of the radiolysis created by the gamma radiation is absent, and the consequent enhanced dissolution of the fuel caused by chemical species such as O_2 or H_2O_2 formed during radiolysis cannot be measured. Most of the studies agree on the steps that take place when spent fuel is dissolved under repository conditions. In a first stage, the oxidized layer at the surface of the matrix is released into the leaching solution. Then, the oxidants attack the UO_2 surface, and more uranium is released and oxidized. The oxidized uranium precipitates as U(VI), and the reaction continues. Oxidizing conditions in a repository enhance the corrosion of UO_2 [27]; however, secondary uranyl alteration minerals can form and grow onto the surface, thus protecting the fuel material [23]. Uranyl oxide hydrates are the first to precipitate, but when the surrounding medium provides other species, uranyl silicates can be found [9,28]. Several studies compare the corrosion rate of uranium from UO_2 under different storage conditions. The results depend upon the experimental conditions selected, but the corrosion rates were found to range between about 0.3 and 2 $mg \bullet m^{-2} \bullet d^{-1}$. A paper on fuel corrosion processes by D.W. Shoesmith [27] reviews the influence of all the parameters that are of importance in a repository.

The durability of basaltic glass, both synthetic as produced in the laboratory and natural as found in nature, has also been studied extensively [29–35], especially to determine the

long-term durability of the high-level waste immobilized in glass. Techer [34] found that the basaltic glass alteration rate dropped by four orders of magnitude after a protective layer of alteration products formed on the surface of the sample. Abdelouas and his team [33] identified hydrotalcite-like compounds as the first alteration products found in a basaltic glass. Crovasier [35] compared the corrosion of synthetic basalt glass with nuclear borosilicate glass and found that they had similar dissolution mechanisms and that the long-term dissolution rate was very low. Basalt glass is actually used as a natural analog for nuclear waste and for predicting its durability over geological periods of time. Crovasier stated that "the available data show that natural basaltic glasses may survive for millions of years under subsurface conditions."

The last parameter that may influence the durability of DUCRETE is the interactions of both the uranium compounds and the basalt glass with the cement matrix. Based on a review of the literature, it has been postulated that dense DUCRETE would develop possible failure mechanisms under oxidizing conditions and with the pore water chemistry of concrete made from Portland cement. Expansive, less-dense oxides would form that could affect the strengths, thermal conductivities, and competence of the shielding made from the DUCRETE in proposed storage and transport casks. For the expected service conditions of DUCRETE in spent fuel casks, the rates and extent of these potential aggregate/cement–paste interactions are unknown. The principal area of concern regarding the stability of DUAGG pellets in concrete is the possible reaction between the sintered DUO_2 particles and the cement pore solution, which is a very basic medium (pH ~12.6) that contains large quantities of alkalies (sodium and potassium).

The potential reaction products of the UO_2 and/or the constituents of the basalt-like binder could create deleterious expansive mineral growths. These reactions could be similar to alkali–aggregate (alkali–silica) reactions (AAR), which can disrupt normal concrete structures by generating cracks and spalling [36,37,38]. Therefore, in an attempt to assess the potential impacts of DUO_2–DUAGG aggregates on the longevity and durability of DUCRETE casks, Oak Ridge National Laboratory (ORNL) is using modified standardized American Society for Testing and Materials (ASTM) exposure tests [39] that accelerate the onset and progress of such surface interactions. Scanning electron miscrope (SEM) examination of the surface of the uranium aggregate allowed for a visualization of the alteration products that were formed.

After the results obtained for the DUAGG aggregate had been studied for a year, a second series of tests was started using pellets of high-fired DUO_2 that were submitted to the same conditions as the DUAGG pellets. These tests would allow a direct comparison of the DUAGG pellets with regular DUO_2 pellets when used in a cement matrix.

2. EXPERIMENTAL

2.1 DESCRIPTION OF THE DURABILITY/LEACHING TEST

Testing at ORNL measured the extent and rates of surface reactions of the DUO_2 materials under the expected service temperatures and the simulated chemical environment of cement paste as it would exist in a cask made of concrete containing SNF. The intact aggregates of DUO_2/DUAGG were tested for reactivity according to the ASTM C289-01[39] method to measure interactions with the cement pore liquids that are expected to occur in concrete pastes. The ASTM method, however, had to be modified to better match the conditions that would exist in a cask as well as the limitation of products (e.g., material, vessels) at our disposal.

The ASTM test called for the reaction of crushed material (150- to 300-µm fraction) with a 1 *N* sodium hydroxide (NaOH) solution at 80°C for 24 h, followed by the analysis of the solution for silicon. In our test, the temperature was modified to cover the range of temperatures that could be seen in a cask containing SNF. A test sponsored by the Electric Power Research Institute (EPRI) [40] indicates that, while the outside of the cask would remain at ambient temperature, the side adjacent to the fuel could reach temperatures varying from 50 to 140°C. The higher temperature was obtained for off-normal conditions when the ventilation channels in the cask were blocked. Therefore, three temperatures were selected for the test: ambient, 67°C, and 150°C.

The exposure to 1 *N* NaOH represents an extreme situation that does not accurately characterize the cement pore solution to which the DUAGG/DUO_2 aggregate would actually be exposed. It represents a worst-case scenario in which the AAR is amplified and could represent the upper limit of reactivity if AAR were to occur within the material. Three leaching media were chosen for the testing that took into account the possibilities of the AAR (1) DI water (to represent a better-case scenario), (2) two cement pore solutions (the actual scenario), and (3) a 1 *N* NaOH solution (the worst-case scenario).

Because we wanted to examine the surface of the DUAGG after exposure, the use of a fine fraction size was not practical. Furthermore, we had a limited quantity of DUAGG material (~1 kg), which would not permit the generation of the amount of the selected fraction size called for by the ASTM method. Therefore, an entire pellet of DUAGG and two pellets of high-fired DUO_2 were used for each test. The pellets were exposed to the solutions for different lengths of time to allow ongoing monitoring of the reaction. The selected times were 30 days, 60 days, 90 days, 180 days, 360 days, and 24 and 27 months. The test were run under atmospheric conditions in a closed system, and the solutions were not changed during the experiment.

The ASTM method called for 25 g of crushed material to be tested with 25 mL of 1 *N*

NaOH solution. In the modified method, using whole pellets, a volume to surface ratio of 10 cm^{-1} was selected. This ratio is often used in leaching tests such as American Nuclear Society (ANS) 16-1 and appeared to be a better choice for this experiment. A ratio of 10 cm^{-1} is much higher than that found in the "real" conditions in a concrete, where the amount of interstitial liquid is very low — especially when the concrete is aging and the liquid is used to form cement hydrates. Using a higher liquid-to-solid ratio is a way to accelerate the reactions taking place in the experiment [41,42].

2.2 DUO_2 MATERIALS TESTED

The DUAGG samples were obtained from Starmet CMI (formerly Carolina Metals, Inc.), and the high-fired DUO_2 pellets were available at ORNL.

The almond-shaped DUAGG aggregates (as shown in Fig. 1) were approximately 1.59 cm long, 0.95 cm wide, and 0.64 cm thick, with a measured average surface area of 5.77 ± 0.01 cm^2. Because of the irregular shape of the pellet, the measurement was made by comparing the weight of a sheet of parafin of the known area and one that covered the outside surface of the pellet. This measurement was repeated several times to allow statistical evaluation of the results. The average weight was found to be 6.39 ± 0.01 g, and the average volume was 0.784 ± 0.002 cm^3. The measured density of the DUAGG pellets was 8.15 g/cm^3. With a pellet surface area measured at 5.8 cm^2 and a leachate surface-to-volume ratio of 1:10 cm^{-1}, the volume of liquid used in the sealed leach vessels was 58 mL for each DUAGG pellet. Some of the pellets had surface defects, and the most regular ones were selected. The irregularity and roughness of the surface (as was later seen when using electron microscopy) probably induced a large error in the surface measurement.

The high-fired DUO_2 pressurized water reactor (PWR) pellets, shown in Fig. 2, were cylindrically shaped with a diameter of 0.685 cm and a height of 1.39 cm. The weight of one pellet was 5.355 g and the density 10.52 $g/cm^{3.}$ Two pellets were used for each test to obtain enough solution for analysis. The outside surface of the pellets presented fewer defects than the DUAGG pellet. The physical characteristics of the two types of pellets are compiled in Table 1.

The chemical composition of both materials was determined. They were both dissolved following standard U.S. Environmental Protection Agency (EPA) methods (SW-846/3051 and 3052 at http://www.epa.gov/SW-836/pdfs/305.pdf) and were analyzed by inductively coupled plasma-atomic emission spectroscopy (ICP-AES) using a Thermo-Jarrell Ash 61E Trace instrument. The standard EPA method followed for the analysis was SW846-6010B. The elemental composition for each material is provided in Table 2.

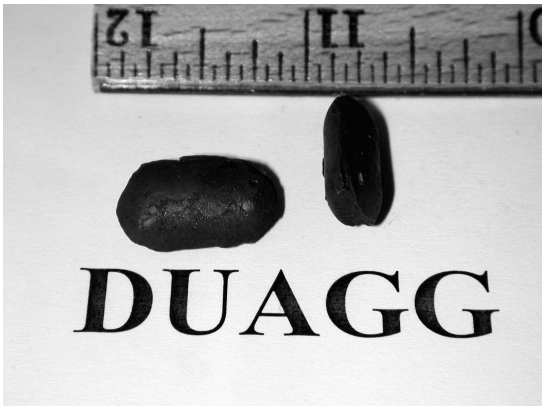

Fig. 1. DUAGG pellet.

Fig. 2. High-fired DUO_2 pellet.

Table 1. Physical characteristics of the two types of DUO_2 pellets used

	DUAGG	**PWR high-fired DUO_2**
Shape	almondlike	cylinder
Size (cm)	1.59 long 0.95 wide 0.64 thick	0.685 diameter 1.39 height
Weight (g)	6.39 ± 0.01	5.355
Density (g/cm^3)	8.15	10.52
Surface area (cm^2)	5.8	2.99
Number of pellets per test	1	2
Volume of leaching solution (mL)	58	60

Table 2. Elemental composition of the UO_2 materials

	DUAGG composition (mg/kg)	PWR-DUO_2 composition (mg/kg)
Silver	< 24	< 100
Aluminum	5200 ± 500	1902 ± 1979
Arsenic	< 180	< 250
Boron	< 1190	< 125
Barium	25 ± 1	< 50
Beryllium	< 10	< 25
Calcium	< 2380	< 7500
Cadmium	29.4 ± 0.4	< 50
Chromium	< 25	< 75
Copper	310 ± 20	< 175
Iron	3600 ± 700	< 2000
Potassium	1200 ± 60	< 2250
Magnesium	1300 ± 200	1650 ± 640
Manganese	< 10	< 50
Molybdenum	< 30	< 100
Sodium	< 1200	< 3750
Niobium	< 180	640 ± 150
Nickel	< 35	< 175
Lead	< 70	< 125
Silicon	18300 ± 100	< 1000
Strontium	46 ± 1	40 ± 2
Titanium	11400 ± 100	< 75
Uranium	795000 ± 10500	802000 ± 135000
Vanadium	20 ± 3	60 ± 20
Zinc	< 800	< 1000
Zirconium	7210 ± 80	< 750

2.3 PREPARATION OF THE LEACHING SOLUTIONS

2.3.1 Leaching solutions for the testing of DUAGG

The ordinary Portland cement (OPC) pore solution (OPC-DUAGG) was prepared by mixing ~300 g of a type I-II Portland cement (Lone Star Industries, Inc.) with ~1 L of deionized (DI) water. The mixture was tumbled for 7 days in a sealed bottle, allowed to settle, and then the supernate was filtered through a 0.45-µm filter. Inductively coupled plasma (ICP) analysis showed that the solution contained ~3 mg/L of barium, ~1800 mg/L of potassium, ~300 mg/L of sodium, and ~50 mg/L of strontium. The results of the analyses are found in table 3. The pH of the solution was ~12.6. Another solution, BFS-

DUAGG, was prepared by mixing a blend of 40% of blast furnace slag (BFS) (Lone Star Industries, Inc.- finesse 6330 blaine, 120 grade) and 60% of the same type I-II OPC with an excess of DI water. Type II DI water was used as well as a commercial 1 *N* NaOH solution. The ICP analyses of the leaching solutions used are found in Table 3.

2.3.2 Leaching solutions for the testing of high-fired DUO_2

In view of the results obtained on DUAGG, two different mixes of cement and additives were prepared for testing of the high-fired DUO_2 pellets. The first cement pore solution was obtained by mixing 400 g of type I-II OPC with 2 L of type II DI water. This solution was called "OPC-DUO_2." A second mixture containing 40% of type I-II OPC (Lone Star Industries, Inc.), 30% Class F fly ash (Southeastern Fly Ash Co., Inc.), and 30% BFS (Lone Star Industries, Inc.) was mixed with excess type II DI water to obtain a cement pore solution named "BFS-DUO_2."

Table 3. Analyses (mg/L) of the solutions used for curing the DUAGG and DUO_2 pellets

	BFS DUAGG	BFS DUO_2	OPC DUAGG	OPC DUO_2	NaOH DUAGG	NaOH DUO_2	DIW DUAGG	DIW DUO_2
Silver	< 0.020	< 0.039	< 0.011	< 0.039	< 0.053	< 0.033	< 0.002	< 0.004
Aluminum	< 0.600	1.257	< 0.600	2.225	< 1.603	3.326	< 0.064	< 0.059
Boron	< 1.000	0.285	< 0.534	< 0.223	< 2.672	< 0.138	< 0.107	< 0.013
Barium	4.7	6.1	3.4	4.7	0.015	< 0.014	< 0.001	< 0.002
Calcium	539	506	485	689	< 5.3	< 2.00	< 0.214	< 0.213
Cadmium	< 0.010	0.032	0.033	0.043	< 0.027	< 0.020	< 0.001	< 0.002
Chromium	< 0.020	< 0.026	0.027	< 0.029	< 0.053	< 0.024	< 0.002	< 0.003
Copper	< 0.040	< 0.126	0.045	< 0.129	< 0.107	< 0.086	< 0.004	< 0.009
Iron	< 1.000	< 1.130	< 0.534	< 1.132	< 2.672	< 0.836	< 0.107	< 0.090
Potassium	921	502	1784	705	< 2.14	1.23	< 0.086	< 0.096
Magnesium	< 0.300	< 0.328	< 0.160	< 0.329	< 0.802	< 0.307	< 0.032	< 0.033
Manganese	< 0.008	< 0.013	< 0.004	< 0.013	< 0.021	< 0.013	< 0.001	< 0.002
Molybdenum	< 0.025	< 0.052	< 0.013	< 0.051	< 0.067	< 0.040	< 0.003	< 0.004
Sodium	264	184	328	150	22157	35868	< 0.107	< 0.302
Nickel	< 0.030	< 0.056	< 0.016	< 0.056	< 0.080	< 0.071	< 0.003	< 0.006
Lead	< 0.060	< 0.063	< 0.032	< 0.063	< 0.160	< 0.048	< 0.006	< 0.005
Selenium	< 0.150	< 0.191	< 0.080	< 0.193	< 0.401	< 0.259	< 0.016	< 0.016
Silicon	< 0.800	0.522	0.511	0.564	< 1.069	< 1.036	< 0.043	< 0.035
Strontium	37	30	63	66	0.014	0.016	< 0.000	< 0.001
Titanium	< 0.006	< 0.014	< 0.003	< 0.014	< 0.016	< 0.016	< 0.001	< 0.002
Uranium	< 0.300	< 0.816	< 0.160	< 0.818	< 0.802	< 0.890	< 0.032	< 0.059
Vanadium	< 0.015	< 0.025	< 0.008	< 0.025	< 0.040	< 0.020	< 0.002	< 0.002
Zinc	< 0.700	< 0.239	< 0.374	< 0.212	< 1.871	< 0.265	< 0.075	< 0.028
Zirconium	< 0.300	< 0.321	< 0.160	< 0.336	< 0.802	< 0.537	< 0.032	< 0.029

2.4 EXPERIMENTAL SETUP

The containers used for the tests at elevated temperatures were vessels from a microwave digestion system (Fig. 3). These vessels are made of an outer shell of Ultem®, a thick

inner shell of tetrafluoroethylene (TFE) Teflon; and, a 20-mil clear perfluoroalkoxy (PFA) liner. These vessels can withstand high temperatures as well as pressures up to 220 psi. The containers used for the tests at room temperature were made of low-density polyethylene (LDPE). They were sealed air tight with electrical tape around the snap cap. Because of the limited number of vessels available and the limited amount of DUAGG, it was not possible to run duplicate tests.

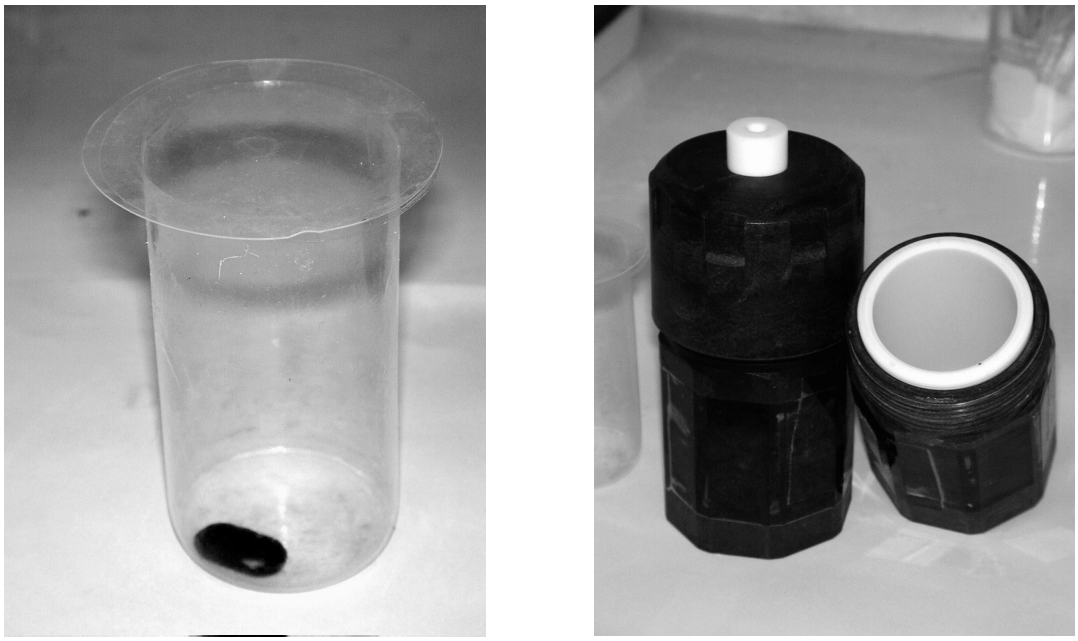

Fig. 3. View of the Teflon liner used in the high-temperatures experiments and the vessel receiving it.

Both the DUAGG and DUO_2 pellets were rinsed with DI water to remove any fine particles attached to them. After the pellets were dried, the selected solution was poured first in the appropriate container and then the pellet was placed in the vessel. Then, the vessel was closed tightly to prevent leakage. The preparation of the solutions and vessels as well as the static corrosion test were performed in aerated conditions. The vessel and its content were placed in an oven set at either 67 or 150°C.

At a consistent surface-to-liquid ratio of 1:10 cm^{-1}, the sintered DUAGG samples and the DUO_2 samples were exposed to (1) type II DI water, (2) a 1 *N* NaOH standard solution, (3) a saturated interstitial solution extracted from an OPC (high-alkali type I-II Portland cement), and (4) a saturated interstitial solution extracted from a mixture of OPC and BFS. Fly ash was also included in the mixture of OPC and BFS for the DUO_2 samples.

The three exposure temperatures were 20, 67, and 150ºC, and the seven time intervals

planned were 30 days, 60 days, 90 days, 180 days, 360 days, and 2 and 3 years. One vessel was prepared for each time interval chosen, and the solutions were not changed at any time during the experiment. Thus the concentration at any given time is a measure of cumulative extraction rather than incremental extractions. The preparation and curing of the samples were performed under atmospheric conditions with no control for CO_2 or O_2 interaction with the uranium pellets or solutions. After the vessels were closed, no new intake of these gases occurred until the vessels were opened at the chosen time interval.

At the end of each exposure period, the vessels were removed from the oven, allowed to cool to room temperature, and opened. The uranium pellets were removed and were rinsed with DI water to eliminate the salts left by the solution and were then dried for further SEM examination. The liquid phase was sampled, and the volume was measured. The solution was acidified with concentrated nitric acid to bring the solution to a pH below 2. The leachate was then analyzed for total composition, including elements such as aluminum, silicon, uranium, alkalies, and other measurable elements, by ICP-AES in a Thermo Jarrell Ash model 61E trace analyzer. The empty containers were rinsed with a solution of 10% nitric acid to dissolve and analyze the deposits/crystals that may have formed on the surface of the Teflon liners.

The quantities of each element leached were compared with the initial content of a DUAGG pellet (see Table 2) to determine the degree of corrosion of the aggregate surfaces. In the case of the high-fired DUO_2, the theoretical composition of 88.148 wt % of uranium was used instead of the analyzed value found during the analysis (80 ± 14 wt %).

Consistent with the guidelines of ASTM C295-98, the surfaces of the exposed aggregates were subsequently examined and compared by SEM and energy dispersive X-ray fluorescence (EDX) analyses with a Phillips XL30FEG from the Metals and Ceramics Division's Shared Research Equipment (SHaRE) Collaborative Research Center and Program at ORNL.

3. RESULTS AND DISCUSSION

3.1 CHEMICAL ANALYSES OF THE LEACHATES

The actual time intervals for the DUAGG pellets kept in DI water, NaOH solution, and OPC solution were 30, 60, 90, 180, 390, 730, and 810 days (1, 2, 3, 6, 13, 24, and 27 months). For the DUAGG samples kept in BFS pore solution, the time intervals were 30, 60, 90, 180, 390, 600, and 730 days (1, 2, 3, 6, 13, 20, and 24 months). The DUO_2 pellets were analyzed after 30, 60, 90, 180, and 270 days (1, 2, 3, 6, and 9 months).

The ICP analysis of the DUAGG revealed that the most abundant elements in the pellets are uranium, silicon, and titanium, as shown in Table 2. For calculating the percentage of uranium released from the DUO_2 pellets, the theoretical value was used instead of the one measured by ICP.

The maximum "normalized" leaching, which is the amount leached relative to the initial amount of the specific element in the DUAGG (from Table 2), is calculated as shown in Eq. (1). The results are presented in Tables 4 through 7. The percentage of uranium leached from the DUO_2 pellet is also shown in the same tables.

$$\%\ Amount\ leached = \frac{\left(\left(CLi \bullet VLi\right) + \left(CRi \bullet VRi\right)\right) - \left(CBi \bullet VBi\right)}{Ai} \qquad (1)$$

where C_{Li} and V_{Li} are the measured concentrations (mg/L) of a specific element (i) and the volume of leachate (L) at the time interval considered, C_{Ri} and V_{Ri} are the measured concentrations (mg/L) in the rinse of the vessel for that element and the volume (L) of acid used to rinse, C_{Bi} and V_{Bi} are the measured concentrations (mg/L) for (i) and the volume (L) of the blank, and, A_i is the amount (mg) of the element (i) in the initial DUAGG pellet. It is important to remember that these results are based on an unique cumulative sample, which can explain some of the scarcity of observations.

Table 4. Quantity of some elements leached in DI water (percentage of the original amount present in the pellet)

Time interval (months)	Temperature (°C)	DUAGG						DUO_2
		Aluminum	Iron	Silicon	Titanium	Uranium	Zirconium	Uranium
1	20	0.000	0.005	0.000	0.0001	0.00002	0.000	0.0006
	67	0.36	0.37	0.32	0.0005	0.00005	0.0007	0.0089
	150	2.41	0.03	2.37	0.0008	0.001	0.0007	0.0396
2	20	0.009	0.009	0.0007	0.002	0.00001	0.0004	0.0007
	67	0.99	0.26	0.92	0.001	0.0002	0.0004	0.0065
	150	3.10	0.098	3.09	0.001	0.002	0.0004	0.0402
3	20	0.000	0.05	0.0065	0.000	0.000	0.000	0.0006
	67	0.12	0.000	0.24	0.000	0.000	0.0002	0.0172
	150	0.13	0.04	0.33	0.0004	0.00005	0.0002	0.0427
6	20	0.000	0.000	0.006	0.000	0.000	0.000	0.0020
	67	0.27	0.000	0.31	0.000	0.000	0.000	0.0542
	150	0.04	0.010	2.17	0.0002	0.00001	0.001	0.3126
9	20	–	–	–	–	–	–	0.0022
	67	–	–	–	–	–	–	0.0208
	150	–	–	–	–	–	–	0.8990
13	20	0.002	0.000	0.000	0.00006	0.0002	0.001	–
	67	3.33	3.04	5.27	0.04	0.13	0.009	–
	150	7.15	5.80	15.5	0.17	0.15	0.27	–
24	20	0.000	0.005	0.000	0.00002	0.00004	0.0007	–
	67	2.10	1.78	1.84	0.05	0.007	0.02	–
	150	5.44	3.13	4.51	0.08	0.10	0.01	–
27	20	0.580	1.53	0.045	0.039	0.035	0.014	–
	67	1.81	1.70	2.82	0.04	0.01	0.001	–
	150	3.63	3.18	6.12	0.12	0.40	0.09	–

Table 5. Quantity of some elements leached in NaOH 1 *N* solution (percentage of the original amount present in the pellet)

Time interval (months)	Temperature (°C)	DUAGG						DUO_2
		Aluminum	Iron	Silicon	Titanium	Uranium	Zirconium	Uranium
1	20	0.000	0.000	0.07	0.007	0.000	0.000	0.0130
	67	3.0	0.000	3.3	0.006	0.000	0.000	0.0096
	150	26	0.87	20	0.15	0.003	0.000	0.0038
2	20	0.000	0.000	0.15	0.005	0.000	0.000	0.0207
	67	6.0	0.04	5.6	0.02	0.0006	0.000	0.0055
	150	34	1.06	27	0.04	0.004	0.000	0.0062
3	20	0.000	0.02	0.27	0.006	0.000	0.000	0.0335
	67	10.2	0.20	8.9	0.01	0.001	0.000	0.0088
	150	40	1.39	31	0.03	0.005	0.000	0.0051
6	20	0.53	0.03	0.46	0.005	0.00004	0.004	0.0388
	67	18.1	0.32	14.8	0.07	0.003	0.04	0.0042
	150	329	1.14	32	0.03	0.005	0.000	0.0142
9	20	–	–	–	–	–	–	0.0266
	67	–	–	–	–	–	–	0.0043
	150	–	–	–	–	–	–	0.0494
13	20	1.28	0.12	1.13	0.004	0.0005	0.007	–
	67	24.8	0.55	22.4	0.11	0.003	0.06	–
	150	50	0.98	52	0.05	0.01	0.007	–
24	20	1.58	0.04	1.41	0.003	0.0001	0.01	–
	67	24.3	0.12	22.5	0.15	0.002	0.01	–
	150	58	0.87	50	0.07	0.008	0.000	–
27	20	1.20	0.03	1.12	0.003	0.0001	0.007	–
	67	22.0	0.02	22.4	0.05	0.002	0.000	–
	150	67	0.81	43	0.26	0.07	0.07	–

Table 6. Quantity of some elements leached in OPC cement solution (percentage of the original amount present in the pellet)

Time interval (months)	Temperature (°C)	DUAGG						DUO_2
		Aluminum	Iron	Silicon	Titanium	Uranium	Zirconium	Uranium
1	20	0.019	0.005	0.005	0.0003	0.00003	0.000	0.0000
	67	0.27	0.007	0.19	0.0005	0.00003	0.0001	0.0001
	150	9.8	0.07	8.7	0.01	0.0005	0.000	0.0001
2	20	0.000	0.000	0.003	0.000	0.000	0.000	0.0000
	67	0.65	0.03	0.48	0.001	0.00007	0.0002	0.0000
	150	3.2	0.02	2.2	0.0001	0.00006	0.0002	0.0000
3	20	0.000	0.000	0.0008	0.000	0.000	0.000	0.0000
	67	0.45	0.05	0.40	0.002	0.00006	0.0002	0.0000
	150	1.9	0.05	1.1	0.0004	0.0001	0.0002	0.0001
6	20	0.000	0.04	0.03	0.001	0.00006	0.003	0.0006
	67	0.78	0.08	0.69	0.001	0.0001	0.003	0.0012
	150	0.4	0.000	0.000	0.000	0.000	0.000	0.0006
9	20	–	–	–	–	–	–	0.0001
	67	–	–	–	–	–	–	0.0003
	150	–	–	–	–	–	–	0.0005
13	20	0.03	0.02	0.03	0.001	0.00005	0.003	–
	67	2.22	0.01	2.24	0.000	0.0001	0.000	–
	150	28.2	0.20	25.4	0.01	0.0004	0.000	–
24	20	0.23	0.08	0.08	0.006	0.006	0.01	–
	67	0.97	0.02	1.07	0.0002	0.00007	0.002	–
	150	22.7	0.000	11.1	0.02	0.000	0.000	–
27	20	0.15	0.01	0.05	0.005	0.000	0.002	–
	67	3.85	0.01	4.06	0.001	0.00006	0.0005	–
	150	24.5	0.02	9.2	0.03	0.0007	0.002	–

Table 7. Quantity of some elements leached in BFS cement solution (percentage of the original amount present in the pellet)

Time interval (months)	Temperature (°C)	DUAGG						DUO_2
		Aluminum	Iron	Silicon	Titanium	Uranium	Zirconium	Uranium
1	20	–	–	–	–	–	–	0.0001
	67	–	–	–	–	–	–	0.0000
	150	–	–	–	–	–	–	0.0001
2	20	–	–	–	–	–	–	0.0000
	67	–	–	–	–	–	–	0.0000
	150	–	–	–	–	–	–	0.0000
3	20	–	–	–	–	–	–	0.0001
	67	–	–	–	–	–	–	0.0000
	150	–	–	–	–	–	–	0.0001
6	20	–	–	–	–	–	–	0.0002
	67	–	–	–	–	–	–	0.0007
	150	–	–	–	–	–	–	0.0032
9	20	–	–	–	–	–	–	0.0002
	67	–	–	–	–	–	–	0.0004
	150	–	–	–	–	–	–	0.0035
13	20	0.0000	0.008	0.000	0.002	0.000	0.000	–
	67	0.88	0.01	0.66	0.0002	0.00002	0.000	–
	150	4.19	0.01	3.66	0.0002	0.0001	0.002	–
20	20	0.18	0.05	0.15	0.003	0.0007	0.000	–
	67	1.27	0.000	1.69	0.0007	0.000	0.000	–
	150	2.21	0.000	3.26	0.02	0.000	0.000	–
24	20	0.15 0.26	0.08 0.09	0.14 0.14	0.004 0.004	0.0001 0.0002	0.000 0.004	–
	67	4.36 6.52	0.06 0.07	3.97 6.27	0.003 0.004	0.0002 0.0002	0.01 0.005	–
	150	2.25 5.69	0.02 0.05	4.80 3.40	0.05 0.02	0.0004 0.0002	0.01 0.02	–

3.2 RELEASE OF URANIUM FROM THE DUO_2 AGGREGATES

The graphs illustrating the release of uranium from the DUAGG pellets are presented in Figs. 4 and 5; the release from the high-fired DUO_2 is shown in Figs. 6 and 7. Even though the tests with DUO_2 did not last as long as those with DUAGG, the results allow some definitive conclusions.

3.2.1 The release of uranium is lower from DUAGG than from the DUO_2 pellet

This is the most important result in that under most conditions, an order of magnitude exists between DUAGG and DUO_2. In Table 8, the maximum amount of uranium leached from DUAGG and DUO_2 is reported, and an extrapolation of the release at 9 months for DUAGG is given. For example, in DI water, the maximum release of 0.40% was observed after 27 months at 150°C for DUAGG; for DUO_2, after 9 months of exposure, 0.9% was released at the same temperature. From the data collected, one can estimate that DUAGG released about 0.075% of uranium after 9 months of exposure at 150°C in DI water—about one order of magnitude lower than for DUO_2.

Table 8. Comparison of the maximum release of uranium in each conservation medium

	DUAGG	DUO_2
DI	0.40 % U released after 27 months at 150°C (~ 0.075 % released after 9 months)	0.90% U released after 9 months at 150°C
NaOH	0.07 % U released after 27 months at 150°C (~ 0.0075% released after 9 months)	~ 0.05% U released after 9 months at 150°C
OPC pore solution	0.007% U released after 27 months at 150°C (~ 0.0002% released after 9 months)	0.0005 % U released after 9 months at 150°C
BFS pore solution	0.0003 % U released after 24 months at 150°C (~ 0.0001 % released after 9 months)	0.0035 % U released after 9 months at 150°C

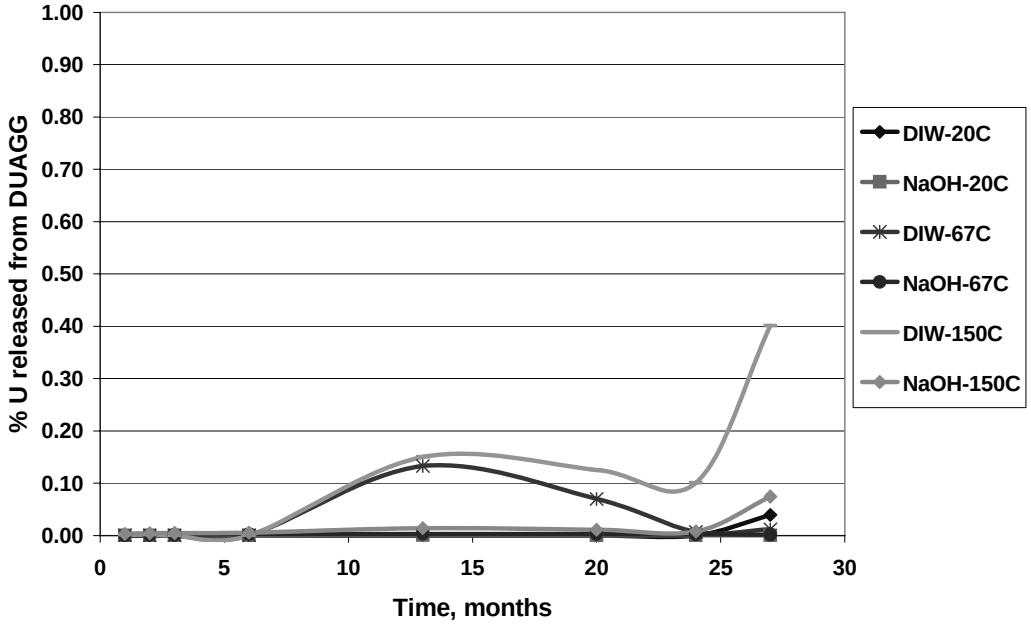

Fig. 4 :Fraction of uranium released from DUAGG kept in DI water and NaOH solution

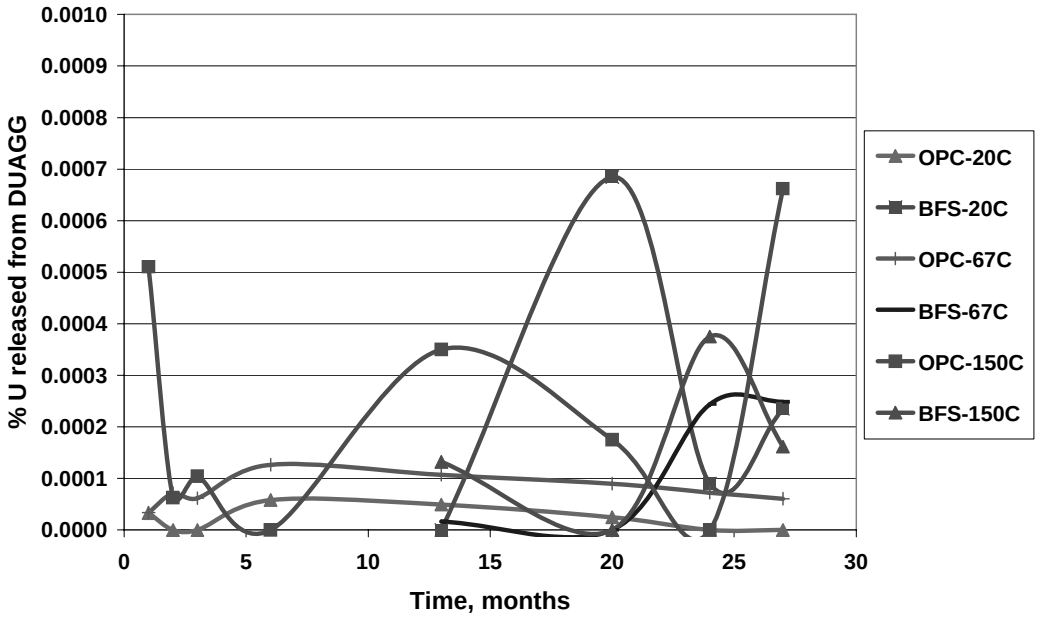

Fig. 5: Fraction of uranium released from DUAGG kept in OPC and BFS cement pore solutions

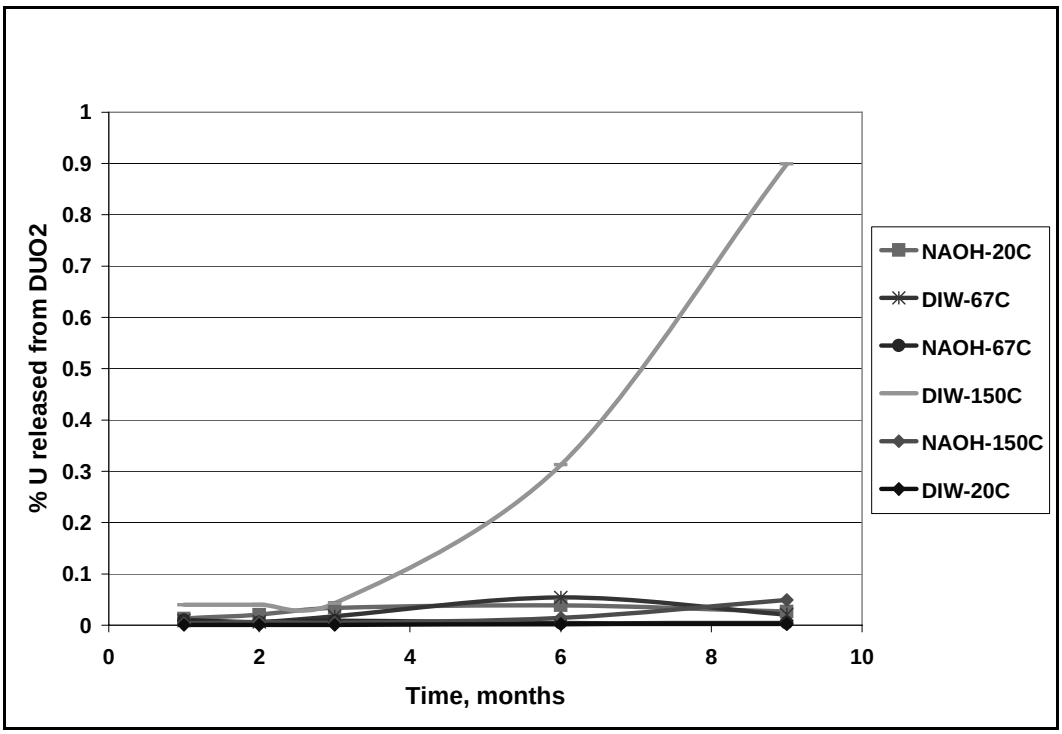

Fig. 6: Fraction of uranium released from DUO_2 kept in DI water and NaOH solution

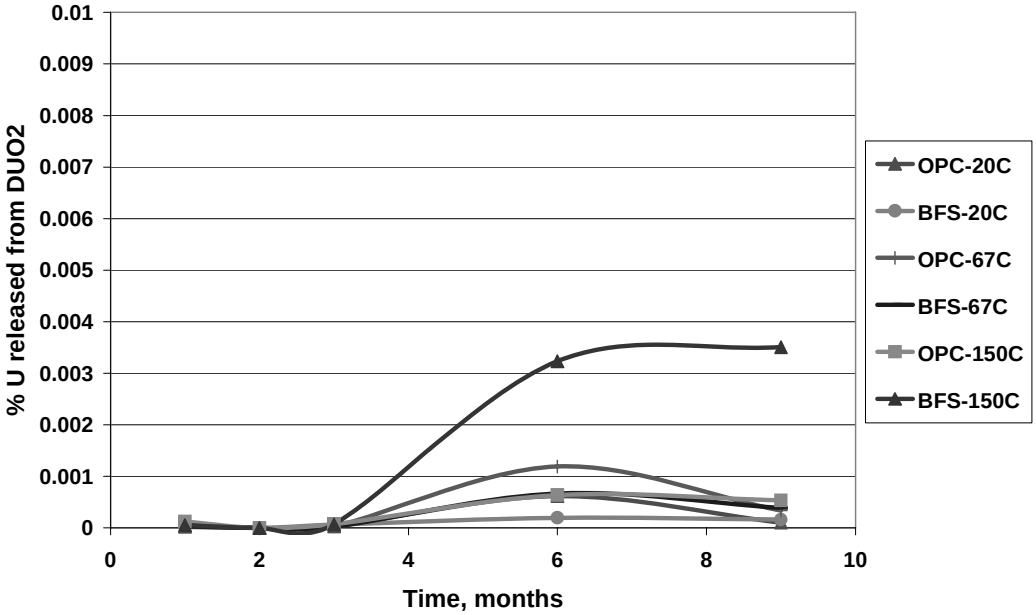

Fig. 7: Fraction of uranium released from DUO_2 kept in OPC and BFS cement pore solutions

3.2.2 The release of uranium increases when the temperature increases in almost all cases

In DI water this phenomenon is the most accentuated and occurs for both DUAGG and DUO_2. Because of the scarcity of the results (i.e., not enough material and equipment to prepare duplicate samples), it is not possible to see whether a common factor exists between temperatures. In OPC and BFS pore solutions, the phenomenon is not as important as in DI water, and a slight increase in the release occurs when the temperature increases. In an NaOH solution, the DUAGG release increases with the temperature, like for DI water; however, until DUO_2 has undergone 6 months of exposure, the release at 20°C is greater than the release at higher temperatures. After 9 months of exposure, the release at 150°C exceeds that at 20°C.

3.2.3 DI water is the worst solution when considering the inhibition of the release of uranium

The NaOH solution is next to the bottom in its ability to inhibit release of uranium. OPC and BFS cement pore solutions, respectively, are increasingly better at inhibiting release.

3.2.4 Cement pore solutions have a beneficial effect for both DUAGG and DUO_2 on the reduction of uranium release

For DUO_2 the maximum release was as much as 260 times lower in BFS and 750 times lower for OPC than in DI water. For DUAGG, the maximum release was as much as 600 times lower in BFS and 70 times lower in OPC than in DI water. This is very evident when comparing Figs. 4 and 6 with Figs. 5 and 7. For the DUAGG pellet, three orders of magnitude are measured between the DI water and NaOH compared to one order of magnitude for the cement pore solutions. For DUO_2 pellets, the difference is two orders of magnitude.

The release of uranium has been compared with data found in the literature for release rates of uranium from UO_2 or simulated nuclear fuel. The results of the release rates of uranium from the DUAGG pellet are presented in Table 9 and illustrated in Figs. 8 through 10. The release rate was calculated as follows:

$$R(mg \bullet m^{-2} \bullet day^{-1}) = \frac{U(mg \bullet L^{-1}) \bullet V(L)}{SA(m^2) \bullet D(day)} \qquad (2)$$

where U is the concentration of uranium in the leachate, V is the volume of leachant, SA is the geometric surface area of the DUAGG pellet, and D is the duration of the leach period. The measurement of the surface area was made in a very crude way, and the error associated with this value is high. Also, especially for the DUAGG pellet, the surface of the pellet was very rough, and the calculation assumed the surface was plane and without

Table 9: Uranium release rates ($mg \bullet m^{-2} \bullet d^{-1}$) obtained for DUAGG and high-fired DUO_2

Time interval (months)	Temperature (°C)	DI Water		NaOH		OPC		BFS	
		DUAGG	DUO_2	DUAGG	DUO_2	DUAGG	DUO_2	DUAGG	DUO_2
1	20	0.065	2.9	0	68	0.10	0.12	-	0.35
	67	0.14	47	0	51	0.10	0.32	-	0.16
	150	3.7	208	9.4	20	1.50	0.64	-	0.30
2	20	0.012	1.9	0	54	0	0	-	0
	67	0.23	17	0.92	15	0.10	0	-	0
	150	2.4	106	6.6	16	0.09	0	-	0
3	20	0	1.1	0	59	0	0.05	-	0.11
	67	0	30	1.08	15	0.06	0.05	-	0.05
	150	0.044	75	4.6	9	0.10	0.13	-	0.12
6	20	0	1.8	0.02	34	0.03	0.54	-	0.17
	67	0	48	1.30	3.7	0.06	1.05	-	0.59
	150	0.006	274	2.7	12	0	0.56	-	2.84
9	20	-	1.3	-	16	-	0.06	-	0.09
	67	-	12	-	2.5	-	0.20	-	0.23
	150	-	526	-	29	-	0.31	-	2.05
13	20	0.046	-	0.12	-	0.01	-	0	-
	67	30	-	0.70	-	0.02	-	0.004	-
	150	34	-	3.2	-	0.08	-	0.03	-
20	20	-	-	-	-	-	-	0.10	-
	67	-	-	-	-	-	-	0	-
	150	-	-	-	-	-	-	0	-
24	20	0.005	-	0.02	-	0.69	-	0.01/0.03	-
	67	0.9	-	0.27	-	0.01	-	0.03/0.03	-
	150	12	-	1.0	-	0	-	0.05/0.02	-
27	20	3.8	-	0.01	-	0	-	-	-
	67	1.3	-	0.17	-	0.01	-	-	-
	150	44	-	8.1	-	0.07	-	-	-

defect. This implies that the release rate is probably lower than the calculation of R indicates.

The work of Thomas and Till [8] was very similar to our project, except that the duration of the tests they performed was limited to 8 days. They found a release rate of 5 $mg \bullet m^{-2} \bullet day^{-1}$ for uranium when UO_2 was kept in DI water at 70°C. In our work, after 1 month of exposure at 67°C in DI water, the amount of uranium released from the DUAGG was found to be only 0.25 $mg \bullet m^{-2} \bullet day^{-1}$, which is 20 times less than reported for the 8-day study.

Jégou [26] studied the alteration of clad spent fuel in groundwater at room temperature and calculated a rate of fuel dissolution in the range of 1 to 2 $mg \bullet m^{-2} \bullet d^{-1}$. He cited the work of Forsyth[18, 19], who obtained a range of 0.6 to 6 $mg \bullet m^{-2} \bullet d^{-1}$. Our work with DUO_2 pellets at 20°C in DI water also falls in the range of 1 to 2 $mg \bullet m^{-2} \bullet d^{-1}$. Interestingly, the results obtained with DUAGG under the same conditions were at least two orders of magnitude lower. The combination of uranium and basalt release results in the difference species (uranium, aluminum, silicon, iron, titanium, and zirconium) competing for interaction with the solution species. The mechanisms will not be explained in this report; only the measured combined effect is presented. This comparison provides strong evidence that the basalt phase effectively protects the UO_2 (Some of this protection may be physical protection as the basalt coats the UO_2). A comparison among different studies is presented in Table 10.

Table 10. Comparison of uranium release rate with data from the literature

Wronkiewicz [7] - 90°C	0.1 to 15 mg•m^{-2}•day^{-1} in EJ-13 silica bicarbonate simulated groundwater
Thomas and Till [8]	5 mg•m^{-2}•day^{-1}in granite groundwater and WN-1 simulated saline groundwater
Jegou [26] - 25°C	1-2 mg•m^{-2}•d^{-1}
This study DUO_2 - 20°C	1.1 to 2.9 mg•m^{-2}•d^{-1} in DI water 0 to 0.54 mg•m^{-2}•d^{-1} in cement pore solutions
This study DUO_2 - 67°C	12 to 48 mg•m^{-2}•d^{-1} in DI water 0 to 1.05 mg•m^{-2}•d^{-1} in cement pore solutions
This study DUAGG - 20°C	0 to 0.0065 mg•m^{-2}•d^{-1} in DI water (higher value of 3.8 probably an outlier) 0 to 0.10 mg•m^{-2}•d^{-1} in cement pore solutions (higher value of 0.69 probably an outlier)
This study DUAGG - 67°C	0 to 1.3 mg•m^{-2}•d^{-1} in DI water (value at 30 is probably an outlier) 0 to 0.10 mg•m^{-2}•d^{-1} in cement pore solutions

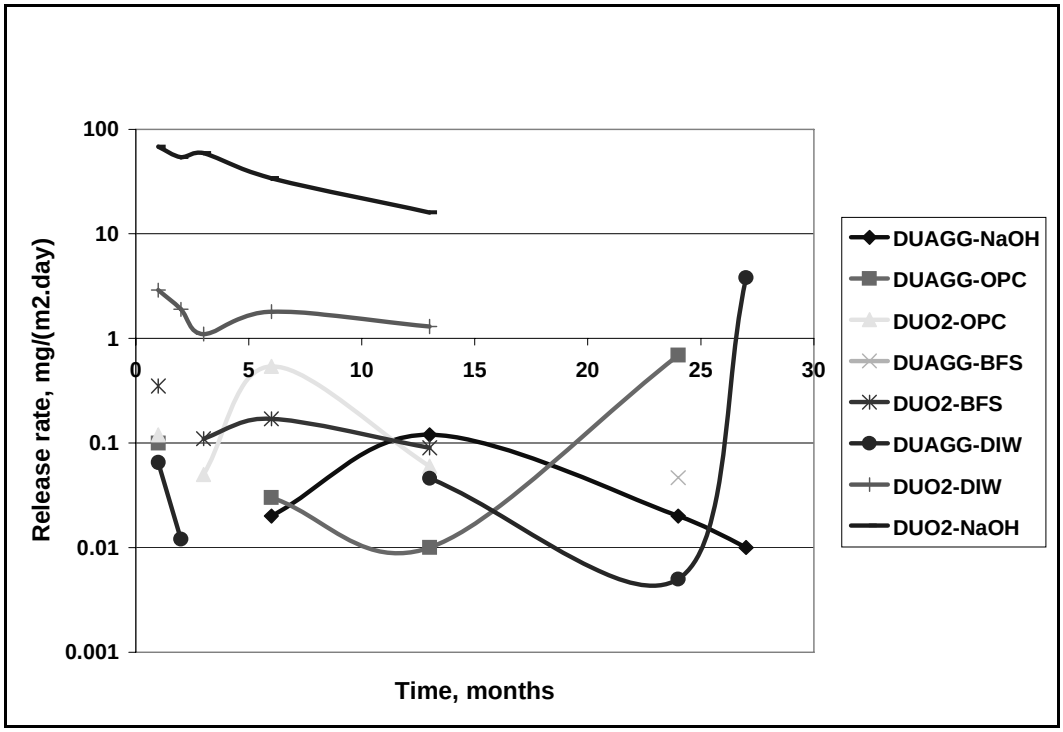

Fig. 8: Release rate of uranium at 20°C

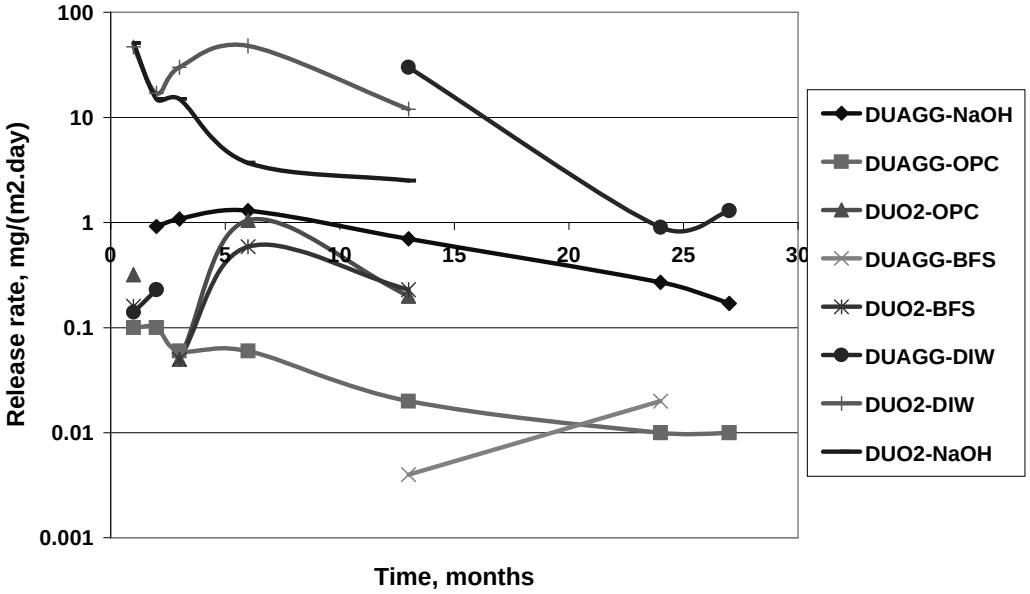

Fig. 9: Release rate of uranium at 67°C

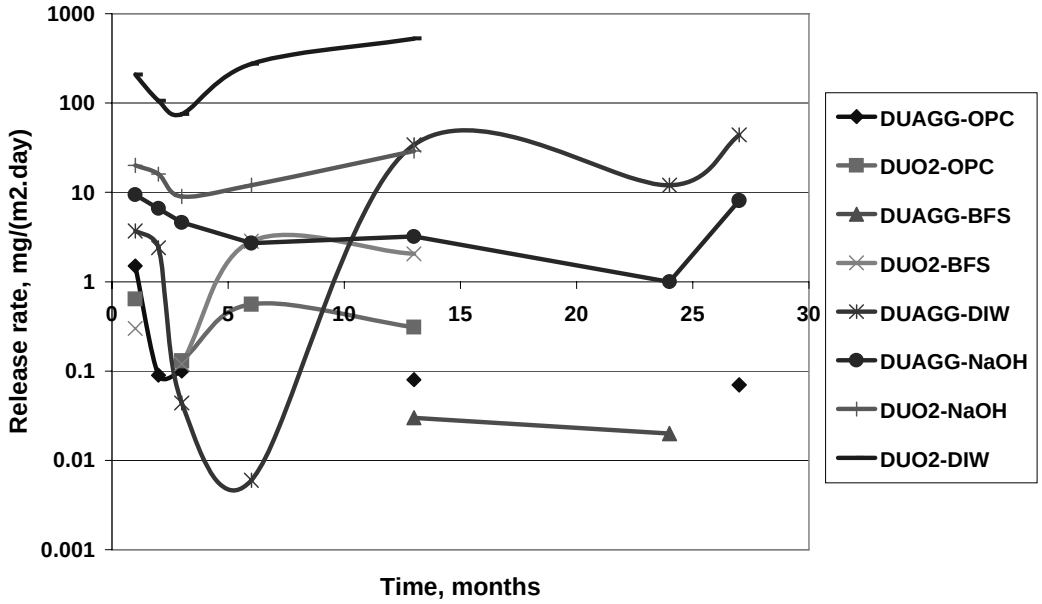

Fig. 10: Release rate of uranium at 150°C

3.3 RELEASE OF THE BASALT COMPONENTS FROM DUAGG

The basalt phase in DUAGG represents only a minor part of the aggregate, about 9 wt % of the mass of the pellet. The release of silicon, aluminum, iron, titanium, and zirconium is illustrated in Figs. 11 through17. The release of each of these glass components was very different, depending upon the leaching solution they were exposed to. As much as ~54 wt % silicon was released from a DUAGG pellet while zirconium did not exceed 0.30 wt %.

For aluminum and silicon, the most aggressive media were the 1 *N* NaOH solution and the DI water. The release was also more pronounced at higher temperatures for these two solutions. In the NaOH solution, the concentration of aluminum and silicon in the leachate increased rapidly for the first 3 months of cure, after which the increase was slower. After 1 year at 150°C, about 50 wt % of the initial aluminum and silicon was measured in the leachate. The changes observed after 1 year are different for the two elements; silicon remained around 50% with perhaps a small decrease, and aluminum appeared to increase slightly. The same pattern was observed for the samples kept at 67°C in NaOH, with the maximum amount leached being around 25 wt % (about half the amount released at 150°C). At 20°C, the amount of silicon and aluminum released was between 1 and 2 wt %.

In DI water, the same pattern of release was found, but instead of aluminum and silicon being about the same amount, silicon appeared to be leached two times more than aluminum. In DI water at 150°C, the maximum release for silicon is at 13 months with ~15 wt % while aluminum is ~7 wt %. At 67°C, the maximum silicon is ~5 wt % while the maximum aluminum is only ~3 wt %. At 20°C, the amount of silicon and aluminum released is very small or none, except for one point at 27 months for aluminum (0.58 wt %).

In cement pore solutions, the release of silicon and aluminum is completely different and much lower than for the other solutions (see Figs. 9 and 11). In OPC pore solution, a fast release occurs; up to ~10% of aluminum and silicon are measured after 1 month. This amount decreased to nearly zero over a period of 6 months; then a large increase (about 25%) is measured at 13 months, and this was followed by another decrease. After 2 years, the release of aluminum was about 20–25%; for silicon it was only around 10%. The variation (up and down) in the leach rate could be caused by the inhomogeneity of the particular samples, or it could have occurred for reasons that we cannot explain at this time based on the resources we had available for the experiment. At 67°C, the release of aluminum and silicon did not exceed 4%. At 20°C, the amount of aluminum released did not exceed 0.2%, and the amount of released silicon was even less. The mixture of OPC and BFS gave even better results; the releases measured at 67 and 150°C were around or less than 5%.

The release of iron was found to be moderate with a maximum amount leached of ~6% in DI water at 150°C. DI water and the NaOH solution are the worst media when considering iron leaching from DUAGG.

Titanium and zirconium appear to be quite stable under all the conditions tested and only very small amounts were leached (less than 0.3% was measured). This could indicate that the basalt glass is not really homogeneous and that some crystalline compounds are present within the glassy phase.

The topic of basaltic glass alteration has been studied extensively since basalt is a natural analogue for nuclear waste glass. All the papers reviewed showed that, after the initial release, the dissolved elements from the basalt increase in the solution and start precipitating. The alteration products form a film around the surface of the sample that slows the release rate considerably. Techer [34] reports four orders of magnitude from the initial maximum rate. The film forms a protective coat that prevents the migration of the mobile species from the glass. In the case of DUAGG, the release rate of uranium is also reduced, as was expected by the developers of this material. The presence of such a protective film in DUAGG was observed by scanning electron miscroscope (SEM).

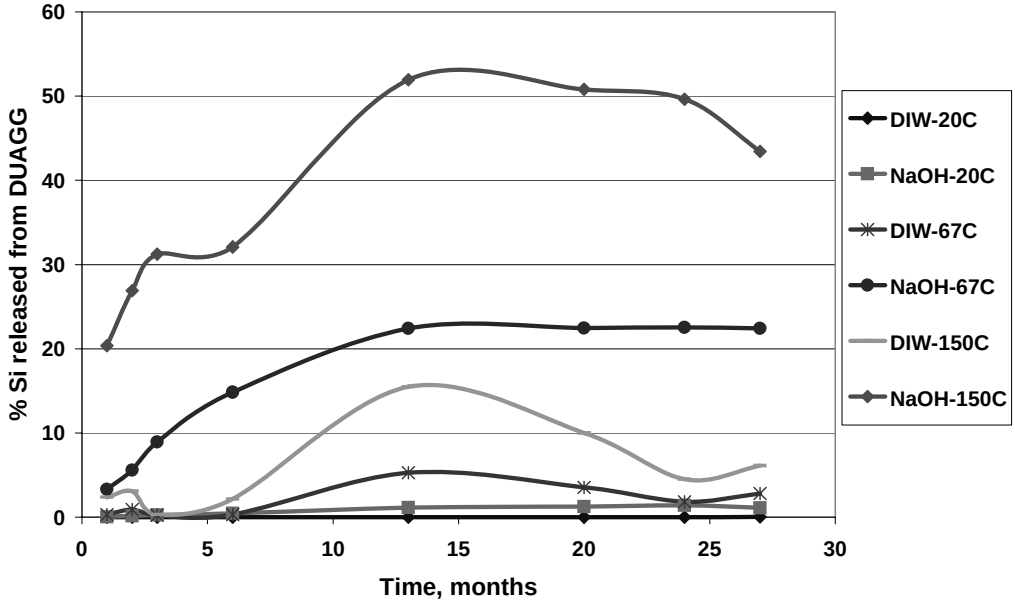

Fig. 11: Fraction of silicon released from DUAGG kept in DI water and NaOH solution

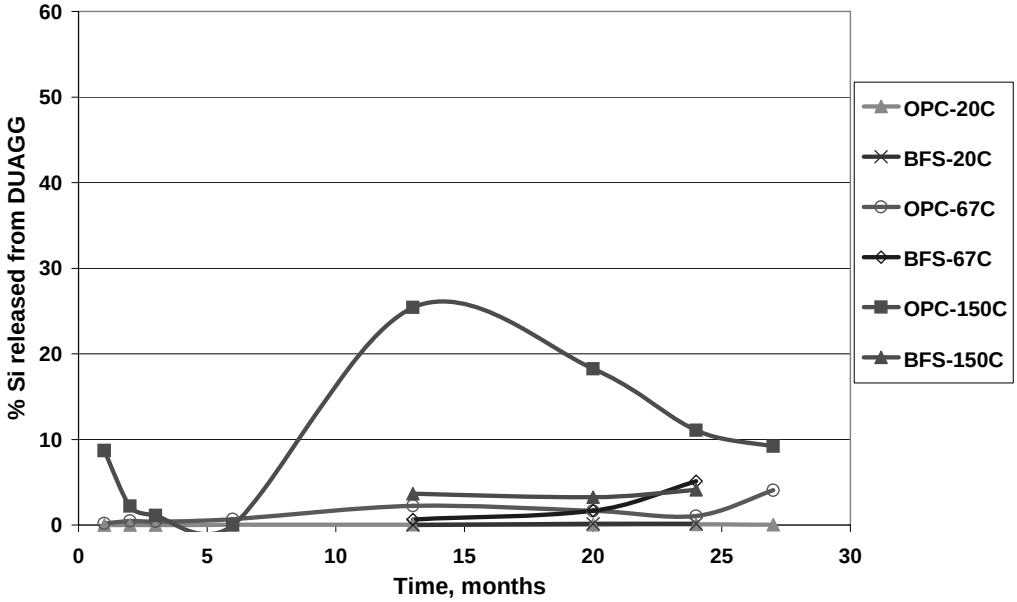

Fig. 12: Fraction of silicon released from DUAGG kept in OPC and BFS cement pore solutions

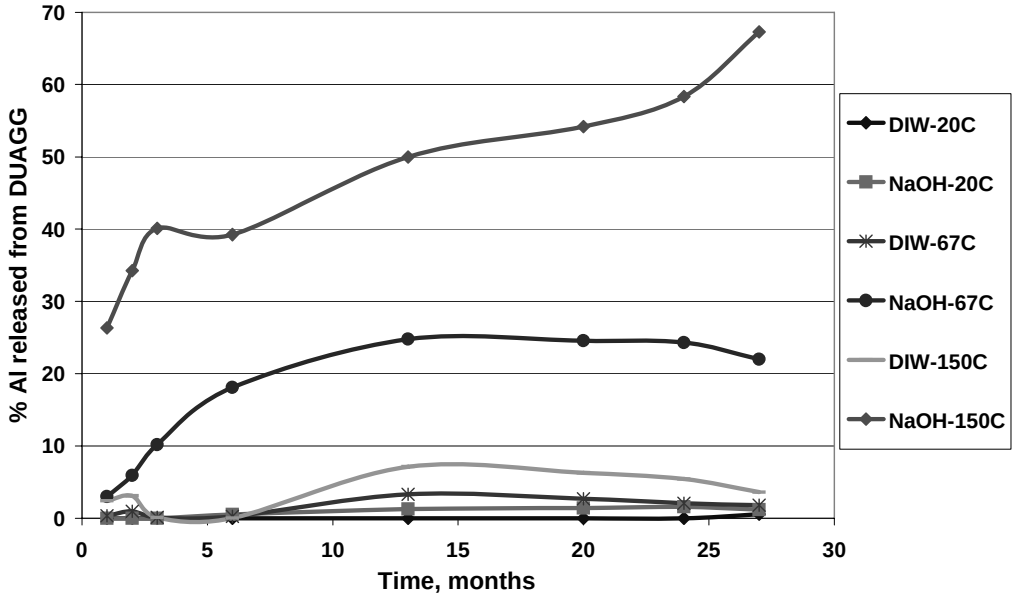

Fig. 13: Fraction of aluminum released from DUAGG kept in DI water and NaOH solution

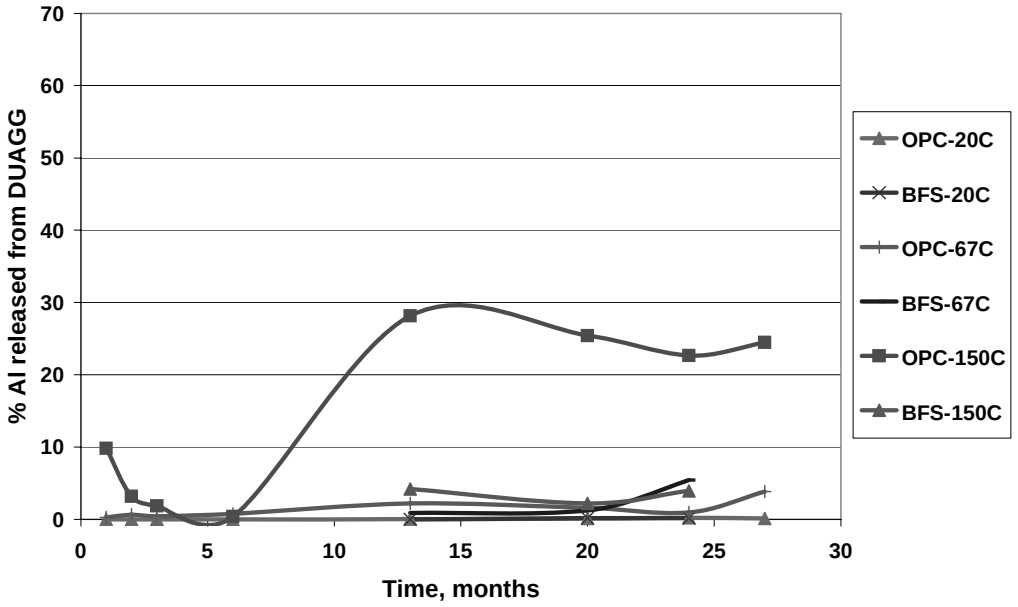

Fig. 14: Fraction of aluminum released from DUAGG kept in OPC and BFS cement pore solutions

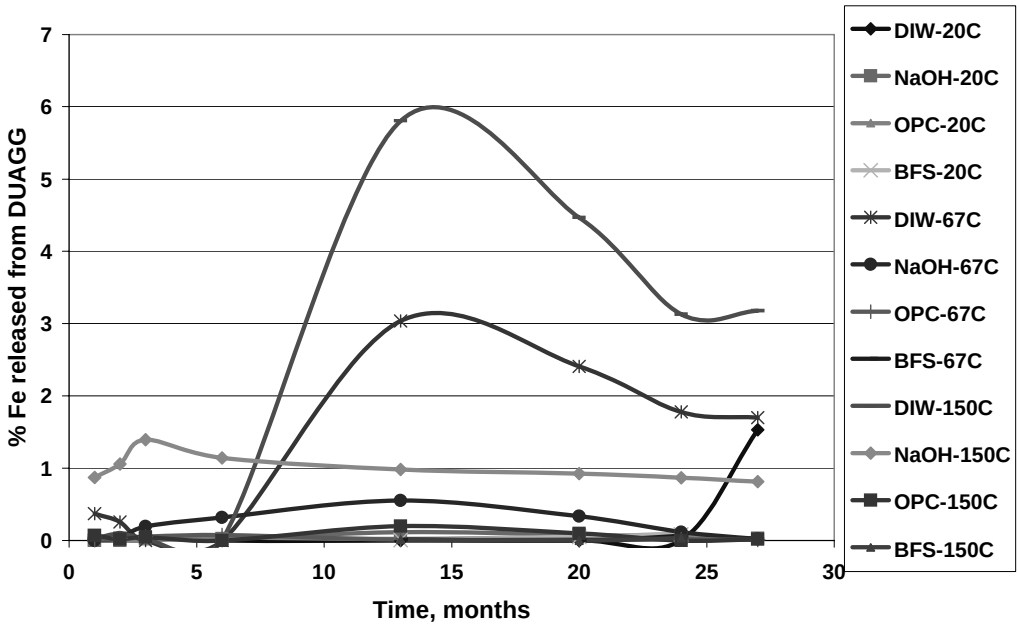

Fig. 15: Fraction of iron released from DUAGG

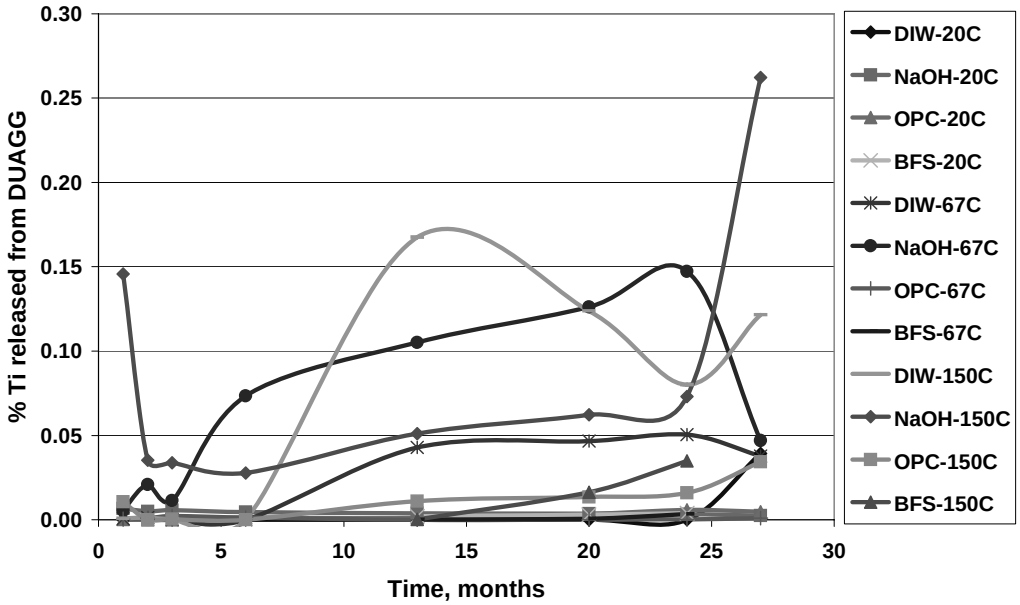

Fig. 16: Fraction of titanium released from DUAGG

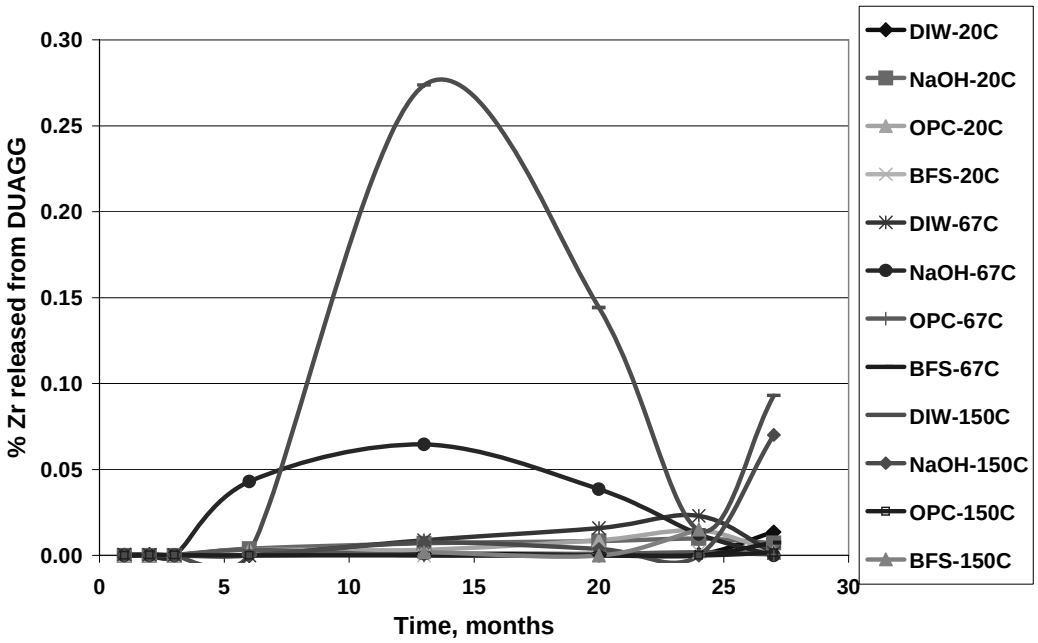

Fig. 17: Fraction of zirconium released from DUAGG

3.4 SEM EXAMINATION OF THE PELLETS

In order to determine whether any deleterious phases were formed, the surfaces of the DUAGG samples at 2, 3, 6, 13, and 27 months of exposure were examined by SEM equipped with EDX. For the high-fired DUO_2 pellets, the samples collected after 9 months of exposure were examined. Each pellet of DUAGG or DUO_2 was cut in the center into two pieces: one piece was the outside surface of the pellet and the other was a fractured piece, allowing a view of the profile from the outside surface to the center of the pellet. These two fragments were coated with a film of carbon to render the surface conductive to electrons and were then examined by SEM.

3.4.1 High-fired DUO_2 pellets

3.4.1.1 NaOH solution

Some representative pictures for these samples are found in Figs. 18, 19, and 20. At 20°C, the outside of the pellet does not show any change from the original morphology. No deposits or alterations are visible except a possible increase of the porosity of the outside layer as seen on the backscattered picture (Fig. 18B). The top surface of the pellet that has recrystallized on the cylinder shows some alteration of DUO_2 grains (Fig. 18D).

The fracture reveals the presence of an alteration zone (Fig. 18C) that is marked by the breakage of the uranium grains along the grain sides. The nonattacked zone shows uranium grains broken inside the grain itself. This is illustrated in Figs. 18E and F, where the individual grains of UO_2 are visible near the outside of the recrystallized pellet on the surface of the cylinder (Fig. 18E) while toward the center of the cylinder, no grain boundary is recognizable (Fig. 18F); the individual grains are still well joined to each other.

At 67°C, the alteration is more pronounced. The outside surface of the pellet (Figs. 19 E and F) shows that DUO_2 has recrystallized onto the sufrace of the cylinder. The fractured cylinder shows an outside layer with a depth of ~1 μm (Figs. 19C and D) made from recrystallized UO_2 crystals, probably schoepite. Locally, on the outside surface, there are greater zones of alteration (Figs. 19A and B). The corrosion is also visible by the appearance of the grains contours (Fig. 19C).

At 150°C, the recrystallized UO_2 on the outside of the pellet resemble dehydrated schoepite crystals (Figs. 20A, B, and C). The outside layer is wider than at 67°C, with a thickness close to 5 μm. The grain corrosion is even more accentuated than at 67°C (Figs. 20D and F).

3.4.1.2 DI water

After 9 months at 20°C, the outside surface of the pellet is corroded and the DUO_2 grains appear pitted, especially on top of the sample (Fig. 21B). Some grain corrosion is visible on the top surface (Fig. 21B). The alteration on the fracture is not very visible (Figs. 21C and D). No recrystallization of DUO_2 is visible at this temperature.

At 67°C, the corrosion is especially visible on the outside surface of the pellet. Most of the UO_2 grains that have recrystallized on the side of the cylinder appear to be cracked and altered (Figs. 22A and B). The fractured pellet shows pitting and cracks (Figs. 22 C and E).

At 150°C, the grain corrosion is extreme on the outside surface of the recrystallized pellet (Figs. 23A and B). The uranium grains are pitted and cracked (Fig. 23C). Locally, on the outside surface of the recrystallized pellet, some crystals of dehydrated schoepite (Fig. 23A) are visible. The fracture showed individual grains that are ready to detach from the pellet (Figs. 23D and E). This illustrates the progression of the corrosion process: the areas around the grains are attacked by the solution. The grains become detached from the material, and then the solution gains access to new grains further inside of the pellet and continues the corrosion process.

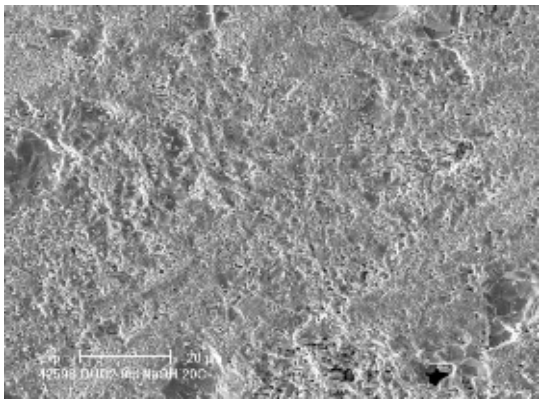

18A: Side of the cylinder-secondary electrons

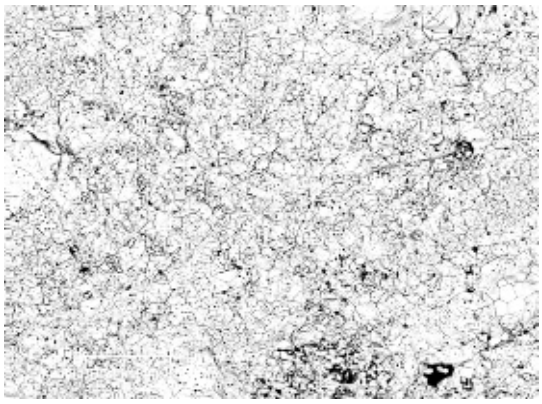

18B: Same area in backscattered electrons

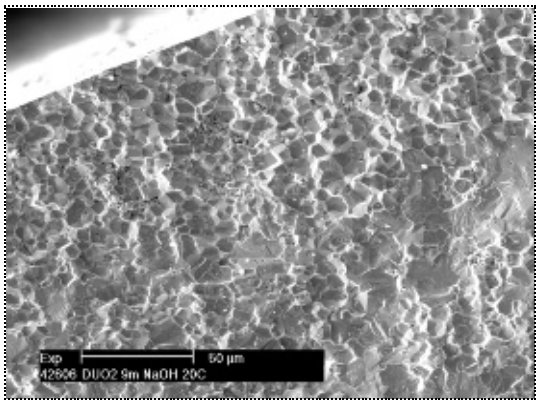

18C: Alteration zone visible on a fracture with a depth of 50-100 µm

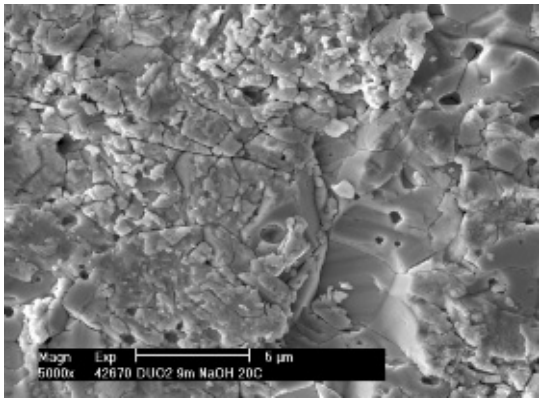

18D: View of the top of the cylinder

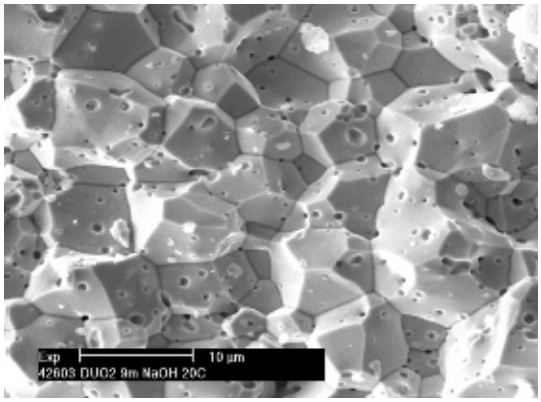

18E: DUO_2 grains near the outside surface of the cylinder

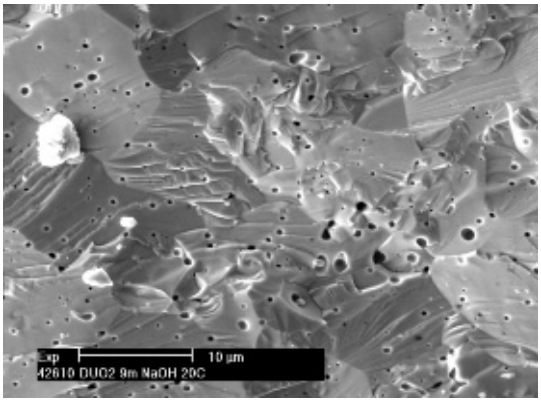

18F: DUO_2 grains at the center of the cylinder

Fig. 18: SEM pictures of DUO_2 cylinder kept in NaOH solution at 20° C for 9 months

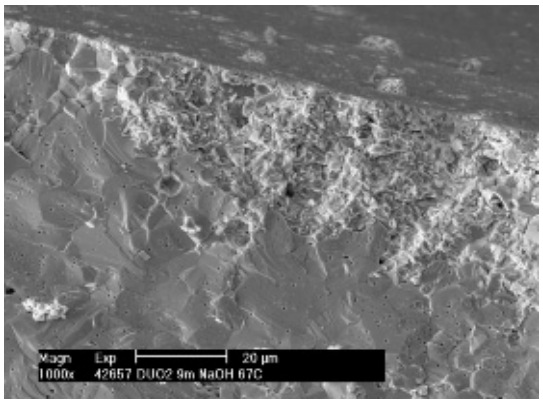

19A: Fracture of the cylinder - DUO_2 has recrystallized on the outside of the cylinder

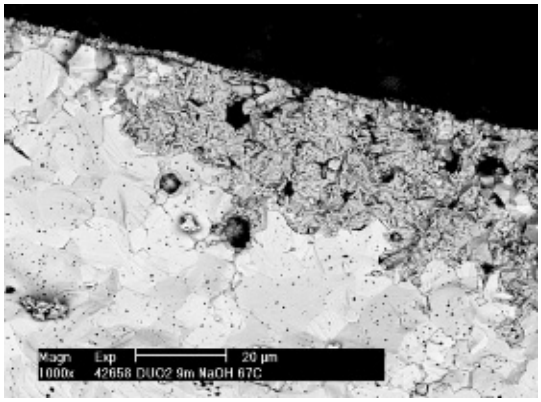

19B: Same area in backscattered electrons - the recrystallization area is porous

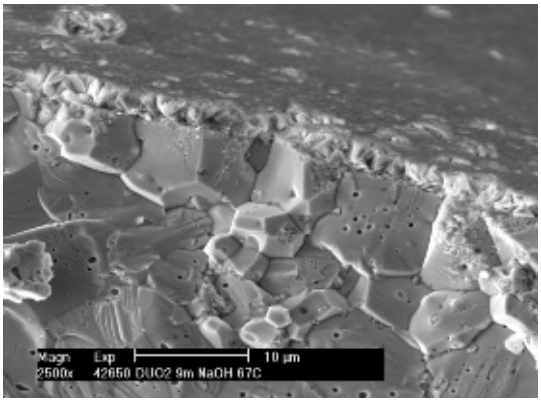

19C: Fracture of the cylinder - DUO_2 recrystallized at the surface of the cylinder

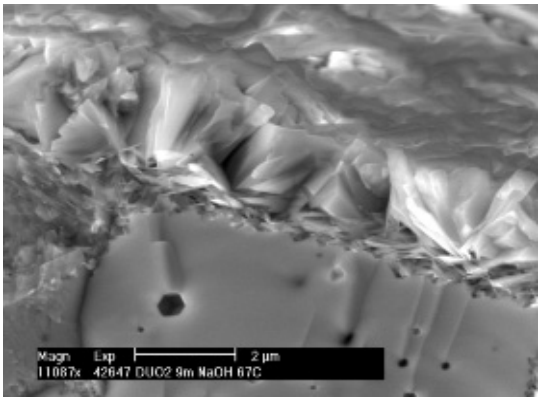

19D: Detail of the recrystallization products

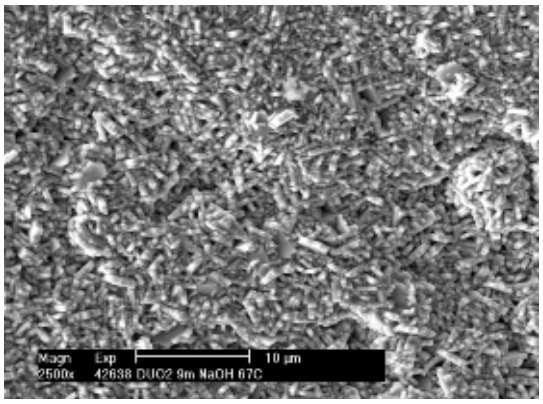

19E: Side of the cylinder - DUO_2 recrystallized - secondary electrons

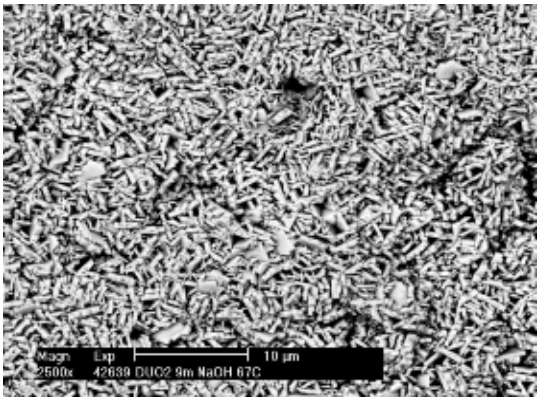

19F: Same area in backscattered electrons

Fig. 19: SEM pictures of DUO_2 cylinder kept in NaOH solution at 67° C for 9 months

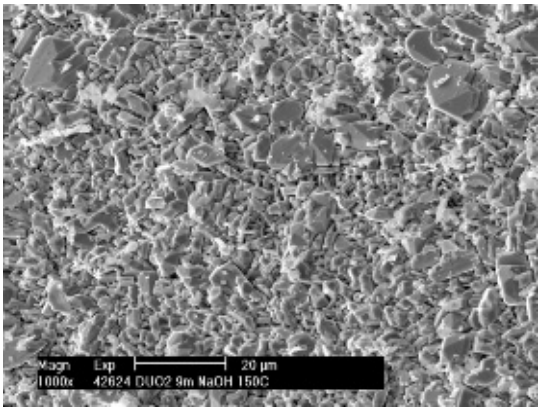

20A: Side of the cylinder - recrystallization of DUO_2

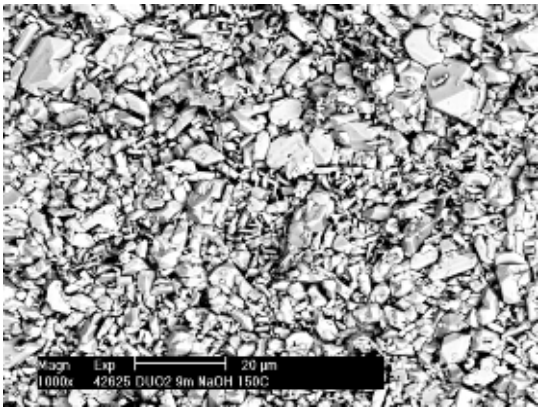

20B: Same area in backscattered electrons

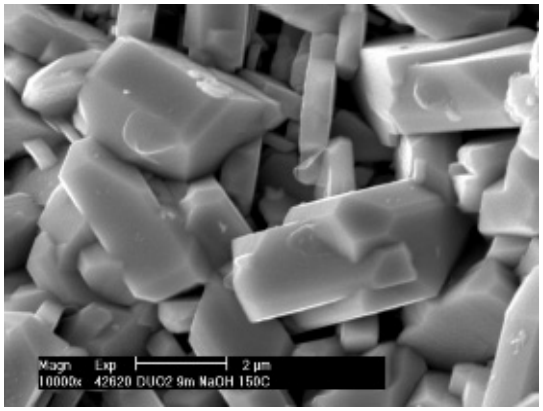

20C: Detail of the new DUO_2 crystals

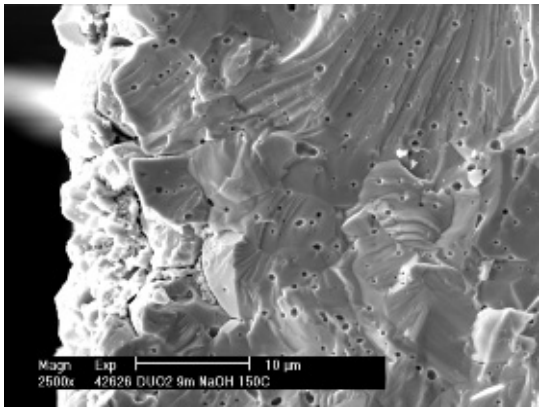

20D: Fracture - the DUO_2 grains are eroded from the surface

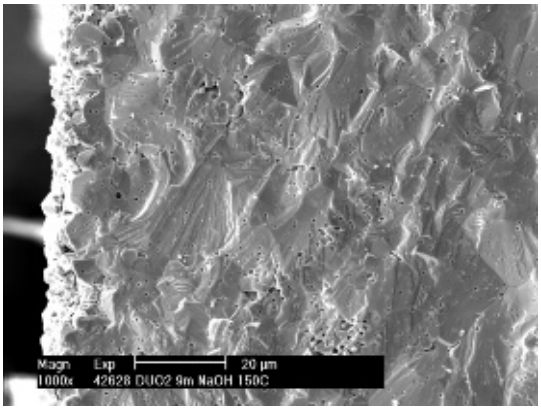

20E: The surface shows signs of erosion

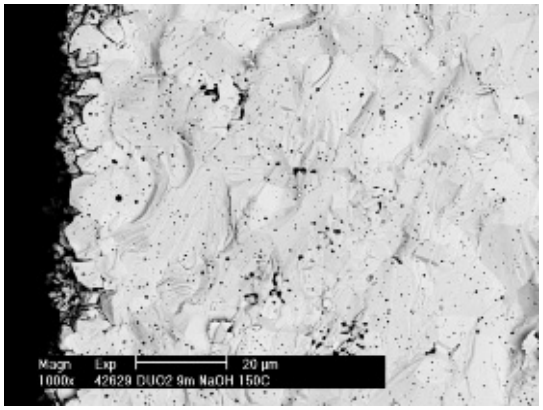

20F: Same area in backscattered electrons

Fig. 20: SEM pictures of DUO_2 cylinder kept in NaOH at 150° C for 9 months

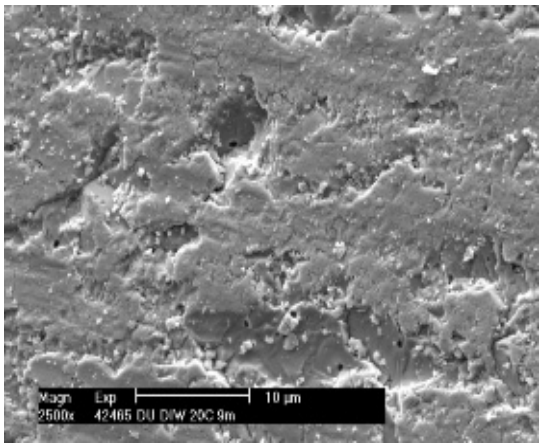

21A: Side of the cylinder

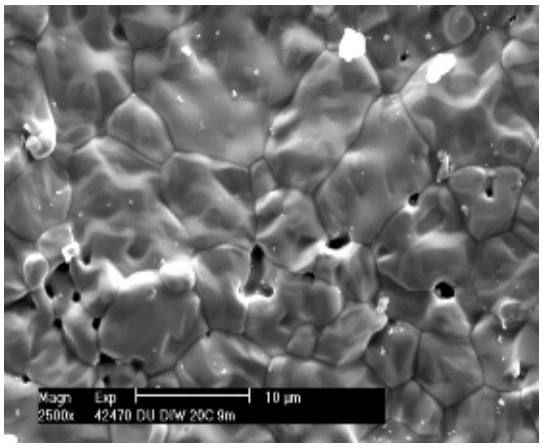

21B: Top of the cylinder

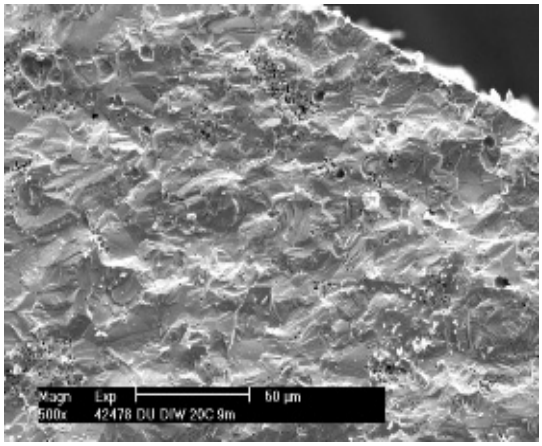

21C: Fracture of the cylinder

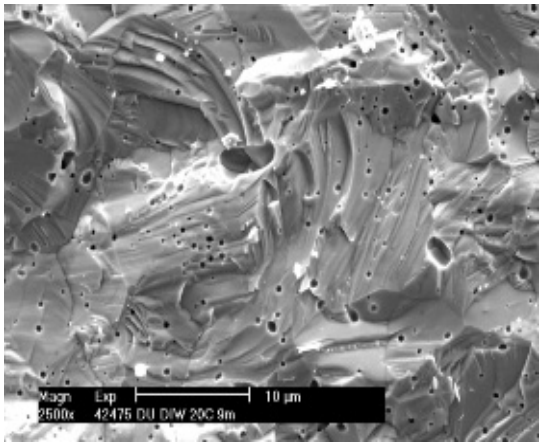

21D: Fracture of the cylinder

Fig. 21: SEM pictures of DUO_2 cylinder kept in DI water at 20° C for 9 months

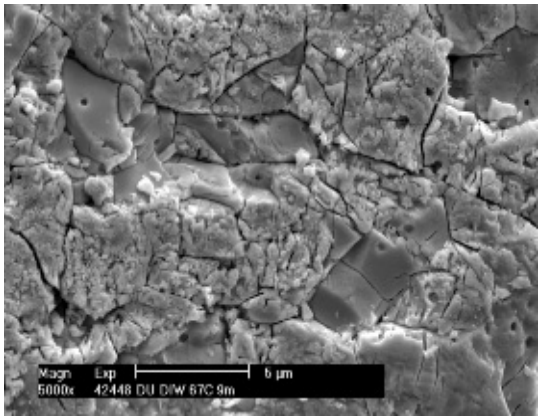

22A: Side of the cylinder

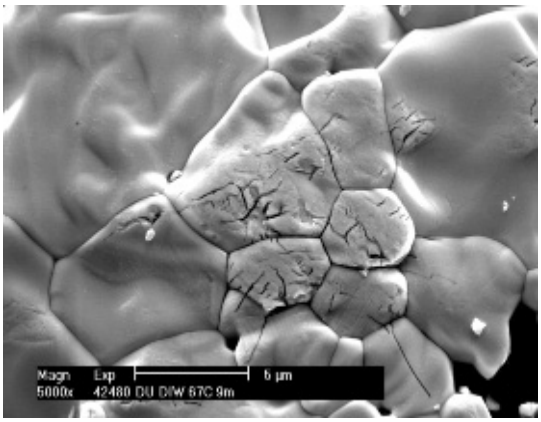

22B: Top of the cylinder

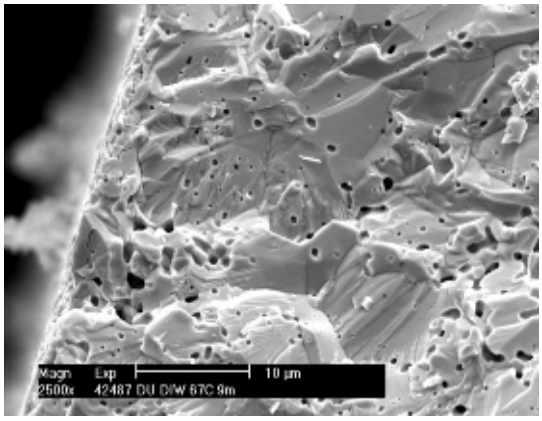

22C: Fracture - secondary electrons

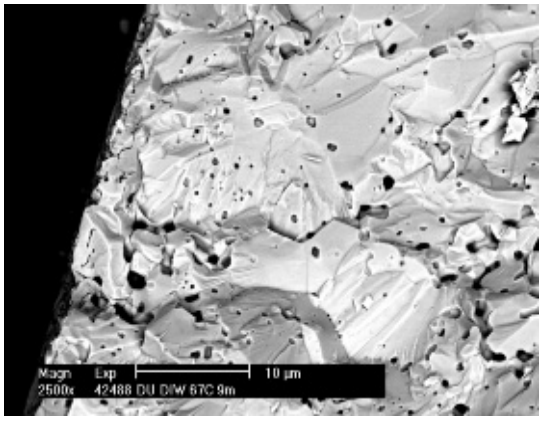

22D: Same area - backscattered electrons

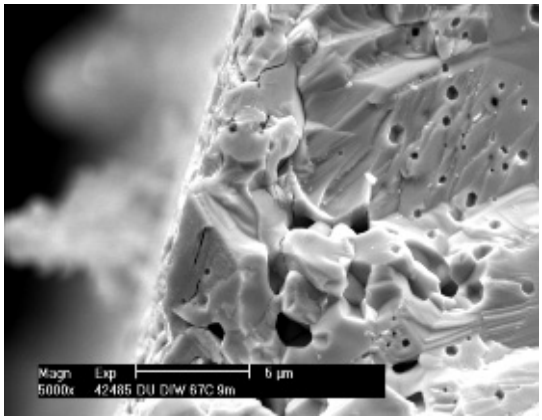

22E: Detail of 22C - secondary electrons

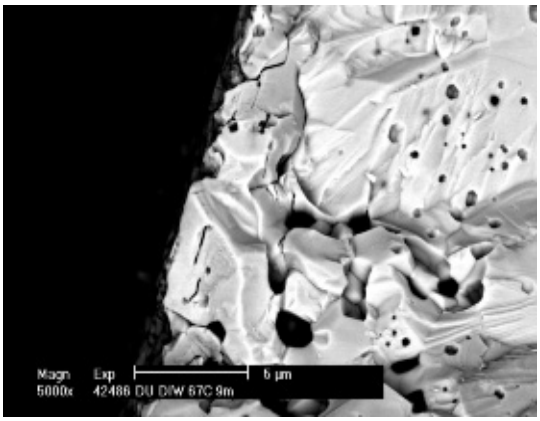

22F: Same area - backscattered electrons

Fig. 22: SEM pictures of DUO_2 cylinder kept in DI water at 67° C for 9 months

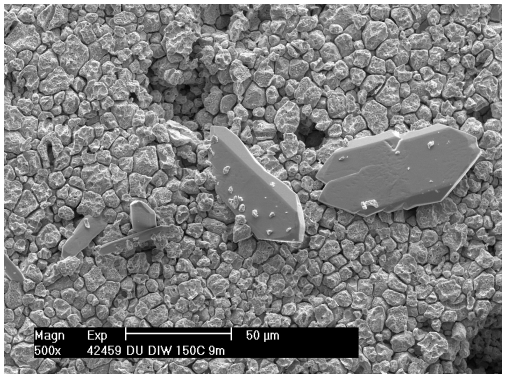

23A: Side of cylinder showing large recrystallized uranium crystals

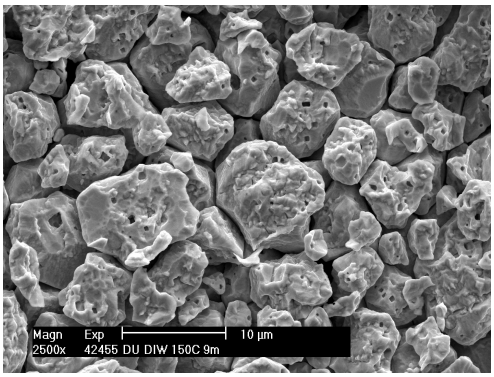

23B: Side of cylinder - external layer of DUO_2 grains do not have much cohesion

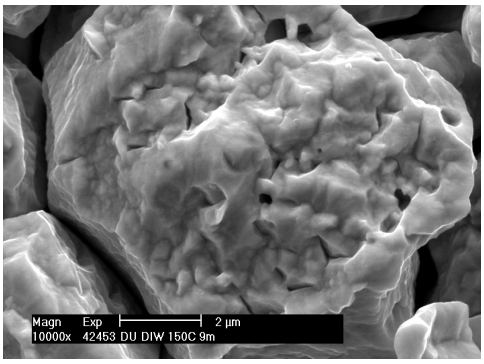

23C: Detail of a DUO_2 grain showing alteration of its surface

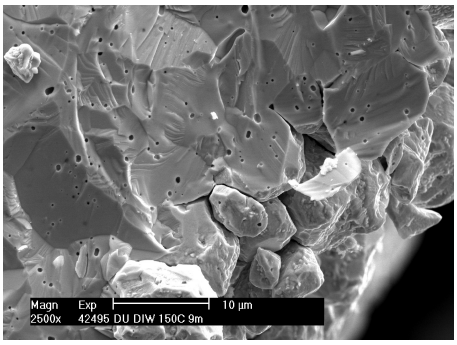

23D: Fracture - DUO_2 grains are detaching

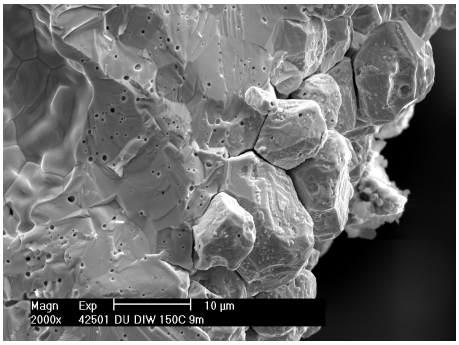

23E: Fracture - secondary electrons

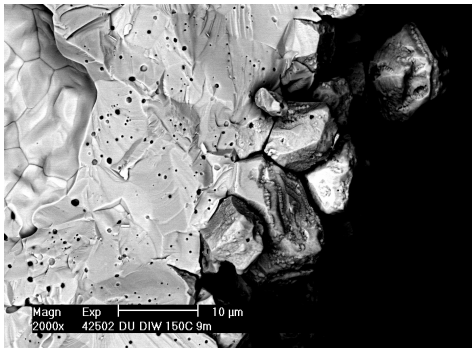

23F: Same area - backscattered electrons

Fig. 23: SEM pictures of DUO_2 cylinder kept in DI water at 150°C for 9 months

3.4.1.3 BFS cement pore solution

The SEM observations are very similar for both cement pore solutions. In BFS cement pore solution after 9 months at 20°C, the outside of the cylinder shows recrystallization of calcium carbonates or calcite (Figs. 24A and B). These crystals are present as an agglomeration of crystals or are found isolated (Fig. 24C). These crystals of calcite do not form a continuous layer; in backscattered electron images, the uranium is visible (Fig. 24B). The fracture of the pellet reveals that the uranium grains are not corroded (Figs. 24D and E). The grain boundaries are not visible, confirming the nonalteration of the pellet.

At 67°C, the amount of calcite appears to be larger than at 20°C. On the side of the pellet, some agglomerations of crystals are also seen (Fig. 25A). The top of the cylinder is locally covered with a thick layer of calcium carbonate (Fig. 25B), but at other places, the crystals of calcite are not abundant (Fig. 25C). The fracture of the cylinder shows that the pellet is not damaged at all (Figs. 25D and E). The contour of the side of the cylinder is almost perfect (Fig. 25E), indicating that the outside layer of DUO_2 grains is not altered at all. Locally, the deposits of calcite can be quite thick (Fig. 25F).

At 150°C, some alteration is visible on top of the cylinder, where the surfaces of some grains show the beginning of etching (Fig. 26A). The outside surface of the pellet shows that the UO_2 has been attacked (Fig. 26B), with some recrystallized uranium phases being formed. The fractured sample shows more cracks than in the samples at the lower temperatures (Figs. 26C and E). The calcite crystals are visible (Fig. 26C). The grain contours are locally visible (Figs. 26E and F), indicating alteration. Some pockets of altered grain are also found within the pellet near the surface (Fig. 26E).

3.4.1.4 OPC cement pore solution

The outside surface of the cylinder appears in very good shape at 20°C (Figs. 27A and B). The backscattered picture (Fig. 27B) especially shows a uniform white background of noncorroded uranium oxide. Crystals of calcium carbonate (Figs. 27A and C) are locally present on the outside surface in contact with the solution. The top of the cylinder (Fig. 27C) does not show pitting or cracking of the grains. The fracture reveals that no corrosion exists inside the cylinder. The outside layer of carbonates is about 5 μm thick. There is no grain corrosion (Fig. 27E), and the border, as seen on the backscattered picture (Fig. 27F), is perfectly intact.

The same conclusions can be made for the sample kept at 67°C. The crystals of calcium carbonate are more abundant on the outside of the cylinder, and they crystallized in a different shape than at 20°C (Figs. 28 A and C). The uranium grains underneath are not

very visible under the carbonate deposits (Fig. 28B). The fracture showed that the thickness of the calcium carbonate layer is about 5 μm. The uranium grains are in perfect condition inside of the cylinder (Figs. 28D, E, and F).

At 150°C, the outside surface of the pellet shows some calcium carbonate crystals, but some deposits are masking the grain contours (Fig. 29A). The top of the cylinder shows some slight grain corrosion (Fig. 29B). The layer of carbonate on the fractured sample is not uniform as it was for 67°C, but the uranium grains appear intact without pitting or cracking (the “holes” that appear in these images are pores) (Figs. 29C and E).

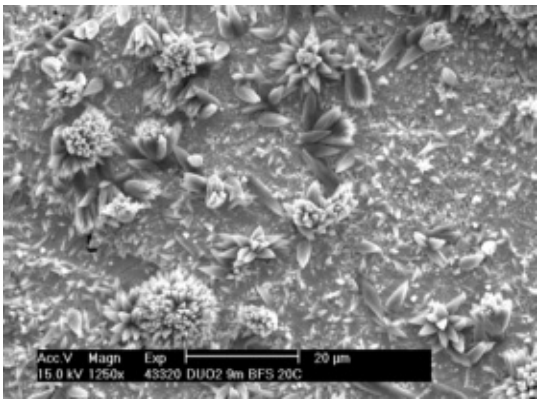

24A: Side of the cylinder - deposits of $CaCO_3$

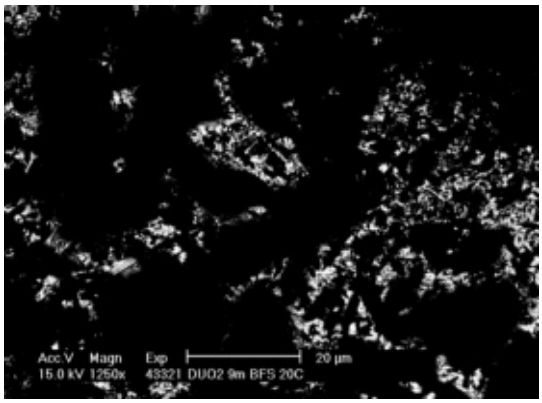

24B: Same area in backscattered electrons

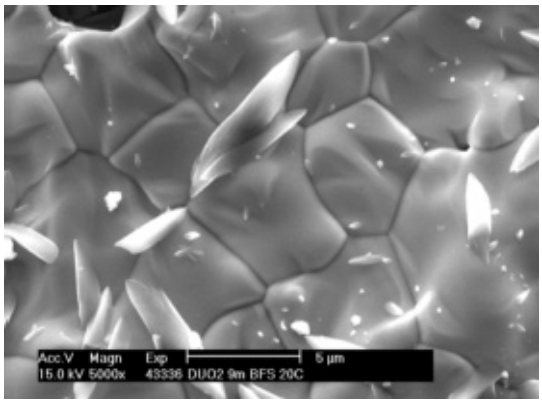

24C: Top of the cylinder with $CaCO_3$ crystals

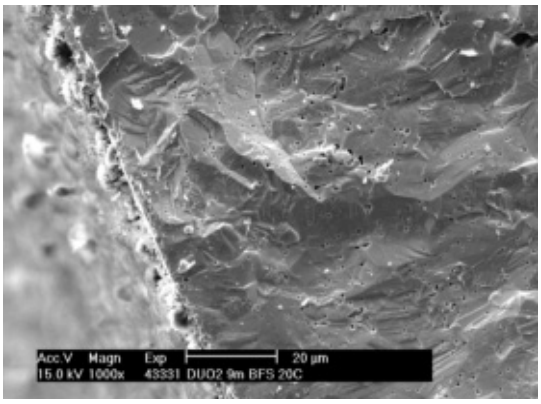

24D: Fracture of the cylinder

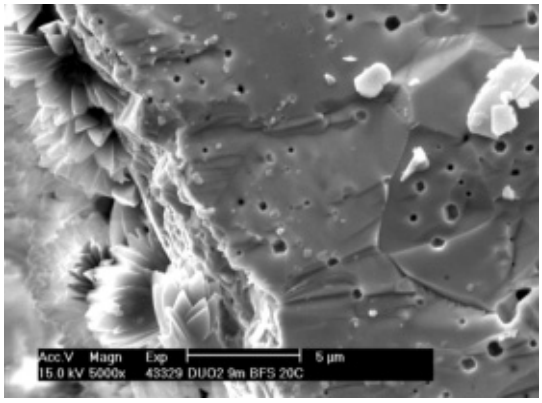

24E: Detail of the border - secondary electrons

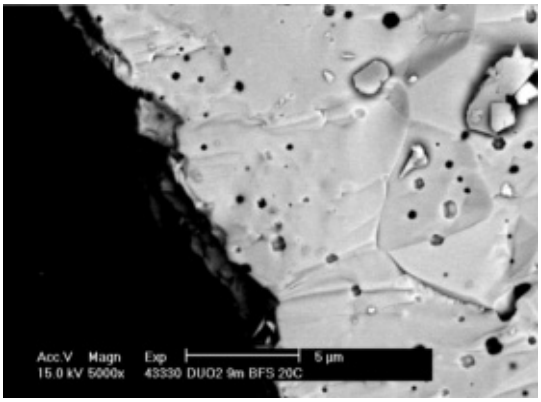

24F: Same area in backscattered electrons

Fig. 24: SEM pictures of DUO_2 cylinder kept in BFS pore solution at 20° C for 9 months

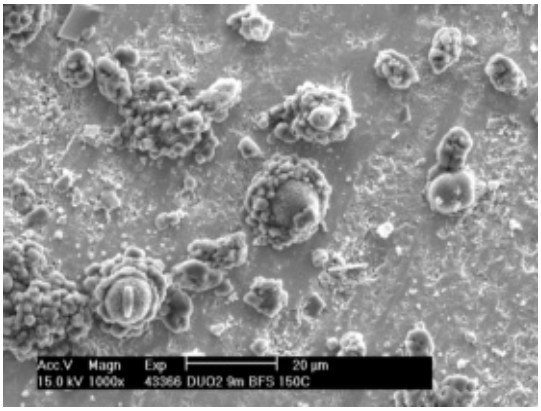

25A: Side of the cylinder with $CaCO_3$ crystals

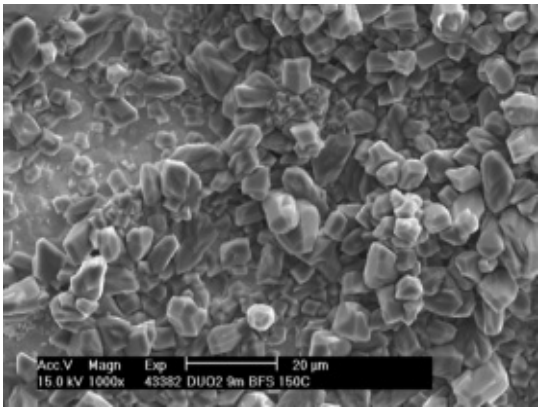

25B: Top of the cylinder with $CaCO_3$ crystals

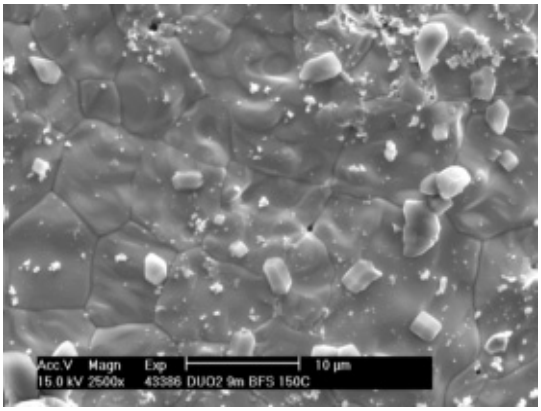

25C: Top of the cylinder

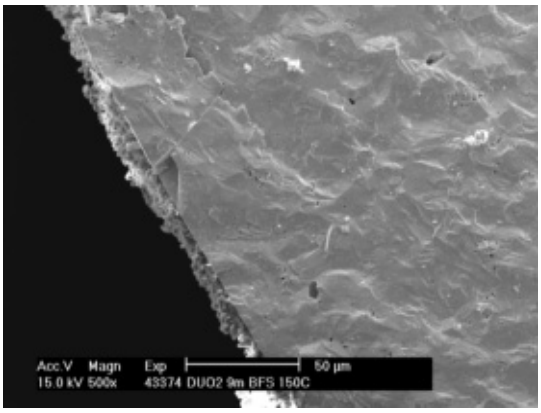

25D: Fracture of the cylinder - the outside layer of $CaCO_3$ is visible

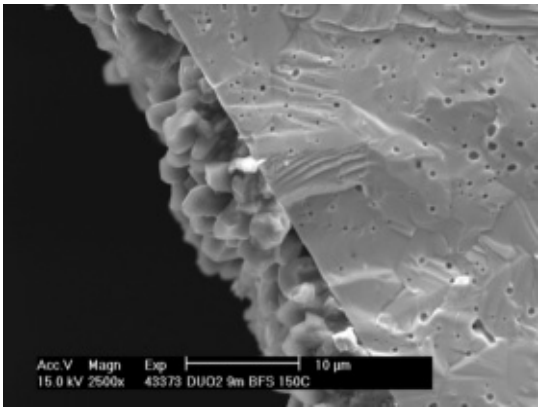

25E: There is no alteration visible of the DUO_2 grains on the outside

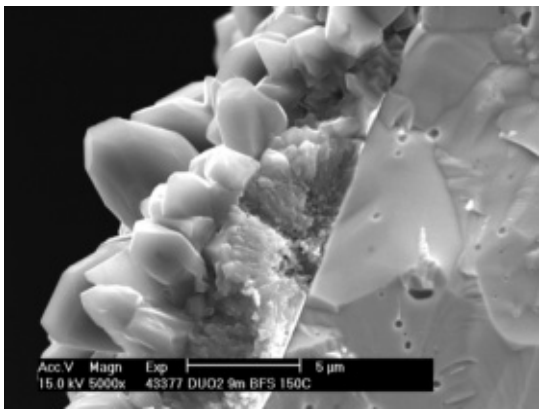

25F: Detail of the contact between $CaCO_3$ and DUO_2

Fig. 25: SEM pictures of DUO_2 cylinder kept in BFS pore solution at 67° C for 9 months

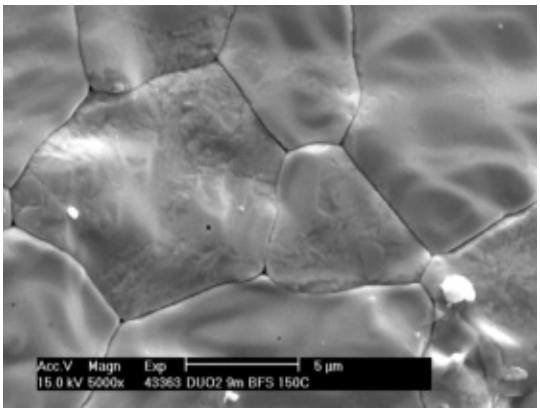

26A: Top of the cylinder - the DUO_2 grains are corroded

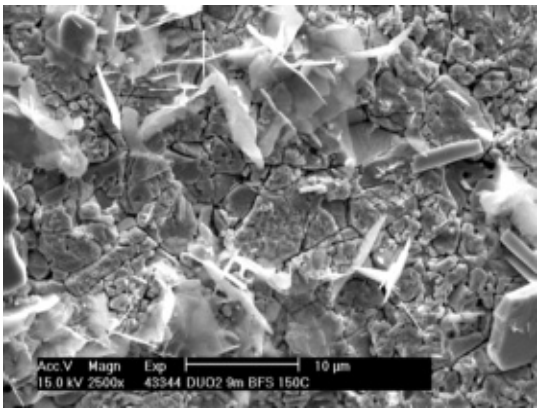

26B: Side of the cylinder

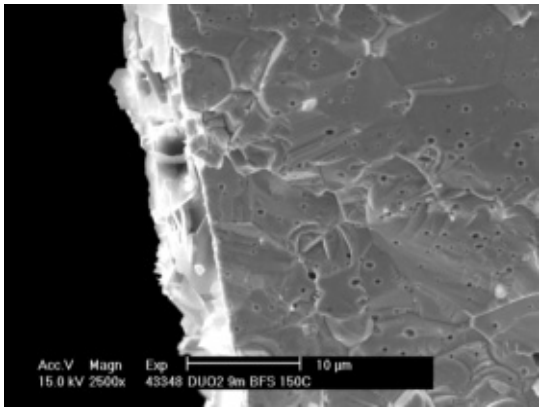

26C: Fracture of the cylinder showing the outside layer of $CaCO_3$

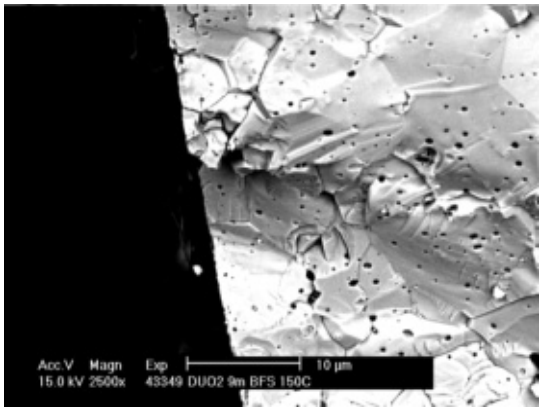

26D: Same area in backscattered electrons

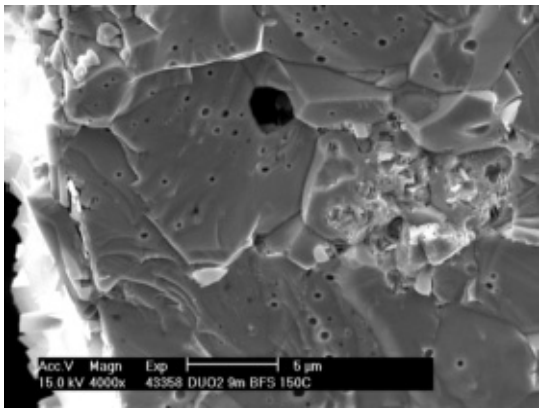

26E: Uranium recrystallization products in a porous area

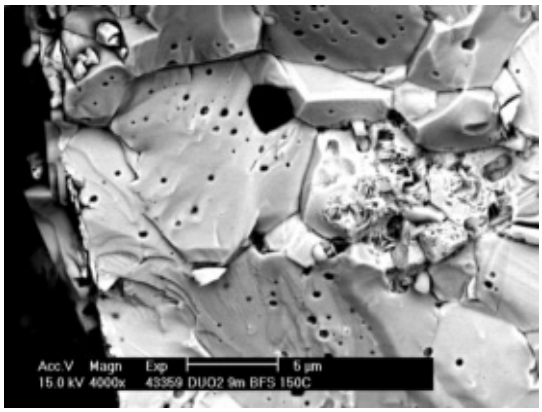

26F: Same area in backscattered electrons

Fig. 26: SEM pictures of DUO_2 cylinder kept in BFS pore solution at 150° C for 9 months

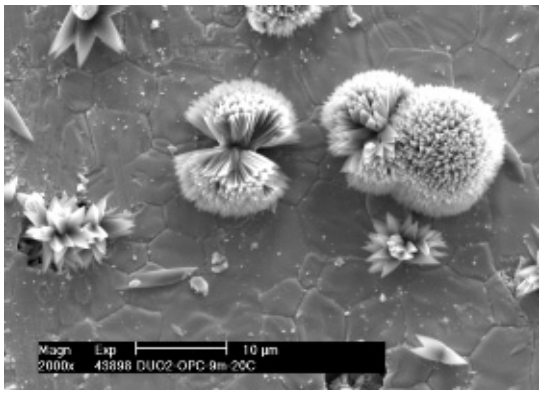

27A: Side of the cylinder - secondary electrons - deposits of $CaCO_3$

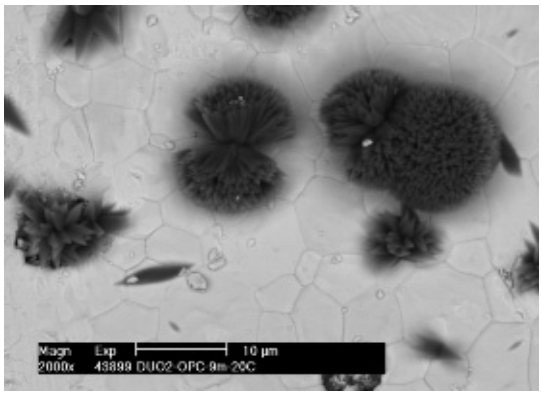

27B: Same area in backscattered electrons

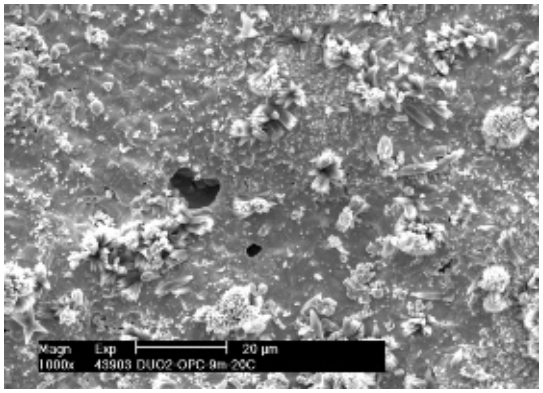

27C: Top of the cylinder with $CaCO_3$ crystals

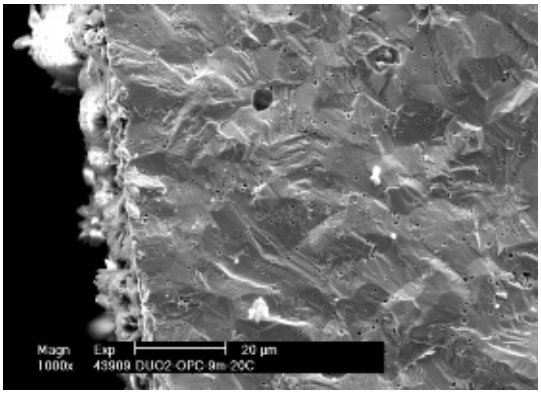

27D: Fracture of the cylinder with the outside layer of $CaCO_3$

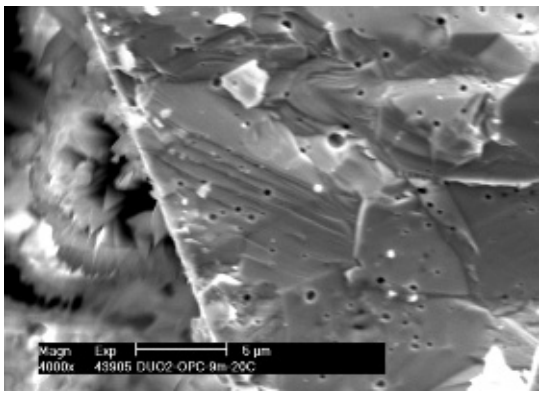

27E: Detail of the outside border, the DUO_2 grains are not eroded

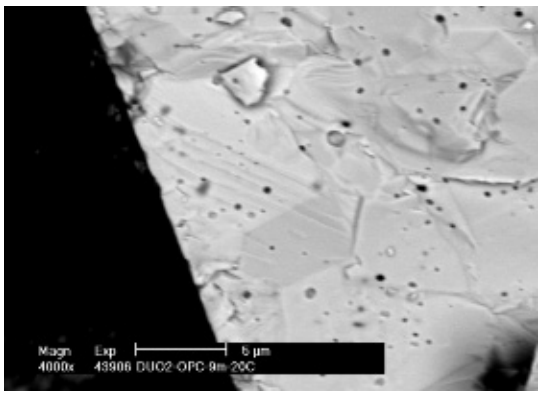

27F: Same area in backscattered electrons

Fig. 27: SEM pictures of DUO_2 cylinder kept in OPC pore solution at 20° C for 9 months

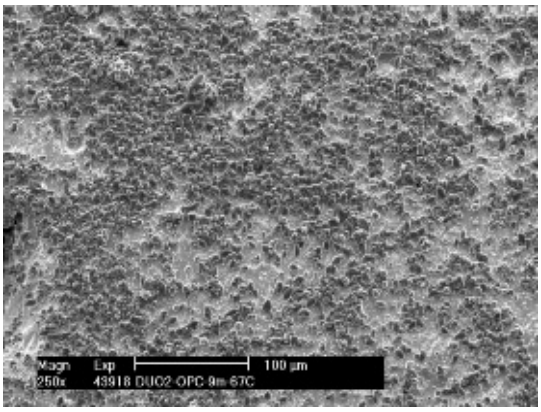

28A: Side of the cylinder almost covered with $CaCO_3$ crystals

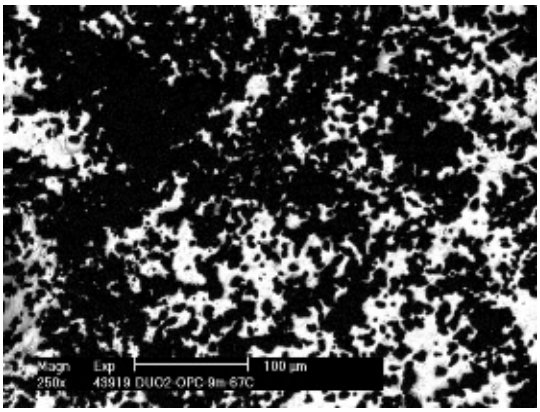

28B: Same area in backscattered electrons

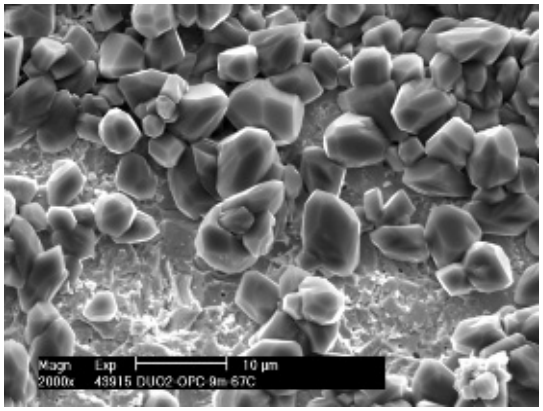

28C: Detail of the side of the cylinder with crystals of $CaCO_3$

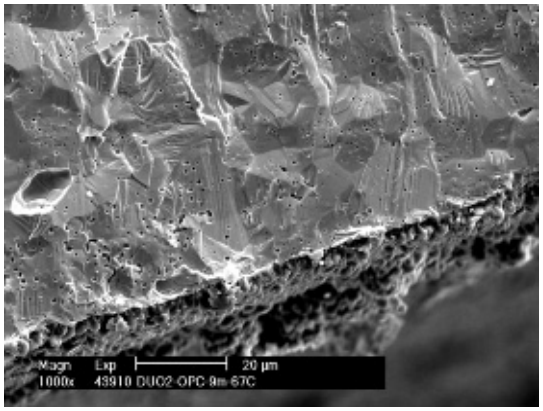

28D: Fracture of the cylinder

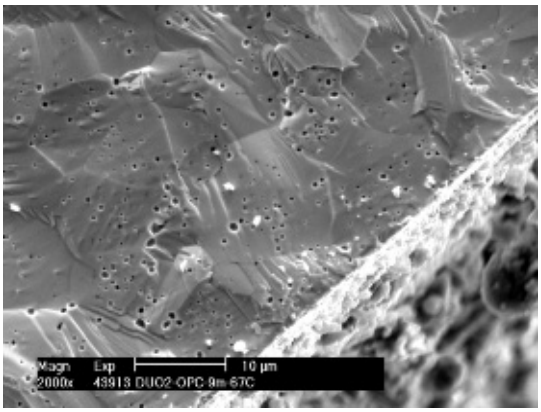

28E: The DUO_2 grains on the outside are not damaged

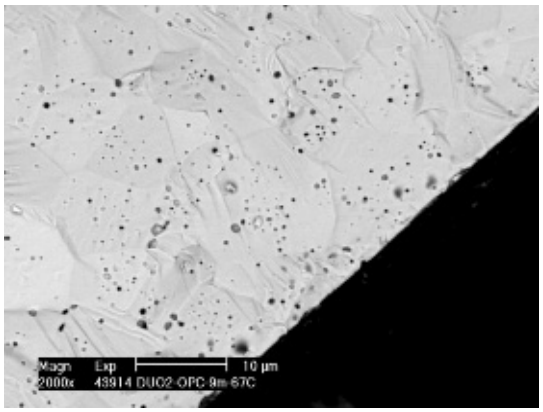

28F: Same area in backscattered electrons

Fig. 28: SEM pictures of DUO_2 cylinder kept in OPC pore solution at 67° C for 9 months

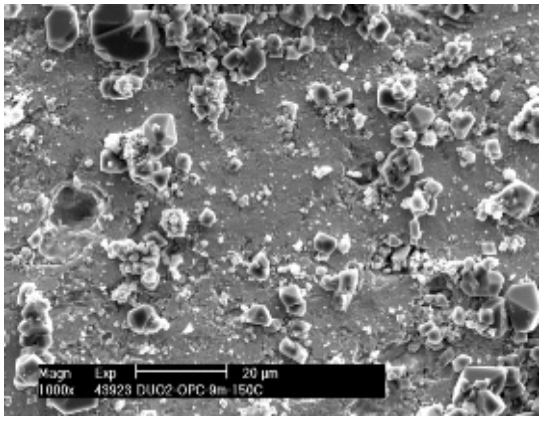

29A: Side of the cylinder with $CaCO_3$ deposits

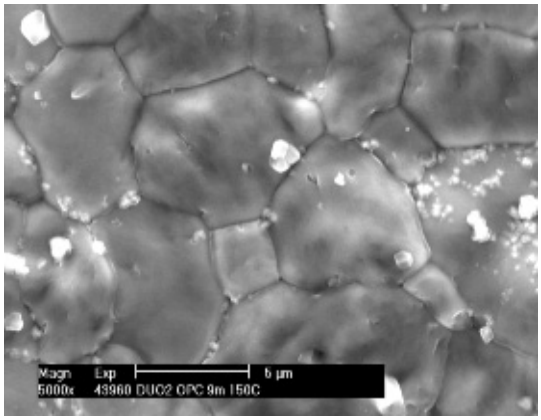

29B: Top of the cylinder

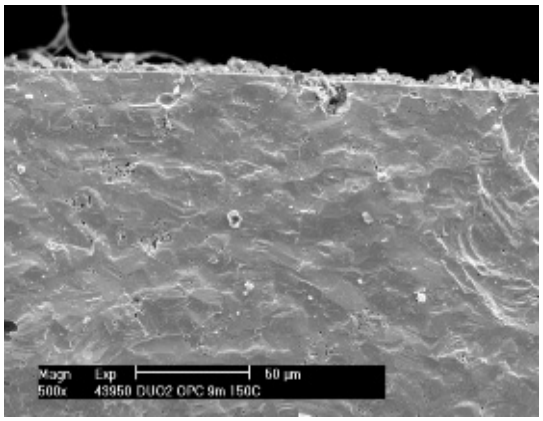

29C: Fracture of the cylinder

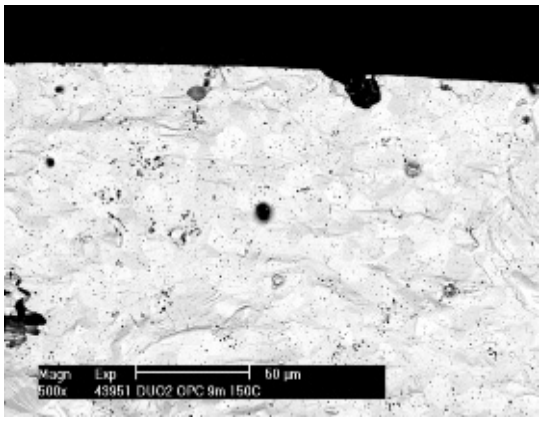

29D: Same area in backscattered electrons

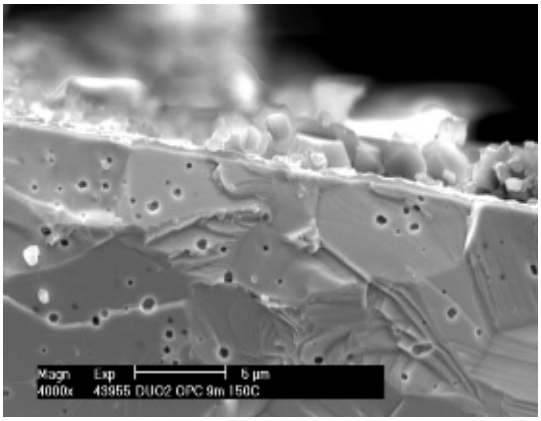

29E: Detail of the outside layer of the cylinder

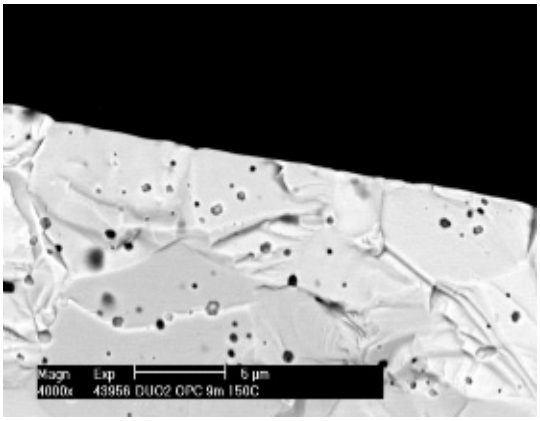

29F: Same area in backscattered electrons

Fig. 29: SEM pictures of DUO_2 cylinder kept in OPC pore solution at 150° C for 9 months

3.4.2 DUAGG

3.4.2.1 DI water

New mineral phases do not form in abundance on the outside surface of the pellet kept at 20°C. The basalt appears to be dissolved, and the relief of the surface is very rough (Fig. 30A). At higher magnification, one can see the presence of small crystals recovering the DUO_2 grains (Fig. 30B). The crystals are too small to be analyzed by EDX, but an analysis of the area shows that the components of the basalt are present, indicating that these crystals are recrystallization products resulting from the dissolved basalt. The fractured sample shows that the layer of recrystallization products from the basalt had penetrated the pellet for less than10 μm (Fig. 30D). This is a superficial change, as seen in pictures 30E and 30F. It confirms that there is no layer of secondary products on the outside of the pellet (Figs. 30C, E, and F).

At 67°C, some rhombohedric crystals are visible on the outside surface of the pellet (Figs. 31A, B, C, and D). They are mixed with some submicron crystals that resemble those seen at 20°C from the dissolution of the basalt. The hexagonal crystals contain aluminum and titanium only and could be a form of aluminum titanate. No outside layer surrounding the pellet was seen on that sample.

At 150°C, the outside surface of the pellet shows only the round grains of DUO_2. The basalt is completely gone (Figs. 32A, D, and E), and only small amounts of recrystallization products are visible (Fig. 32B). Because of the fracture, it can be seen that the zone where the basalt was attacked is about 100 μm thick (Fig. 32C). The grains of UO_2 are also being attacked (Fig. 32D). A typical picture of the surface was taken close to the surface and in the center of the pellet (Figs. 32E and F). One can see that the disappearance of the basalt caused the breakage of the pellet to be different. Next to the outside of the pellet, the fracture follows the contours of the DUO_2 grains (like a 3D relief), while in the center of the pellet, the grains of DUO_2 are fractured and appear as a 2D picture.

3.4.2.2 NaOH solution

The outside surface of the pellet kept at 20°C is covered with deposits (Figs. 33A and B), but they are very finely crystallized. It is clear that the deposits are not thick because the backscattered pictures show the uranium grains (Fig. 33B). At higher magnification, the observation reveals the presence of small plates, about 1 μm or less (Fig. 33D), that contain uranium, magnesium, titanium, and iron. Some others have mostly iron and magnesium. The images of the fractured pellet (Figs. 33E and F) indicate that no outside layer formed and that the basalt is not damaged because the fracture occurred within the DUO_2 grains and not around them.

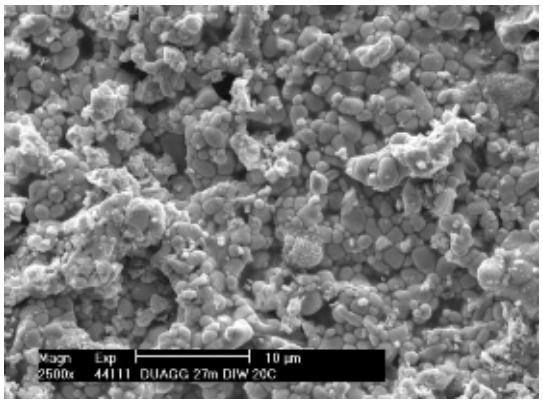

30A: Outside surface of the pellet

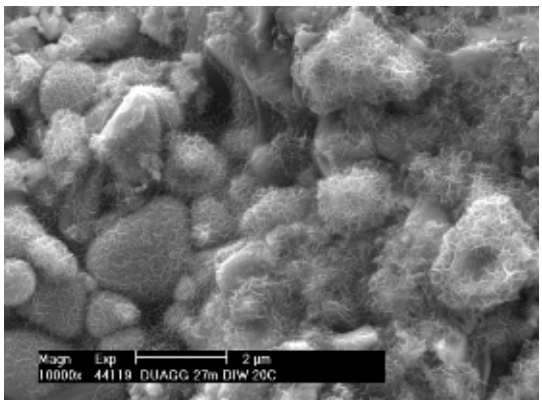

30B: Outside of the pellet with recrystallization products from the basalt phase

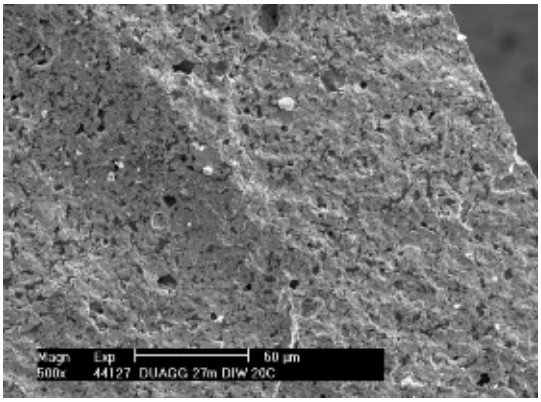

30C: Fracture of the pellet

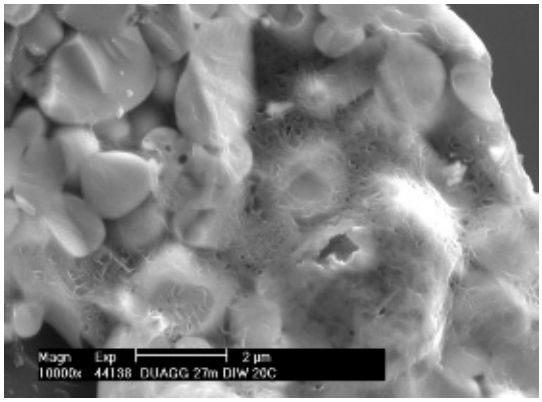

30D: Outside border of the pellet with some basalt recrystallization products

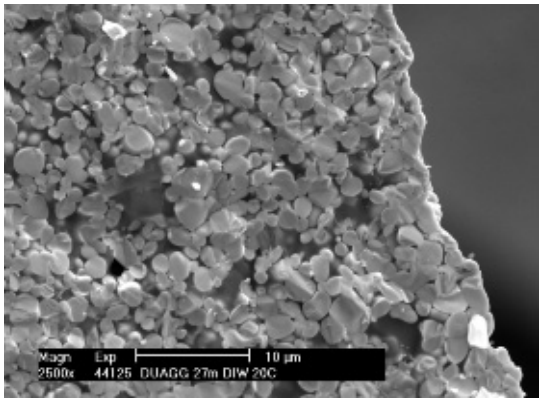

30E: Outside border of the pellet after fracture

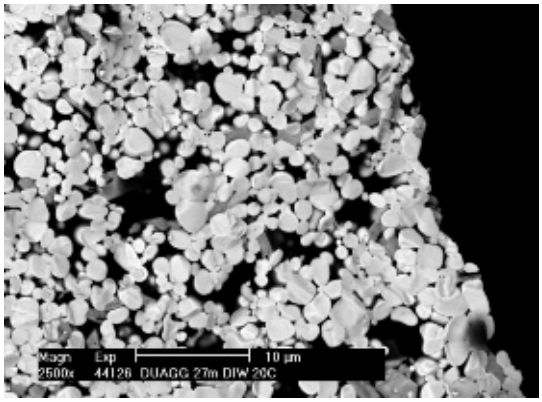

30F: Same area in backscattered electrons

Fig. 30: SEM pictures of DUAGG pellet kept in DI water at 20° C for 27 months

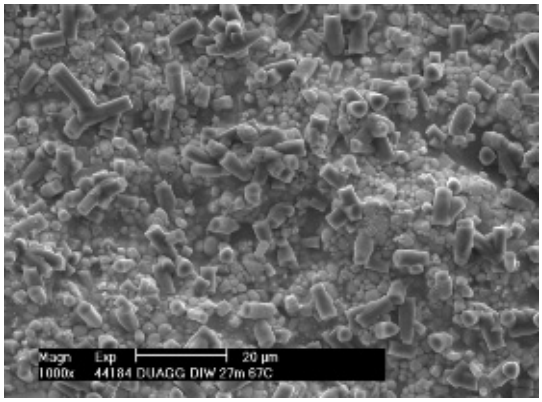

31A: Outside surface of the pellet covered with crystals rich in Ti and Al

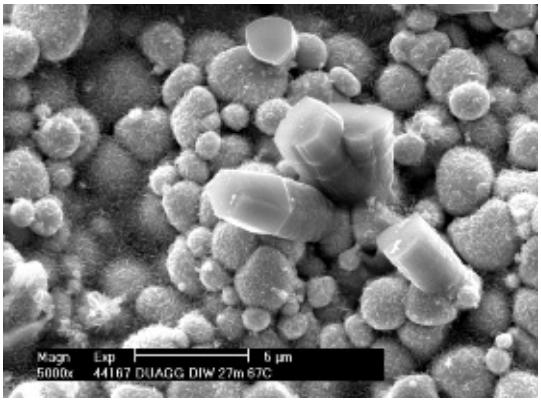

31B: Surface of the pellet with recrystallization products from the basalt

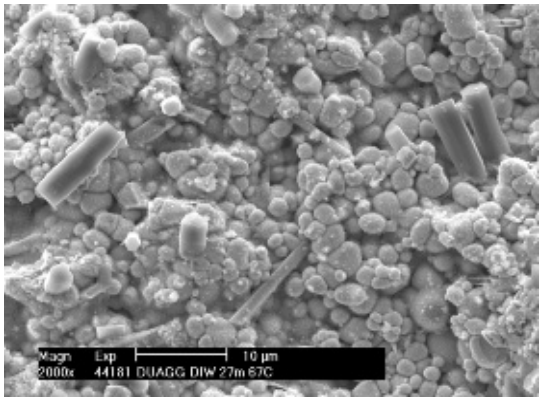

31C: Other view of the surface of the pellet

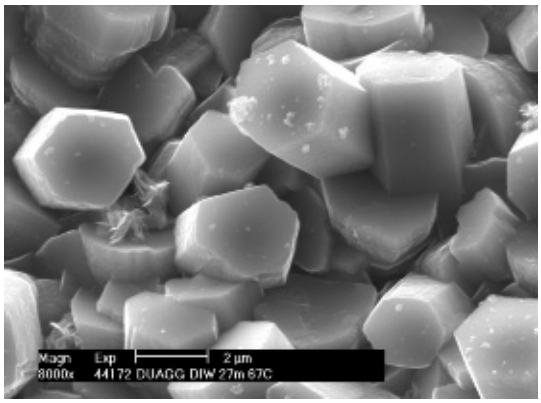

31D: Detail of the crystals containing Ti and Al.

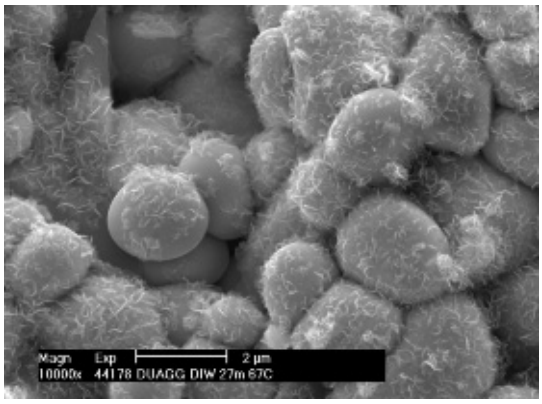

31E: This area contains U and Ti as major elements and Al, Si, Zr, and Fe as minors

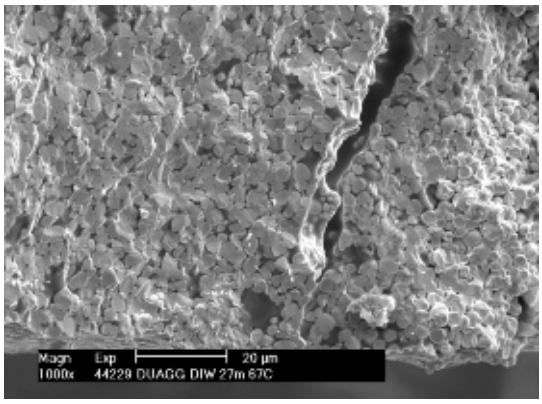

31F: Fracture of the pellet

Fig. 31: SEM pictures of DUAGG pellet kept in DI water at 67° C for 27 months

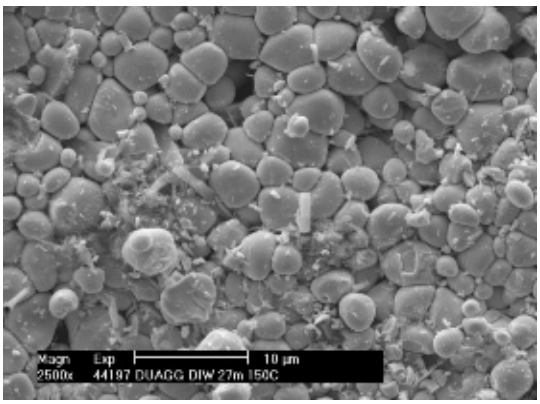

32A: Outside surface of the pellet; the basalt is not visible

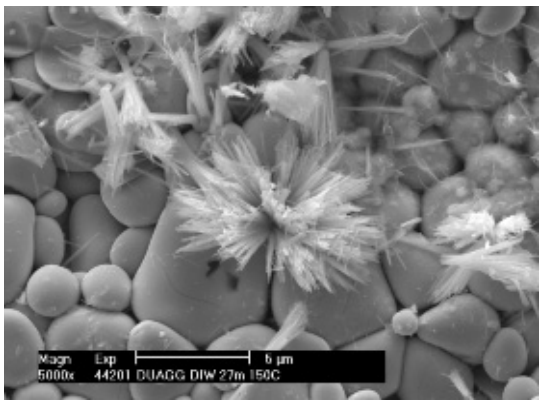

32B: Outside surface of the pellet; the needles contain Ti, Al, and U

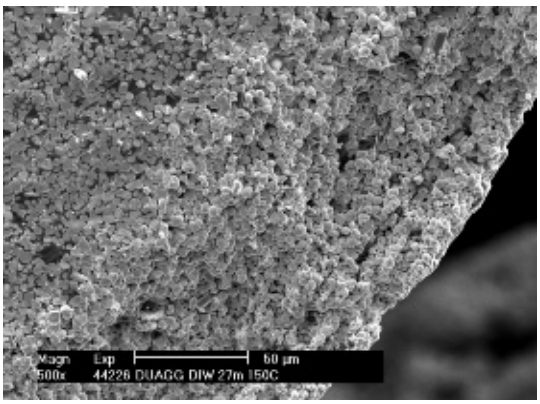

32C: Fracture of the pellet; the zone of altered basalt is about 100µm thick

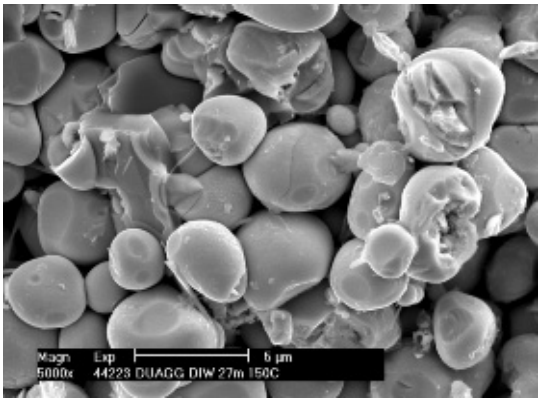

32D: Detail of the alteration layer; the basalt is not visible any longer and the DUO_2 grains are damaged

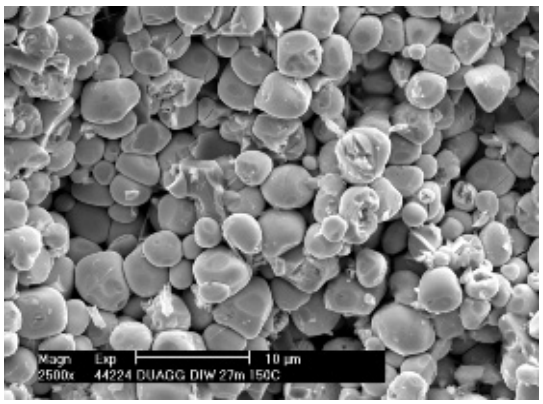

32E: DUAGG near the outside of the pellet

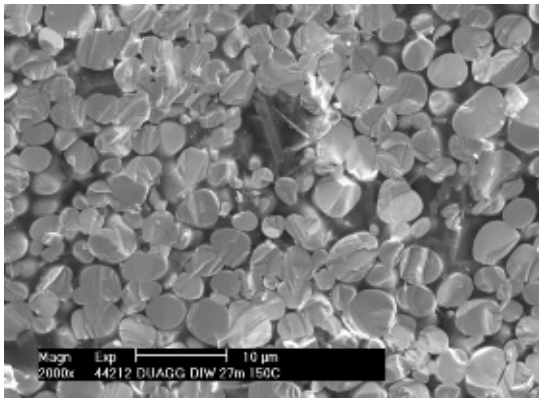

32F: DUAGG toward the center of the pellet

Fig. 32: SEM pictures of DUAGG pellet kept in DI water at 150° C for 27 months

At 67°C, the outside surface is completely covered by needle-like crystals that contain sodium, silicon, and calcium (Fig. 34A). The original morphology of the DUAGG pellet is not visible. The needles are present in a thick layer, and no uranium is present on the EDX spectrum. The fractured pellet shows that these needles are deposited above a dense layer surrounding the DUAGG constituents (Figs. 34B, C, and E). This layer is made up of mostly aluminum, silicon, and calcium with some sodium. Next to the border, the basalt phase appears to be gel-like with lots of cracks (Fig. 34D). The EDX analyses indicates that this phase contains aluminum, silicon, sodium, calcium, and uranium. Locally on the outside or close to it, some agglomeration of very large crystals are found (Fig. 34B) that sometimes contain only sodium and other times sodium with silicon and uranium or sodium and uranium. Titanium and calcium can also be found locally in addition to the other elements. Some of the needle-like crystals are also seen within 50 μm inside of the pellet. They contain uranium and sodium. The uranium grains next to the border are rounded, meaning that the fracture took place within the basalt phase, not the DUO_2 grains. Except on the very border, the uranium grains are not attacked or pitted.

At 150°C, the outside surface of the pellet has a dense layer of needles (Fig. 35A) made of uranium, titanium, sodium, and silicon. Locally on the surface, some large agglomerations of crystals containing sodium, aluminum, and silicon are visible. Other recrystallization products are spherical and contain silicon, calcium, titanium, and iron. The fractured sample shows a dense layer surrounding the pellet that is between 5 and 10 μm thick (Fig. 35B). The uranium grains are not fractured but appear rounded (Fig. 35B). They are also damaged (Fig. 35F). The protective layer contains some crystals in which uranium is mixed with the basalt components (Fig. 35D).

3.4.2.3 OPC cement pore solution

At 20°C, there appears to be little change from the original morphology of the pellet. On the outside surface, some crystals are sporadically present (Figs. 36A ,B and C). These crystals are from the basalt and do not contain uranium. Underneath, the uranium oxide grains are visible but the basalt is slightly eroded (Fig. 36C). The fracture shows the DUO_2 grains fractured through the grain (Fig. 36F), indicating that the basalt is in good condition. No outside products are visible along the border (Figs.36D, E and F). This sample appears to have sustained no or almost no corrosion.

The outside surface of the sample at 67°C is covered with large needle-like crystals (Fig. 37A) containing calcium, silicon and some titanium. Locally within the needles, orthorhombic pseudo-cubic crystals of perovskite-like crystals (calcium and titanium oxide) are visible (Fig. 37B). The fracture shows the presence of a dense layer of the needles on the surface being as thick as 20 to 30 μm (Fig. 37D). On other part of the outside border of the pellet, some looser needles are seen (Fig. 37C). The basalt appears

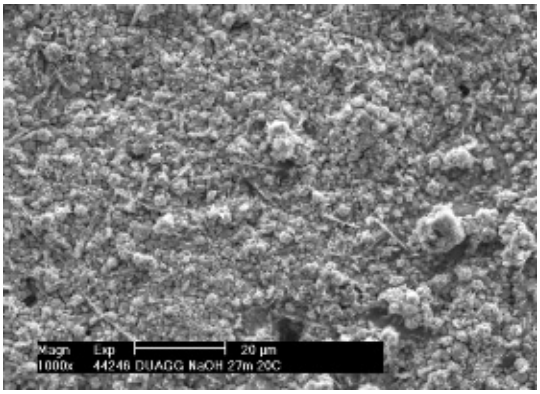

33A: The surface of the pellet is not covered with abundant deposits

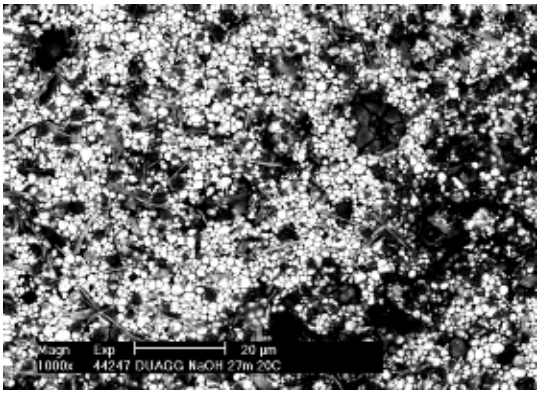

33B: Same area in backscattered electrons; the uranium particles are well visible

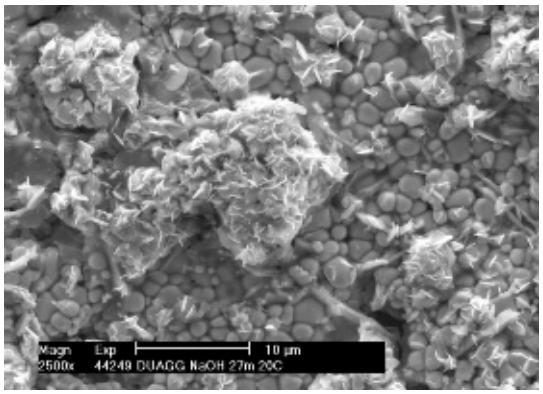

33C: Detail of the surface; small crystals locally cover the DUAGG pellet

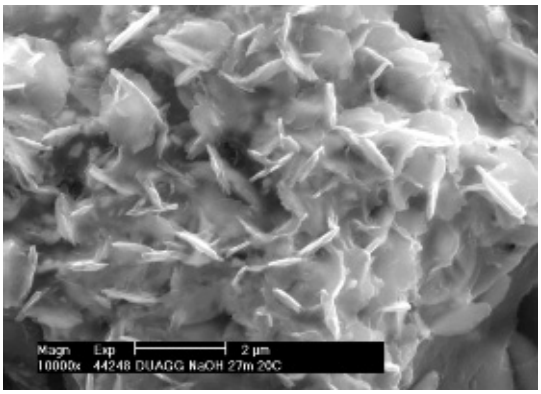

33D: Detail of the small plates; they contain U, Mg, Ti, and Fe.

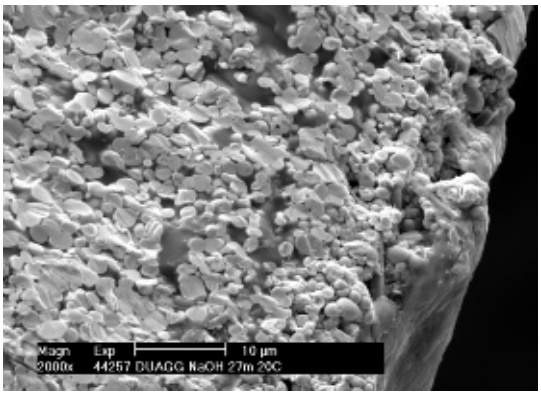

33E: Fracture of the pellet: there are no deposits visible on the outside border

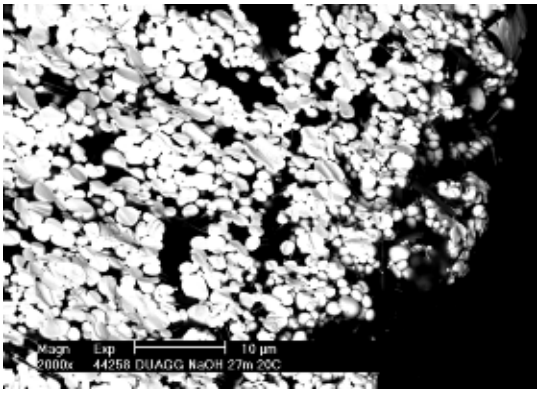

33F: Same area in backscattered electrons

Fig. 33: SEM pictures of DUAGG pellet kept in NaOH solution at 20° C for 27 months

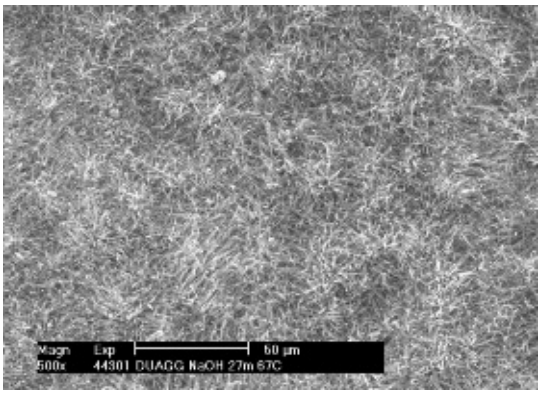

34A: Surface of the pellet covered with a thick layer of needle-like crystals containing Na, Si, and Ca

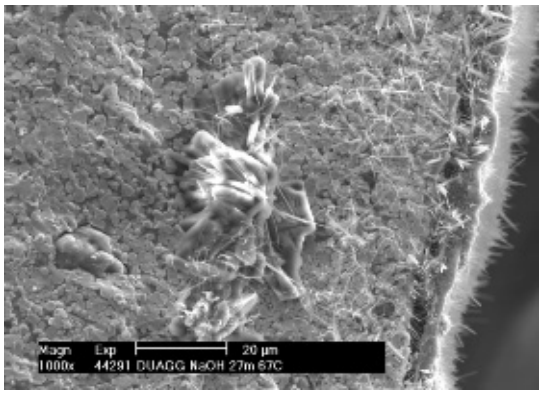

34B: Fracture of the pellet: the layer of needle-like crystals is on the outside. Then a compact layer of mostly Na and small amount of Si and U follows. Recrystallization of Na took place in pores inside the pellet.

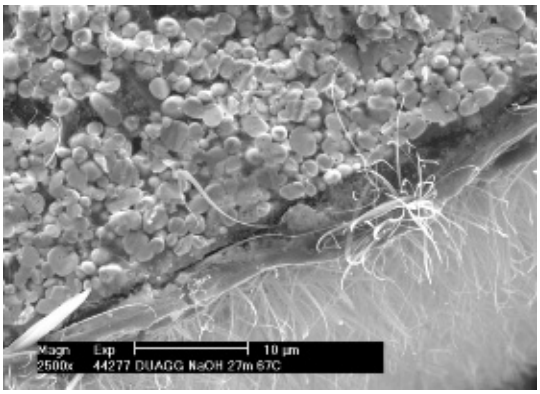

34C: Detail of the layers around the pellet

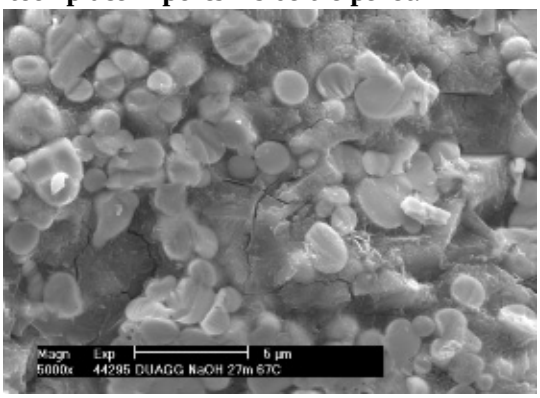

34D: Near the border, the basalt phase is replaced with a gel-like recrystallization phase containing Al, Si, Na, U, and Ca

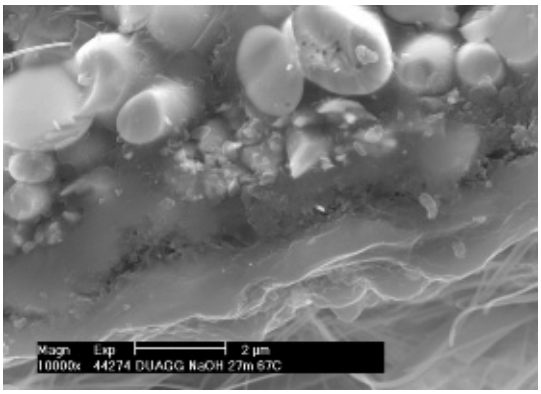

34E: The outside recrystallization products form a dense protective layer

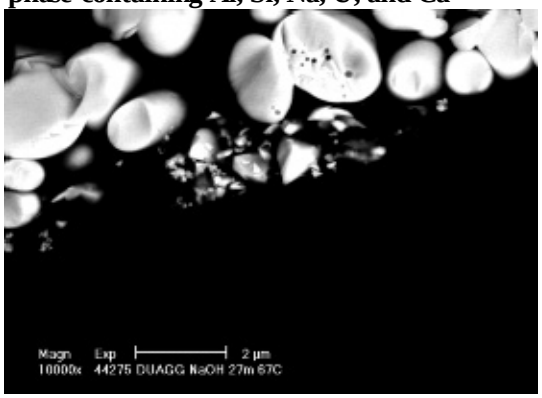

34F: Same area in backscattered electrons

Fig. 34: SEM pictures of DUAGG pellet kept in NaOH solution at 67° C for 27 months

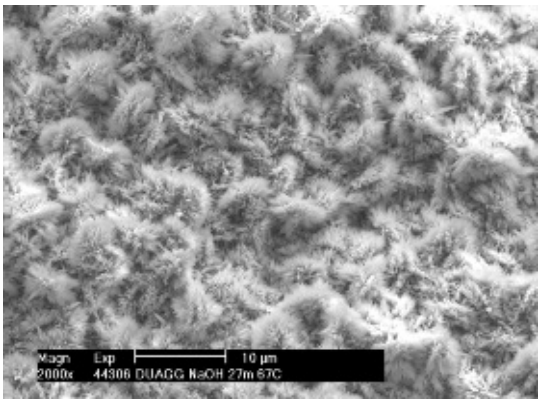

35A: Surface of the pellet covered with thick needle-like crystals

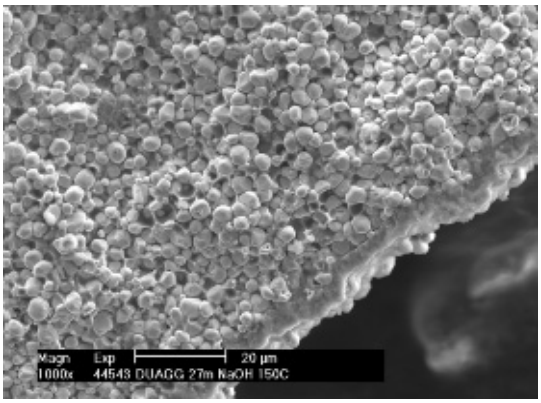

35B: Fracture of the pellet; a dense protective layer is surrounding the pellet

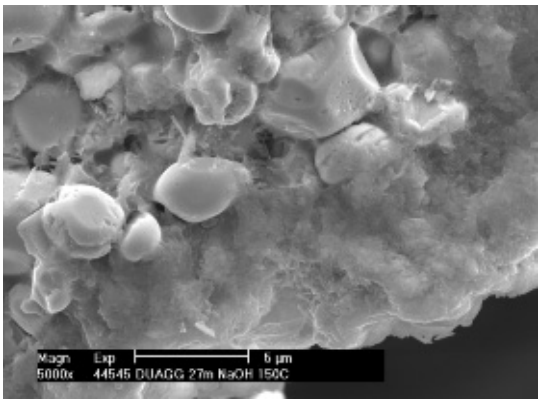

35C: The protective layer is about 5 µm thick and is very dense

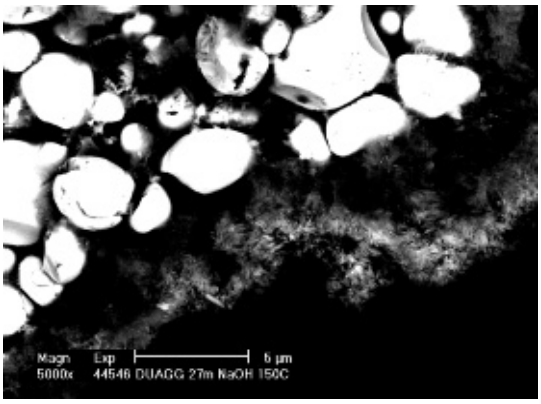

35D: Same area in backscattered electrons; some uranium is present in the recrystallization products

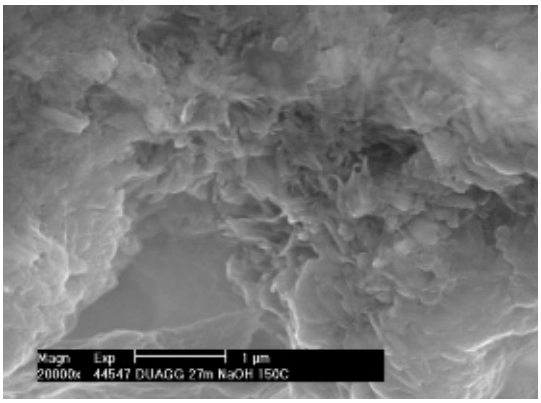

35E: Detail of the protective layer

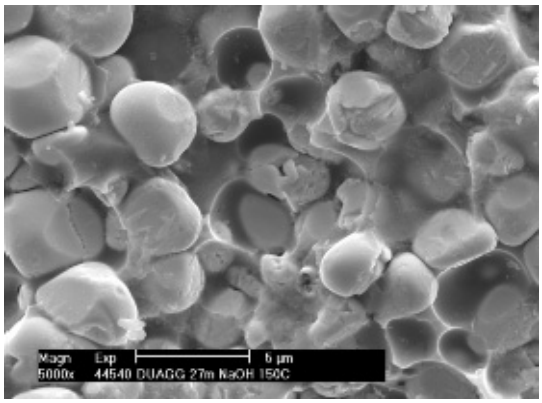

35F: Next to the surface the basalt phase and the DUO_2 grains are altered

Fig. 35: SEM pictures of DUAGG pellet kept in NaOH solution at 150° C for 27 months

to be altered within a depth of ~ 50 μm inside the pellet (Fig. 37E). The transition between the zone where the basalt is altered and not altered is visible on picture 37F.

The surface of the sample kept at 150°C is also covered with recrystallization products containing calcium, silicon, aluminum, and titanium (Fig. 38A). Instead of needles, the crystals are in the form of plates (Fig. 38C) but in the backscattered-electrons image, some uranium is visible underneath the layer of crystals (Fig. 38B). This indicates that the layer of crystals is not very dense. The fractured sample shows this layer, which is less than 5 μm thick (Fig. 38D). The composition of the layer is the same as the crystals on the surface. Next to the outside, the DUO_2 grains are rounded, indicating that the fracture occurred in the damaged basalt phase (Figs. 38E and F).

3.4.2.4 BFS cement pore solution

Like the surface of a pellet in the OPC solution, at 20°C, the surface of the pellet is covered with recrystallization products containing calcium and titanium (Fig. 39A). These crystals appear as agglomerations of needles (Figs. 39A and C) deposited on top of the pellet. The DUO_2 grains are visible when they are not covered by these crystals (Figs. 39B and D). The fracture of the sample shows that there is not a continuous layer around the pellet. Also, the basalt is intact, even next to the border (Figs. 39E and F).

At 67°C, the surface is covered with recrystallization products (Fig. 40A) that are not as well crystalized as those at 20°C (Fig. 40C). These products are dense enough to let very little uranium be seen in backscattered electrons (Fig. 40B). Locally some of the products resemble hydrated calcium silicates (CSH) as seen in cement paste. The fractured sample shows the basalt to be altered within a depth of ~200 μm (Fig. 40D). The porosity is higher where the basalt is altered, with the recrystallization products not filling the voids between the DUO_2 grains as completely as did the initial basalt (Fig. 40F).

At 150°C, the surface of the pellet is covered with a thick layer of crystals agglomerations (Fig. 41B). These agglomerations appear to be made up of mainly two types of crystals: some massive prisms containing aluminum, silicon, and potassium (Fig. 41C) and others that look more like pellets (Fig. 41D) and that contain aluminum, silicon, potassium, and calcium. Locally, some needle-like crystals containing mostly silicon and calcium are visible.

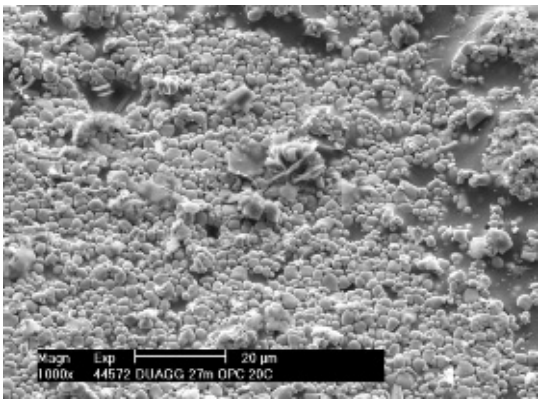

36A: Surface of the pellet; no abundant recrystallization products visible

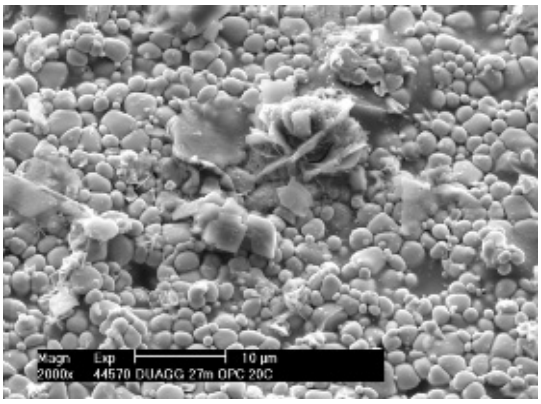

36B: Detail of the surface

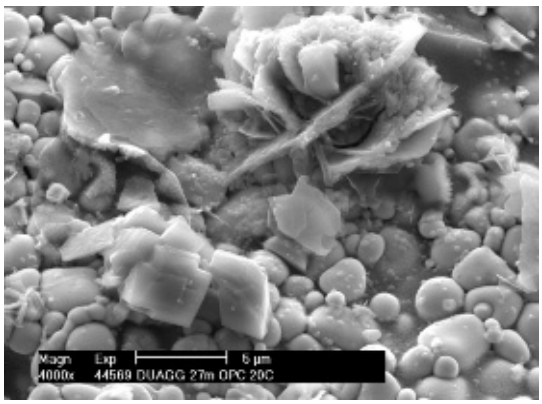

36C: The prismatic crystals contain Ca and Ti while the plates contain Ca, Ti, Al, Zr, and Fe

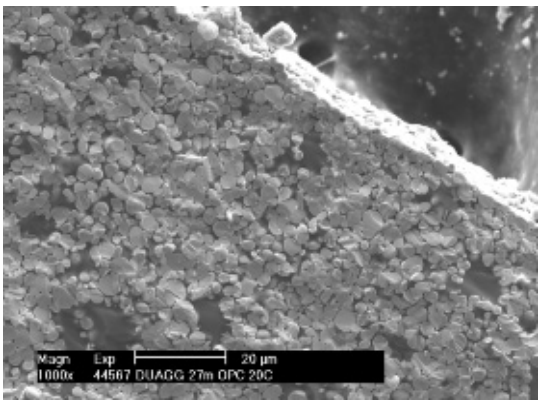

36D: Fracture of the pellet: no crystals visible on the outside

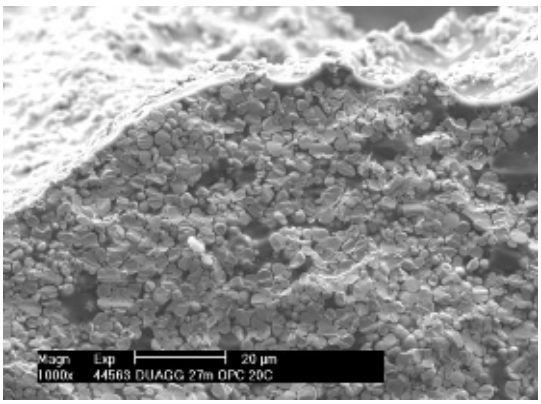

36E: The pellet appears intact with no alteration visible

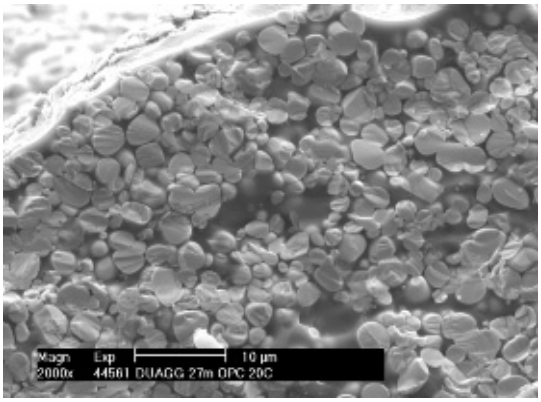

36F: Detail of the outside border; the basalt is unchanged

Fig. 36: SEM pictures of DUAGG pellet kept in OPC pore solution at 20°C for 27 months

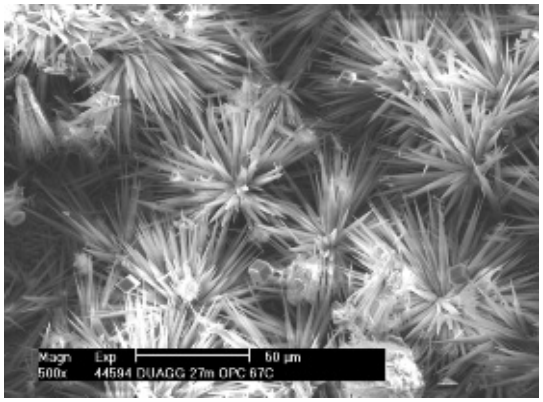

37A: Surface of the pellet covered with these needle-like crystals containing Ca, Si, and some Ti

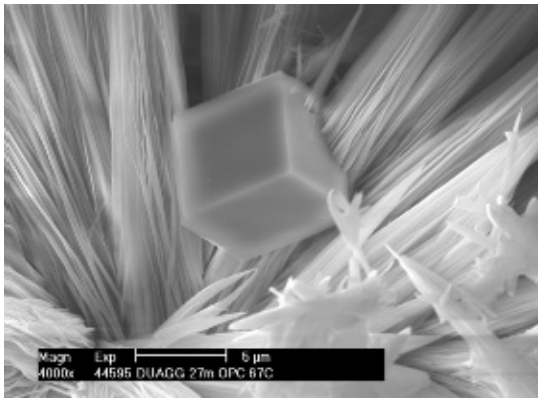

37B: Some crystals containing Ca and Ti are also found with the needles

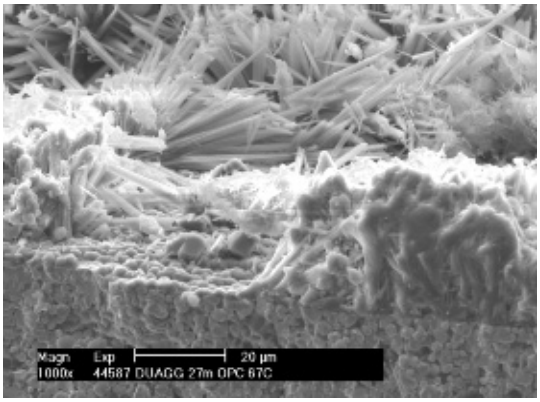

37C: Fracture of the pellet; dense recrystallization products and the needles are seen outside the pellet

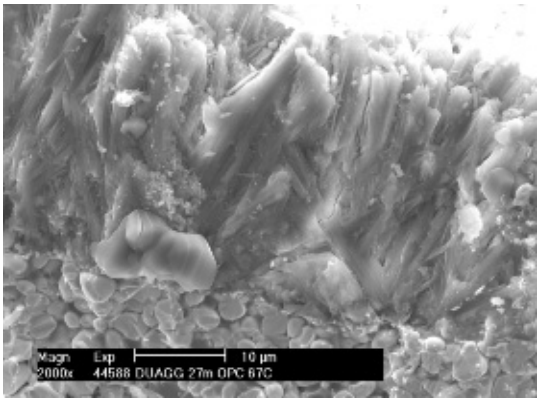

37D: The layer is about 20-30 µm thick and contains Ca, Si, and some Ti

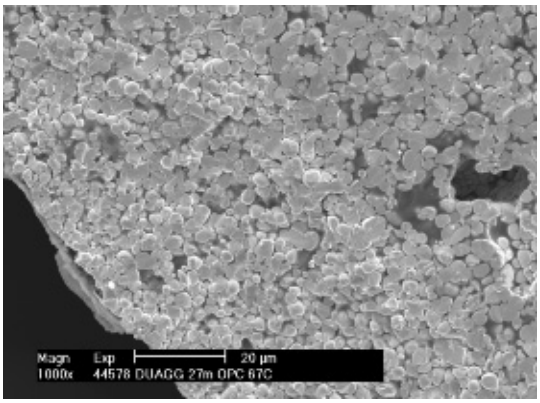

37E: Inside the pellet the basalt is altered in a layer of about 50 µm thickness

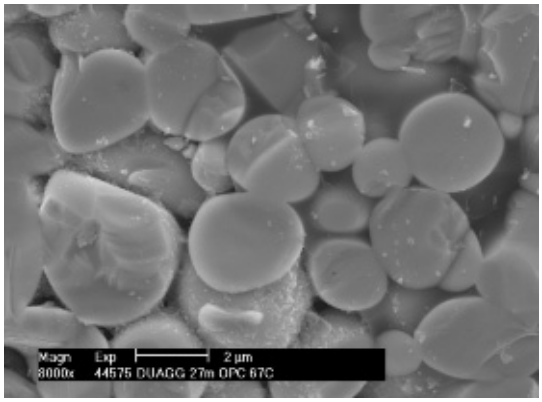

37F: Transition zone for the basalt: on the left altered, on the right intact

Fig. 37: SEM pictures of DUAGG pellet kept in OPC pore solution at 67°C for 27 months

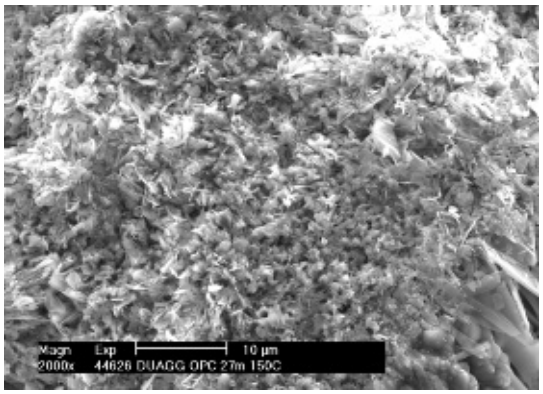

38A: Surface of the pellet mostly covered with recrystallization products

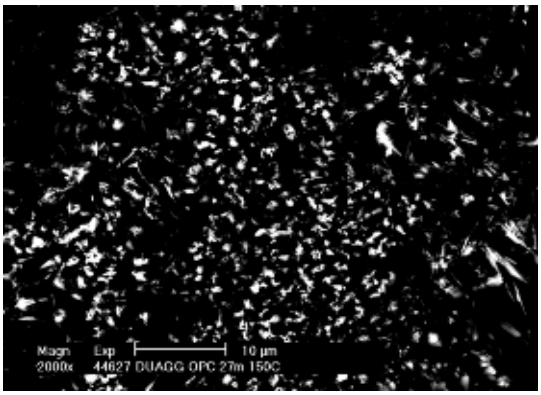

38B: Same area in backscattered electrons

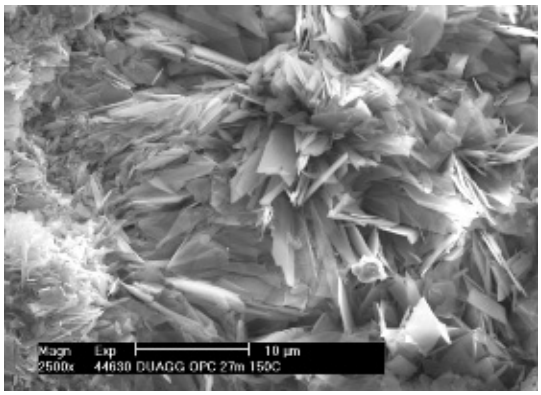

38C: These plates contain Ca, Si, Al, and Ti

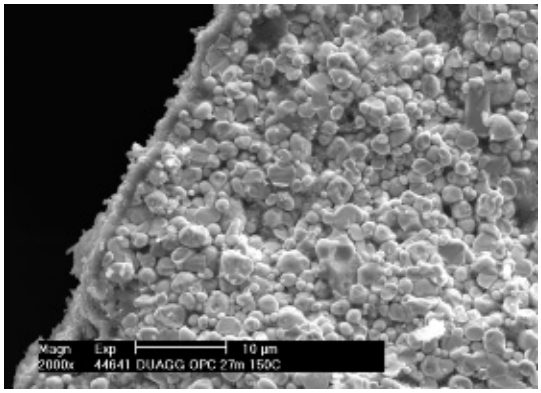

38D: Fracture of the pellet; the outside layer is visible

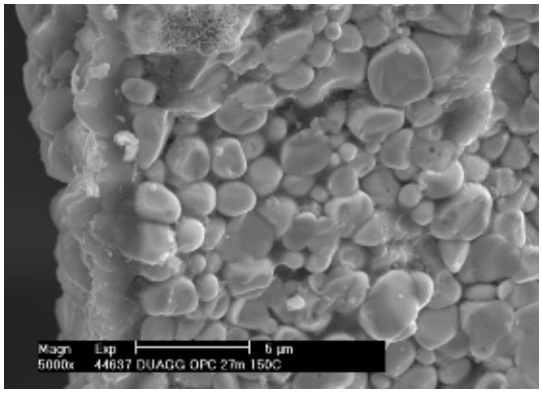

38E: Detail of the fracture

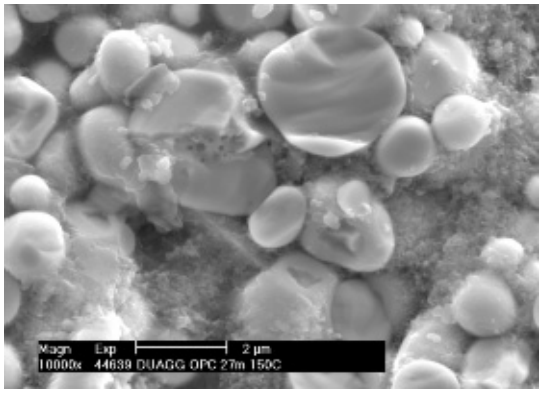

38F: View of DUAGG next to the surface, the basalt phase recrystallized

Fig. 38: SEM pictures of DUAGG pellet kept in OPC pore solution at 150°C for 27 months

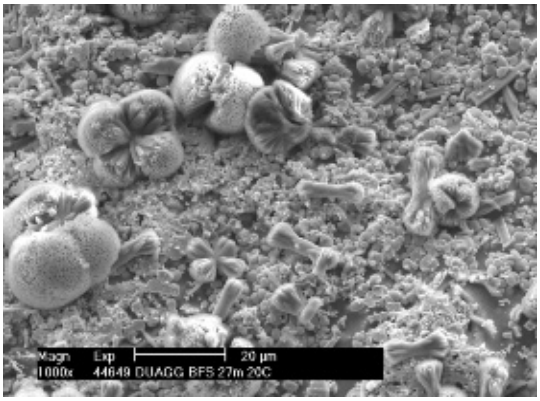

39A: Surface of the pellet: recrystallization products containing Ca and Ti cover a large part of the surface

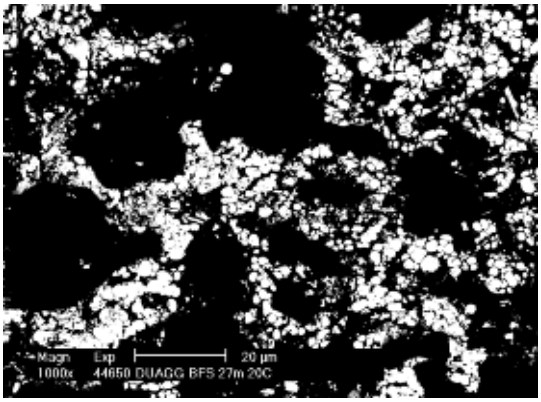

39B: Same area in backscattered electrons; the DUO_2 grains are still visible at places

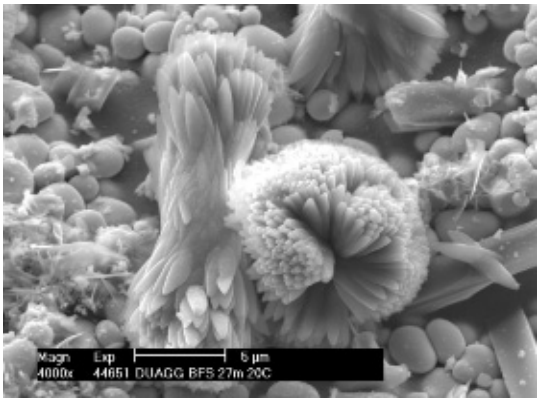

39C: Detail of the recrystallization products containing Ca and Ti

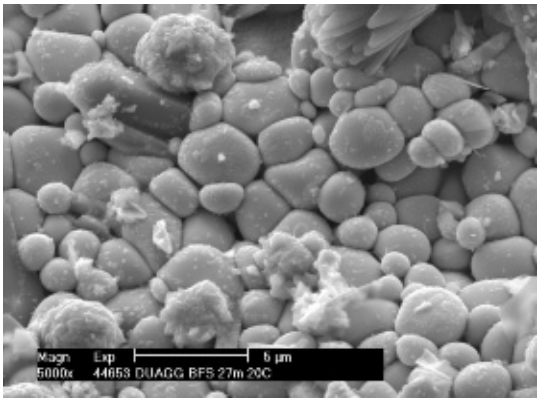

39D: The DUO_2 grains are visible in between the recrystallization phases

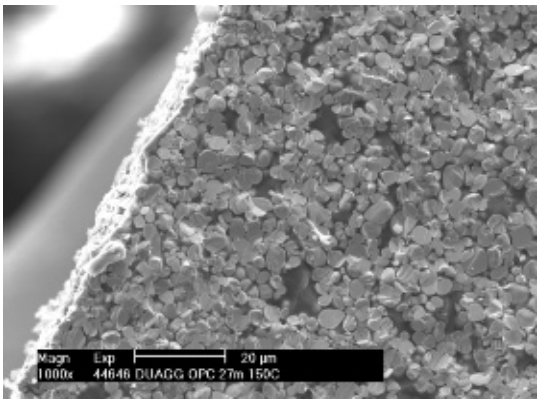

39E: Fracture of the pellet; there is no alteration zone of the basalt visible

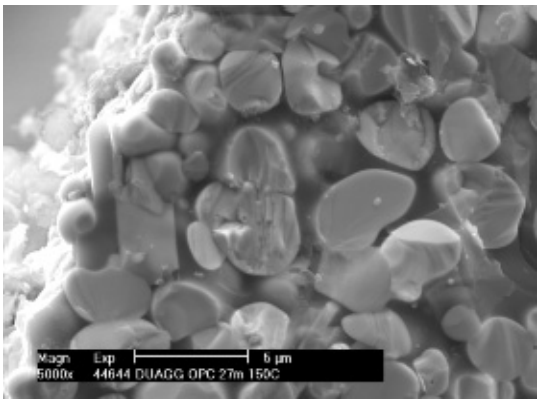

39F: Detail of the outside surface showing no visible alteration of DUAGG

Fig. 39: SEM pictures of DUAGG pellet kept in BFS pore solution at 20°C for 24 months

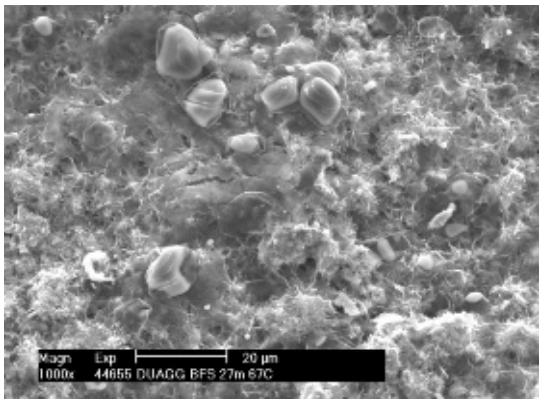

40A: Surface of the pellet, recrystallization products containing Ti, Si, and Ca are covering almost all the DUO_2 grains

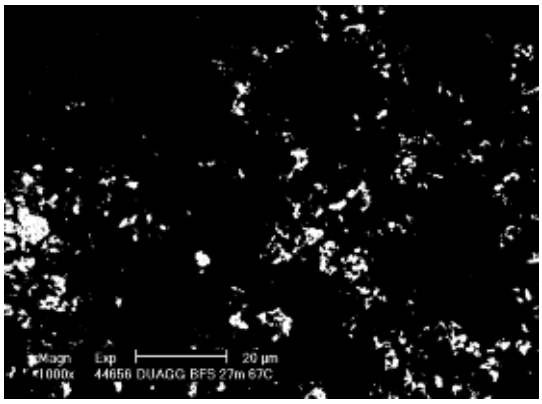

40B: Same area in backscattered electrons, DUO_2 is barely visible

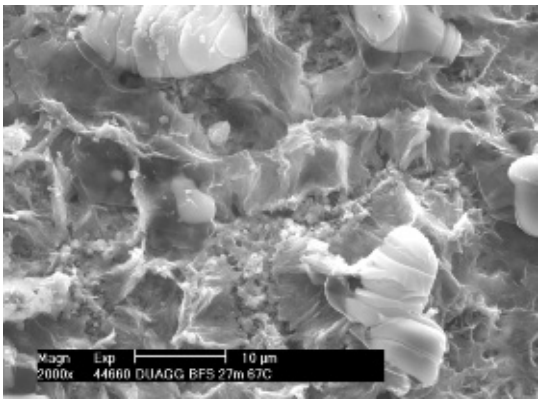

40C: Other view of recrystallization products on the surface of the pellet

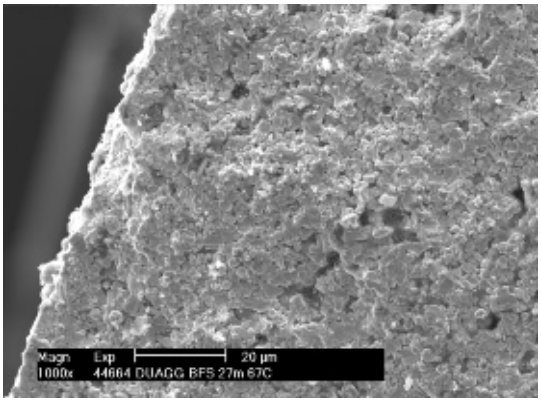

40D: Fracture of the pellet; the basalt appears changed up to a depth of 200 µm

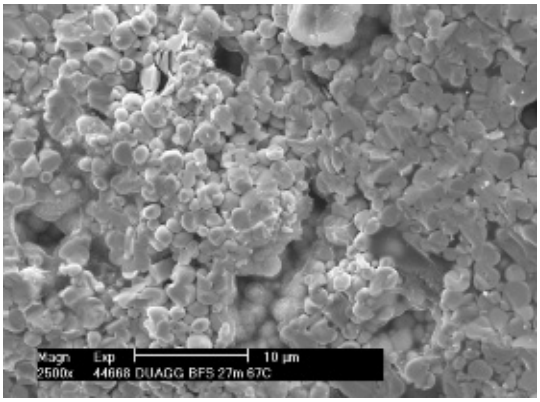

40E: Transition zone with the altered basalt on the left and the intact one on the right

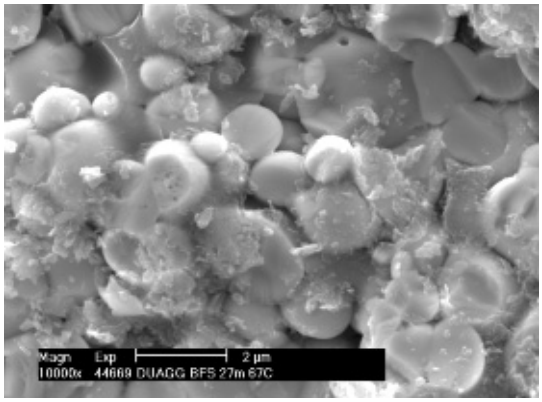

40F: View of the altered basalt on the outside of the pellet

Fig. 40: SEM pictures of DUAGG pellet kept in BFS pore solution at 67°C for 24 months

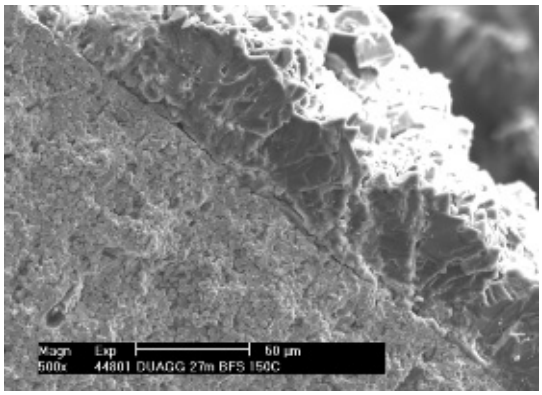

41A: Fracture of the pellet showing an outside layer of about 50 µm thickness

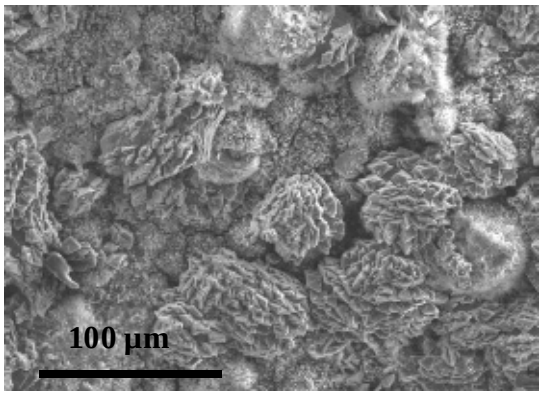

41B: Surface of the pellet covered with thick recrystallization products

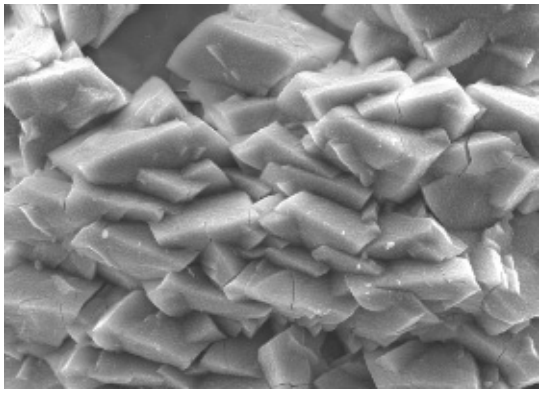

41C: Detail of some of these products: they contain mostly Al, Si, and K

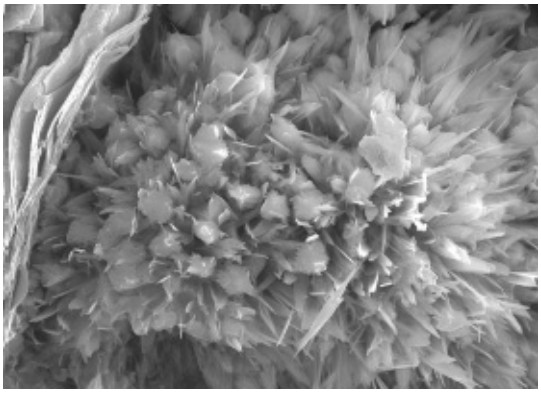

41D: Other types of crystals found on the surface; these contain Si, Ca, K, Al, and some Zr and Ti

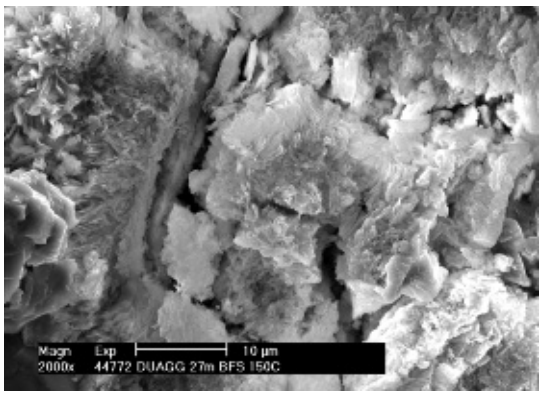

41E: These recrystallization products contain also some U beside Ca, Si, and Al

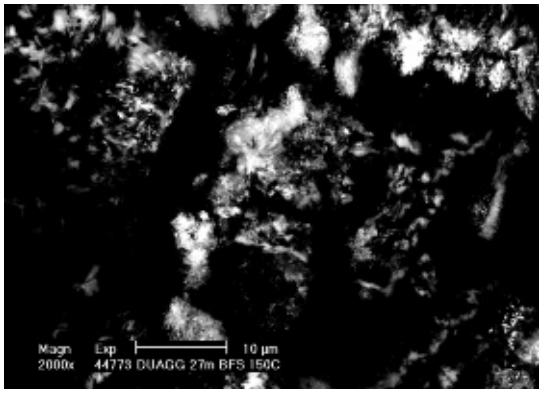

41F: Same area in backscattered electrons showing the crystals containing U

Fig. 41: SEM pictures of DUAGG pellet kept in BFS pore solution at 150° C for 24 months

4. CONCLUSIONS

The corrosion of DUAGG pellets was studied for as long as 27 months at three temperatures, 20, 67, and 150˚C in DI water, 1 *N* NaOH solution, and saturated cement pore solutions made from (a) OPC and (b) a mix of OPC, BFS, and fly ash. The pellets were completely immersed in the solution with a 10 to 1 cm^{-1} ratio of the volume of leachant to the surface area of the pellet with no change of the solution during the test (static cumulative test). No special handling of the pellets or the solutions was made to control the oxidation state. The analyses of the leachates were made, and the pellets were observed by SEM to identify the nature of the products formed during curing. For comparison, the same conditions and testing were performed on pellets of high-fired DUO_2 for 9 months.

Several conclusions can be drawn from the results gathered:

- The total release of uranium is minimal in the conditions of our tests: after 27 months at 150°C, the maximum amount of uranium ranged from 0.40% to 0.0003% (the amount leached divided by the total amount of uranium present in the pellet before testing) was released from DUAGG and the maximum of 0.90 to 0.0005% from high-fired DUO_2 was released after 9 months at 150°C.

- The release of uranium from DUAGG is lower than that released from a DUO_2 pellet: under most conditions at least one order of magnitude difference exists between DUAGG and DUO_2.

- The release of uranium is higher in DI water than in the 1*N* NaOH solution.

- The cement pore solutions have a beneficial effect for both DUAGG and DUO_2 on the uranium release. For DUO_2, the maximum release was as much as 260 times lower in BFS and 750 times lower for OPC than in DI water. For DUAGG, the maximum release was as much as 600 times lower in BFS and 70 times lower in OPC than in DI water.

- The release rate of uranium has been compared with data found in the literature for release rates of uranium from UO_2 or simulated nuclear fuel, and the release rate is lower for DUAGG. It is comparable for DUO_2 in the presence of DI water, but the contact of pure uranium pellets with cement pore solutions decreased the release rate.

The combination of uranium and basalt in DUAGG results in a competition between the different species (uranium, aluminum, silicon, iron, titanium, and zirconium) for interaction with the solution species. The examination of the samples after more than 2

years of cure provides strong evidence that the basalt phase effectively protects the UO_2. A protective coating of recrystallization of basalt dissolution products covers the DU particles and forms a very dense layer that slows or stops the exchange of species between the pellet and the solution. The examination showed no deleterious crystals that may have resulted from AAR when the samples were kept in cement pore solution. The nature of the compounds formed after curing for the high-fired DUO_2 is similar to those reported in the literature for SNF or surrogate SIMFUEL with observation of crystals, such as schoepite. For the DUAGG pellets such products are not visible, and the protective crystals, such as those found in alteration of nuclear glasses, were observed. The results obtained tend to prove that DUAGG behaves as a nuclear glass. Such glasses are currently used for the long-term storage of high-level nuclear wastes; they have been studied extensively during the years and are approved as being safe for storage of long-lived radionuclides.

5. REFERENCES

1. R. R. Price, M. J. Haire, and A. G. Croff, "Depleted Uranium Uses Research and Development Program," Waste Management 2001 Symposium, Tucson, AZ (Feb. 25–Mar. 1, 2001).

2. W. J. Quapp and P. A. Lessing, "Radiation Shielding Composition," U.S. Patent No. 5,786,611 (July 28, 1998).

3. W. J. Quapp and P. A. Lessing, "Radiation Shielding Composition," U.S. Patent No. 6,166,390 (December 26, 2000).

4. P. A. Lessing, "Development of DU-AGG (Depleted Uranium Aggregate)," INEL-95/3015, Idaho National Engineering Laboratory (September 1995).

5. W. J. Quapp, "An Advanced Solution for the Storage, Transportation and Disposal of Spent Fuel and Vitrified High Level Waste," presented at Global 1999 (August 1999).

6. L. R. Dole and W. J. Quapp, "Radiation Shielding Using Depleted Uranium Oxide in Nonmetallic Matrices," ORNL/TM-2002/111, Oak Ridge National Laboratory (August 2002).

7. D. J. Wronkiewicz et al., "Ten-Year Results from Unsaturated Drip Tests with UO_2 at 90°C: Implications for the Corrosion of Spent Nuclear Fuel," *J. Nucl. Mater.* **238**, 78–95 (1996).

8. G. F. Thomas and G. Till, "The Dissolution of Unirradiated UO_2 Fuel Pellets under Simulated Disposal Conditions," *Nucl. Chem. Waste Manage.* **5**, 141–147 (1984).

9. D. J. Wronkiewicz et al., "Uranium Release and Secondary Phase Formation during Unsaturated Testing of UO_2 at 90°C," *J. Nucl. Mater.* **190**, 107–127 (1992).

10. P. Taylor, D.D. Wood, and D.G. Owen, "Microstructures of Corrosion Films on UO_2 Fuel Oxidized in Air-stream Mixtures at 225°C," *J. Nucl. Mater.* **223**, 316–320 (1995).

11. J. Bruno, I. Casas, and A. Sandino, "Static and Dynamic SIMFUEL Dissolution

Studies Under Oxic Conditions," *J. Nucl. Mater.* **190,** 61–69 (1992).

12. K. Ollila, "SIMFUEL Dissolution Studies in Granitic Groundwater," *J. Nucl. Mater.* **190,** 70–77 (1992).

13. J.P. Glatz et al., "Influence of Granite on the Leaching Behavior of Different Nuclear Waste Forms," *J. Nucl. Mater.* **223,** 84–89 (1995).

14. J. Bruno et al., " A Kinetic Model for the Stability of Spent Fuel Matrix under Oxic Conditions," *J. Nucl. Mater.* **238,** 110–120 (1996).

15. Hj. Matzke and A. Turos, "Mechanisms and Kinetics of Leaching of UO_2 in Water," *Solid State Ionic* **49**, 189**–**194 (1991).

16. L.P. Moroni and F.P. Glasser, "Reactions Between Cement Components and U(VI) Oxide," *Waste Management* **Vol. 15, N○3**, 243-254 (1995).

17. W.J. Gray, H.R. Leider and S.A. Steward, "Parametric Study of LWR Spent Fuel Dissolution Kinetics," *J. Nucl. Mater.* **190,** 46–52 (1992).

18. R.S. Forsyth, L.O. Werme and J. Bruno, "Preliminary Study of Spent UO_2 Fuel Corrosion in the Presence of Bentonite," *J. Nucl. Mater.* **160,** 218–223 (1988).

19. R.S. Forsyth, L.O. Werme and J. Bruno, "The Corrosion of Spent UO_2 Fuel in Synthetic Groundwater," *J. Nucl. Mater.* **138,** 1–15 (1986).

20. J.A. Serrano et al., "Comparison of the Leaching Behavior of Irradiated Fuel, SIMFUEL, and Non-Irradiated UO_2 under Oxic Conditions," *Radiochim. Acta* **82**, 33**–**37 (1998).

21. R.S. Forsyth and L.O. Werme, "Spent Fuel Corrosion and Dissolution," *J. Nucl. Mater.* **190,** 3–19 (1992).

22. V.V. Rondinella and Hj. Matzke, " Leaching of SIMFUEL in Simulated Granitic Water: Comparison to Results in Demineralized Water," *J. Nucl. Mater.* **238,** 44–57 (1996).

23. P. Trocellier, C. Cachoir and S. Guilbert, "A Simple Thermodynamical Model to Describe the Control of the Dissolution of Uranium Dioxide in Granitic Groundwater by Secondary Phase Formation," *J. Nucl. Mater.* **256,** 197–206 (1998).

24. S. Sunder and N.H. Miller, "XPS and XRD Studies of $(Th,U)O_2$ Fuel Corrosion in Water," *J. Nucl. Mater.* **279,** 118–126 (2000).

25. L. Mazeina et al., "Characterization of Secondary products of Uranium-Aluminium Material test Reactor Fuel Element Corrosion in Repository-Relevant Brine," *J. Nucl. Mater.* **323,** 1–7 (2003).

26. C. Jegou et al., "Identification of the Mechanisms Limiting the Alteration of Clad Fuel Segments in Aerated Carbonated Groundwater," *J. Nucl. Mater.* **326,** 144–155 (2004).

27. D.W. Shoesmith, "Fuel Corrosion Processes Under Waste Disposal Conditions," *J. Nucl. Mater.* **282,** 1–31 (2000).

28. P.C. Burns, R.C. Ewing, and M.L. Miller, "Incorporation Mechanisms of Actinides Elements into the Stuctures of U^{6+} Phases Formed during the Oxidation of Spent Nuclear Fuel," *J. Nucl. Mater.* **245,** 1–9 (1997).

29. G. Berger, J. Schott and M. Loubert, "Fundamental Processes Controlling the First Stage of Alteration of a Basalt Glass by Seawater: an Experimental Study between 200° and 320°C," *Earth and Planetary Science Letters* **84**, 431–445 (1987).

30. I. Techer et al., "Basaltic Glass: Aletration Mechanisms and Analogy with Nuclear Waste Glasses," *J. Nucl. Mater.* **282,** 40–46 (2000).

31. G. Leturcq et al., "Initial and Long-Term Dissolution Rates of Aluminosilicate Glasses Enriched with Ti, Zr and Nd," *Chemical Geology* **160**, 39–62 (1999).

32. A. Abdelouas et al., "Surface Layers on a Borosilicate Nuclear Waste Glass Corroded in $MgCl_2$ Solution," *J. Nucl. Mater.* **240,** 100–111 (1997).

33. A. Abdelouas et al., "Formation of Hydrotalcite-Like Compounds During R7T7 Nuclear Waste Glass and Basaltic Glass Alteration," *Clay and Clay Minerals* **42**(5), 526–533 (1994).

34. I. Techer et al., "Dissolution Kinetics of Basaltic Glasses: Control by Solution

Chemistry and Protectrive Effect of the Alteration Film," *Geological Geology* **176**, 235–263 (2001).

35. J.L. Crovisier, T. Advocat, and J.L. Dussossoy, "Nature and Role of Natural Alteration Gels Formed on the Surface of Ancient Volcanic Glasses (Natural Analogs of Waste Containment Glasses)," *J. Nucl. Mater.* **321,** 91–109 (2003).

36. S. A. Marfil et al., "Relationship Between SiO_2 , Al_2O_3 , CaO , K_2O, and Expansion in the Determination of the Alkali Reactivity of Basaltic Rocks," *Cement Concrete Res.* **28**(2), 189–196 (1998).

37. W. A. Tasong et al., "Aggregate-Cement Chemical Interactions," *Cement Concrete Res.* **28**(7), 1037–1048 (1998).

38. W. Prince et al., "Similarity Between Alkali-Aggregate Reaction and the Natural Alteration of Rocks," *Cement Concrete Res.* **31**(2), 271–276 (2001) .

39. ASTM C289-01, Standard Method for Potential Alkali-Silica Reactivity of Aggregates (Chemical method).

40. "Performance Testing and Analyses of the VSC-17 Ventilated Concrete Cask," EPRI report TR-100305, Project 3073-1, PNL-7831, UC-85, final report 1992, Pacific Northwest Laboratory and Idaho National Engineering Laboratory (1992).

41. H. A. van der Sloot et al., "Approach Toward International Standardization: A Concise Scheme for Testing of Granular Waste Leachability," pp. 453–466 in *Environmental Aspects of Construction with Waste Materials*, J. J. J. M. Gourmans, H.A. van der Sloot, and Th. G. Aalbers (Editors), Elsevier Science (1994).

42. H. A. van der Sloot, "Quick Techniques for Evaluating the Leaching Properties of Waste Materials: Their Relation to Decisions on Utilization and Disposal," *Trends Anal. Chem.* **17**(5), 298–310, (1998).